

LA-5172

C.B.

CIC-14 REPORT COLLECTION  
**REPRODUCTION**  
**COPY**

Evaluated Neutron-Induced Cross Sections for  
 $^{239}\text{Pu}$  and  $^{240}\text{Pu}$



This report was prepared as an account of work sponsored by the United States Government. Neither the United States nor the United States Atomic Energy Commission, nor any of their employees, nor any of their contractors, subcontractors, or their employees, makes any warranty, express or implied, or assumes any legal liability or responsibility for the accuracy, completeness or usefulness of any information, apparatus, product or process disclosed, or represents that its use would not infringe privately owned rights.

Printed in the United States of America. Available from  
National Technical Information Service  
U. S. Department of Commerce  
5285 Port Royal Road  
Springfield, Virginia 22151  
Price: Printed Copy \$3.00; Microfiche \$0.95



LA-5172  
UC-34  
ISSUED: June 1973

# Evaluated Neutron-Induced Cross Sections for $^{239}\text{Pu}$ and $^{240}\text{Pu}$

by

R. E. Hunter  
L. Stewart  
T. J. Hirons



Work supported by the Defense Nuclear Agency under Subtask Code W99QAXPC102 (Cross Section Evaluations) and Work Unit 09 (Cross Section Evaluations and Translations).



CONTENTS

I.	INTRODUCTION . . . . .	1
II.	PLUTONIUM-239. . . . .	1
A.	<u>Total Cross Section.</u> . . . . .	1
B.	<u>Elastic Scattering Cross Section</u> . . . . .	3
C.	<u>Fission Cross Section.</u> . . . . .	3
D.	<u>Mean Number of Prompt Neutrons per Fission</u> . . . . .	8
E.	<u>Delayed Neutrons from Fission.</u> . . . . .	8
F.	<u>Fission Neutron Energy Distribution.</u> . . . . .	10
G.	<u>Radiative Capture Cross Section.</u> . . . . .	11
H.	<u>Inelastic Scattering Cross Section</u> . . . . .	12
I.	<u><math>\sigma_{n,2n}</math> and <math>\sigma_{n,3n}</math>.</u> . . . . .	14
J.	<u>Angular Distributions</u> . . . . .	16
K.	<u>Charged-Particle Cross Sections.</u> . . . . .	16
L.	<u>Tabulated Cross Sections</u> . . . . .	16
III.	PLUTONIUM-240. . . . .	32
A.	<u>Total Cross Section.</u> . . . . .	32
B.	<u>Elastic-Scattering Cross Section</u> . . . . .	32
C.	<u>Fission Cross Section.</u> . . . . .	32
D.	<u>Mean Number of Prompt Neutrons from Fission.</u> . . . . .	32
E.	<u>Delayed Neutrons from Fission.</u> . . . . .	32
F.	<u>Fission Neutron Energy Distribution.</u> . . . . .	34
G.	<u>Inelastic Scattering</u> . . . . .	34
H.	<u>Radiative Capture Cross Section.</u> . . . . .	36
I.	<u><math>\sigma_{n,2n}</math> and <math>\sigma_{n,3n}</math>.</u> . . . . .	36
J.	<u>Tabulated Cross Sections</u> . . . . .	42
IV.	INTEGRAL TESTING . . . . .	47
V.	DISCUSSION . . . . .	48
	ACKNOWLEDGMENTS. . . . .	49
	REFERENCES . . . . .	49

EVALUATED NEUTRON-INDUCED CROSS SECTIONS

FOR  $^{239}\text{Pu}$  AND  $^{240}\text{Pu}$

by

R. E. Hunter, L. Stewart, T. J. Hirona

ABSTRACT

The neutron-induced cross sections for  $^{239}\text{Pu}$  and  $^{240}\text{Pu}$  have been evaluated for incident-neutron energies from about 100 keV to 20 MeV. Tabulated values are presented, and recommended curves are compared with the experimental data. These cross sections are merged with the ENDF/B-III evaluated curves from 10-100 keV. Below 10 keV, the ENDF/B-III files are recommended. The complete cross-section sets have been tested by comparing calculated and measured values for a series of integral experiments. These integral results are presented and discussed.

I. INTRODUCTION

The neutron cross sections for  $^{239}\text{Pu}$  and  $^{240}\text{Pu}$  have been studied and values recommended for neutron energies from 100 keV to 20 MeV. These data are available in the ENDF/B format and extrapolate smoothly when combined with the low-energy data on MAT 1159 and MAT 1105, the  $^{239}\text{Pu}$  and  $^{240}\text{Pu}$  evaluations, respectively, in ENDF/B-III.

This evaluation effort was concentrated at higher energies with the primary emphasis in two regions: 100 keV to 3 MeV and from 13-15 MeV. Extensions to the representation currently in the ENDF/B files are the treatment of first-, second-, and third-chance fission and the inclusion of "direct-interaction" processes for high-energy neutrons.

The complete evaluations were used in checking an extensive set of integral experiments, including bare and reflected critical assemblies, spectral indices, central core reactivity worths, and leakage spectra. For most of the calculations the processing and neutronics codes were ETOG and DTF, respectively. A few comparisons were run with SIGMA\* and MDN,\* primarily for high-energy tests where the current ENDF codes are not adequate for handling many

processes, for example, multiple-chance fission and spectral representation for direct inelastic scattering.

The cross-section evaluations are discussed in Secs. II and III, with the integral comparisons described in Sec. IV.

II. PLUTONIUM-239

A. Total Cross Section

Measurements of the total cross section of  $^{239}\text{Pu}$  have been presented by Hibdon and Langsdorf,<sup>1</sup> Meads, Bratenahl et al.,<sup>2</sup> Peterson et al.,<sup>3</sup> Foster and Glasgow,<sup>4</sup> and for a number of unpublished Los Alamos results. Recently, Schwartz et al.<sup>5</sup> reported measurements over the energy range from 500 keV to 15 MeV which show good agreement with the higher-energy data of Foster and Glasgow.<sup>5</sup> The evaluated curve above 2.5 MeV is the average of these data, except that above 13 MeV the recommended values lie somewhat above the measurements.

Below approximately 1 MeV, the ENDF/B-III values which lie within the spread of the experimental data (although a bit low) were followed except for minor deviations. The curve between 1.0 and 2.5 MeV was obtained by merging into the average obtained from the measurements by Foster and Glasgow. The recommended curve is shown in Fig. 1.

\* Los Alamos Scientific Laboratory (LASL) cross-section processing and neutronics codes.

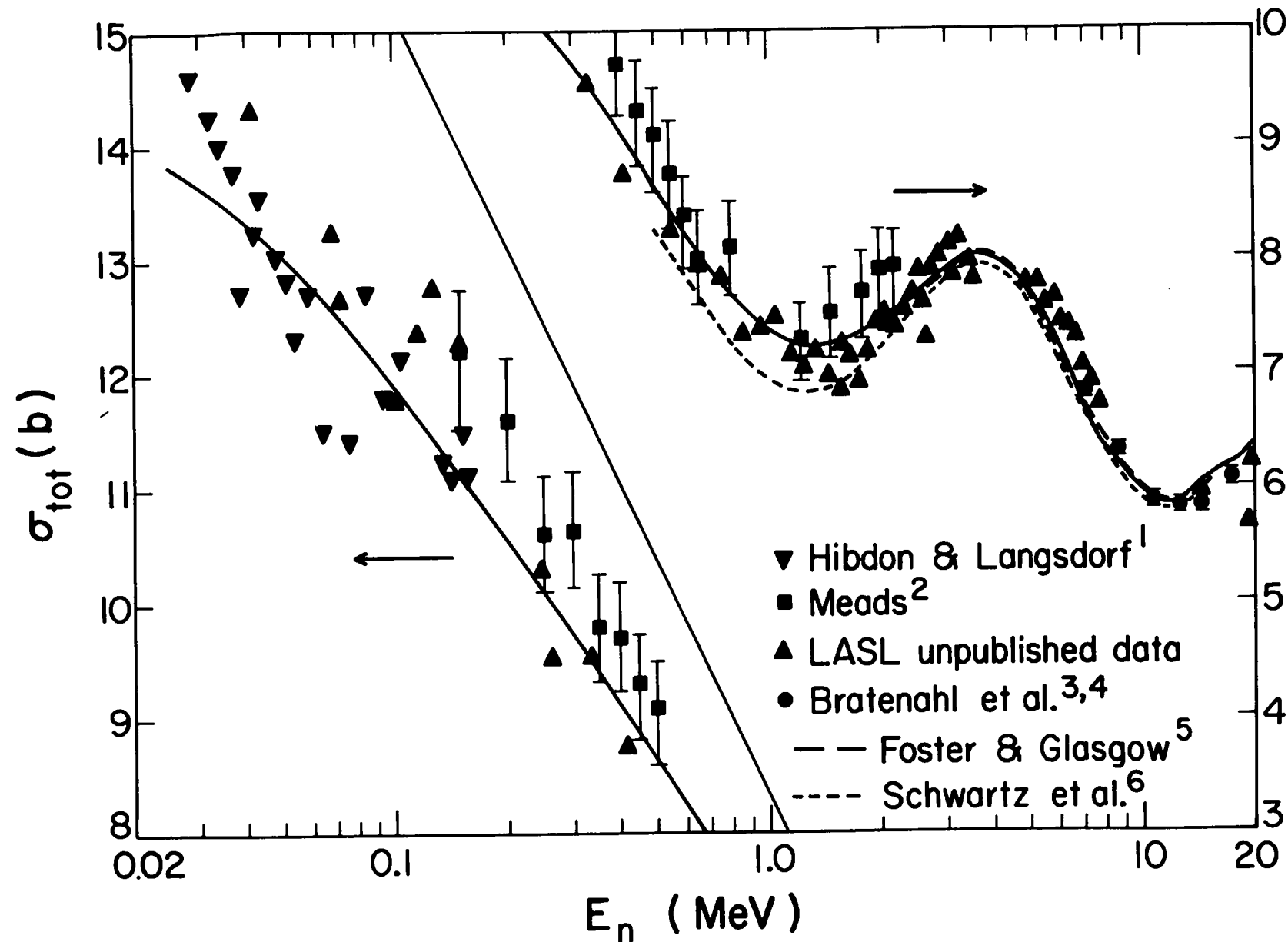


Fig. 1. Total cross section for  $^{239}\text{Pu}$ . The curves representing the data of Foster and Glasgow, and of Schwartz et al. were obtained by averaging their data.

### B. Elastic Scattering Cross Section

Knitter and Coppola,<sup>7</sup> Coppola and Knitter,<sup>8</sup> and Allen et al.<sup>9</sup> made measurements of the angular distributions. Above 6-7 MeV,  $\sigma_{n,n}$  was obtained by continuously "boot-strapping" nearly all cross sections in order to maintain a smooth curve. Also, the elastic cross section was specified to be greater than one-half of the total cross section at each point. The recommended curve is shown in Fig. 2.

### C. Fission Cross Section

The resonance parameters from MAT 1159 of ENDF/B-III were not modified in this evaluation; the fission cross section is represented by resonance parameters up to 25 keV.

In the ENDF/B-III file, the fission cross section is represented by resonance parameters below 25 keV. No attempt has been made here to reevaluate these parameters; instead it is recommended that they be lifted directly from MAT 1159.

Most experimental differential  $^{239}\text{Pu}$  fission cross sections are measured as a ratio of the fission

cross section of  $^{239}\text{Pu}$  to that of  $^{235}\text{U}$ . In this evaluation, the data of Poenitz,<sup>10,11</sup> Pfletschinger and Käppeler,<sup>12</sup> Soleilac et al.,<sup>13</sup> White et al.,<sup>14</sup> Nesterov and Smirenkin,<sup>15</sup> Savin et al.,<sup>16</sup> Lehto,<sup>17</sup> Smith et al.,<sup>18</sup> and White and Warner<sup>19</sup> were employed. All of these measurements were reported within the past seven years, although the data of Smith et al. result from corrections to an older experiment.

In addition, recent "absolute" measurements have been reported by James,<sup>20</sup> Perkin et al.,<sup>21</sup> and Dubrovina and Shigin.<sup>22</sup> Older measurements by Allen and Ferguson<sup>23</sup> and by Dorofeev and Dobrynnin<sup>24</sup> were also used.

Some earlier experiments are not included here on the assumption that they would not appreciably affect the end results. On the basis of the measurements considered, the evaluated curve follows generally the measurements of Savin et al.<sup>16</sup> and Nesterov and Smirenkin,<sup>15</sup> although it falls a bit below their measurements at energies less than 2 MeV. At energies above 1 MeV, the ratio measurements actually

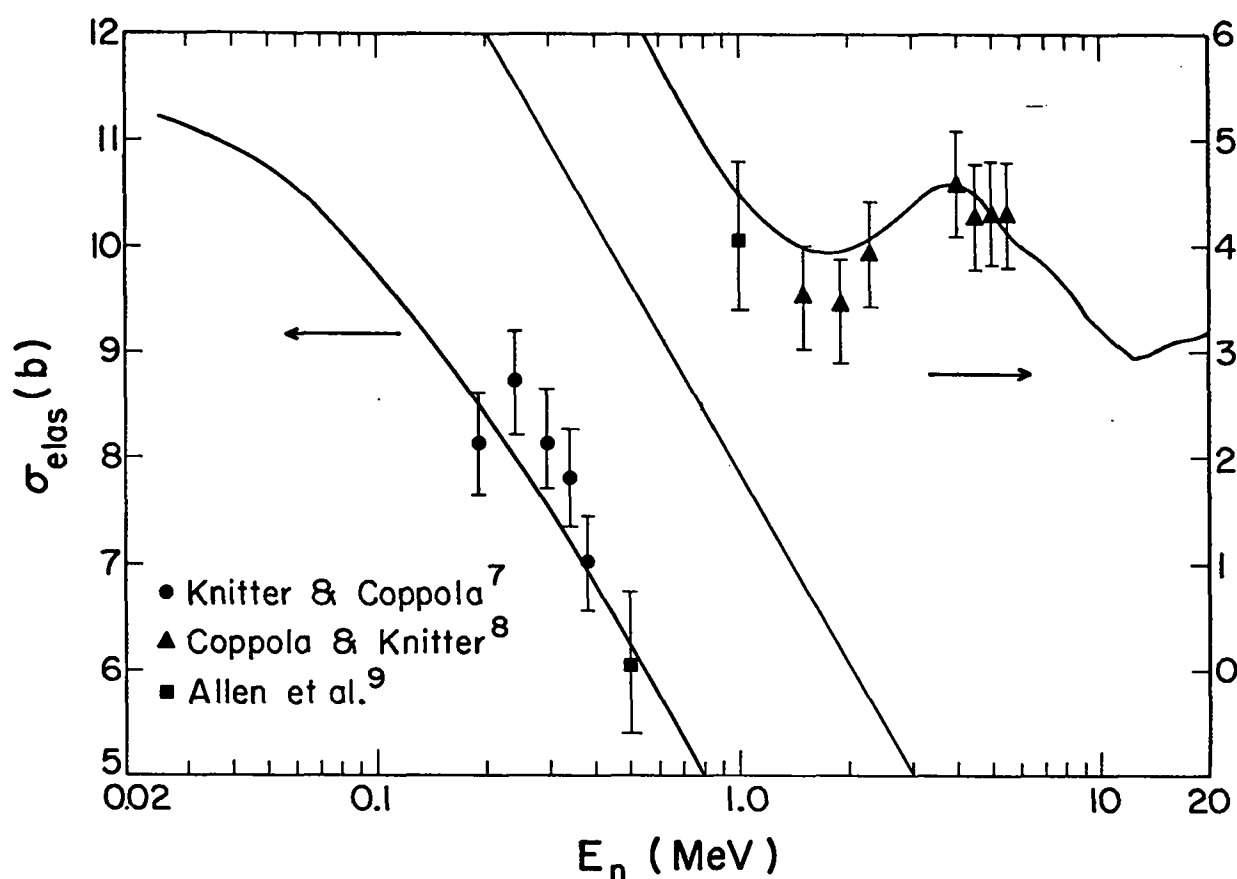


Fig. 2. Elastic-scattering cross section for  $^{239}\text{Pu}$ .

diverge; Soleilac et al.,<sup>13</sup> for example, find a rapidly decreasing ratio while other data indicate an increase.

Above 6-7 MeV, the curve is even more uncertain. The data were taken from Smith et al.,<sup>18</sup> who measured separately the ratio to  $^{235}\text{U}$  and to  $^{238}\text{U}$ . The latter measurements were converted to ratios with respect to  $^{235}\text{U}$  via the  $^{235}\text{U}/^{238}\text{U}$  ratios, as evaluated by Pitterle et al.<sup>25</sup> There is also a value at 14.2 MeV from White and Warner.<sup>19</sup> The uncertainties on the data of Smith et al. are relatively large.

Also, Adams et al.<sup>26</sup> measured separately  $\sigma_f(^{239}\text{Pu})$  and  $\sigma_f(^{235}\text{U})$  relative to  $\sigma_f(^{238}\text{U})$  above 12.6 MeV. From these, the ratio  $\sigma_f(^{239}\text{Pu})/\sigma_f(^{235}\text{U})$  was obtained. Unfortunately, these measured ratios provide little constraint on the absolute cross section above 1 MeV--precisely that region where "hard spectrum" assembly fluxes are large.

A rather pronounced dip in the ratio between 850 keV and 1.0 MeV is fairly well established. This dip seems to indicate a corresponding increase in the  $^{235}\text{U}$  fission cross section rather than a drop in the  $^{239}\text{Pu}$  fission cross section. The recommended curve for the ratio of  $\sigma_f(^{239}\text{Pu})$  to  $\sigma_f(^{235}\text{U})$  is shown in Figs. 3 and 4.

The  $^{235}\text{U}$  fission cross section used to obtain the corresponding curve for  $^{239}\text{Pu}$  was established by Pitterle et al.,<sup>25</sup> and is based largely on recent data (not reviewed here) which tend to raise the curve above 1 MeV and lower it below that point, relative to current published evaluations. The  $^{235}\text{U}$  fission cross-section evaluation shown in Fig. 5 has not been tested extensively by integral comparisons. Small changes in  $^{235}\text{U}$  fission can easily be accommodated by adjustments in evaluating the ratio, without doing violence to the uncertainty in either quantity.

The  $^{239}\text{Pu}$  cross section obtained from this ratio generally falls within the experimental errors of the "absolute" measurements, except that it lies below the data of Dubrovina and Shigin<sup>22</sup> between 80 and about 400 keV and above about 1 MeV. It also lies below the cross sections of Allen and Ferguson<sup>23</sup> at 550 keV and 1.5 MeV. The recommended curve for  $\sigma_f(^{239}\text{Pu})$ , together with the experimental data, is shown in Fig. 6.

As is well known, the "total" fission cross section (which is the measured quantity) is composed of several processes, referred to as first-, second-, third-, ... chance fission:

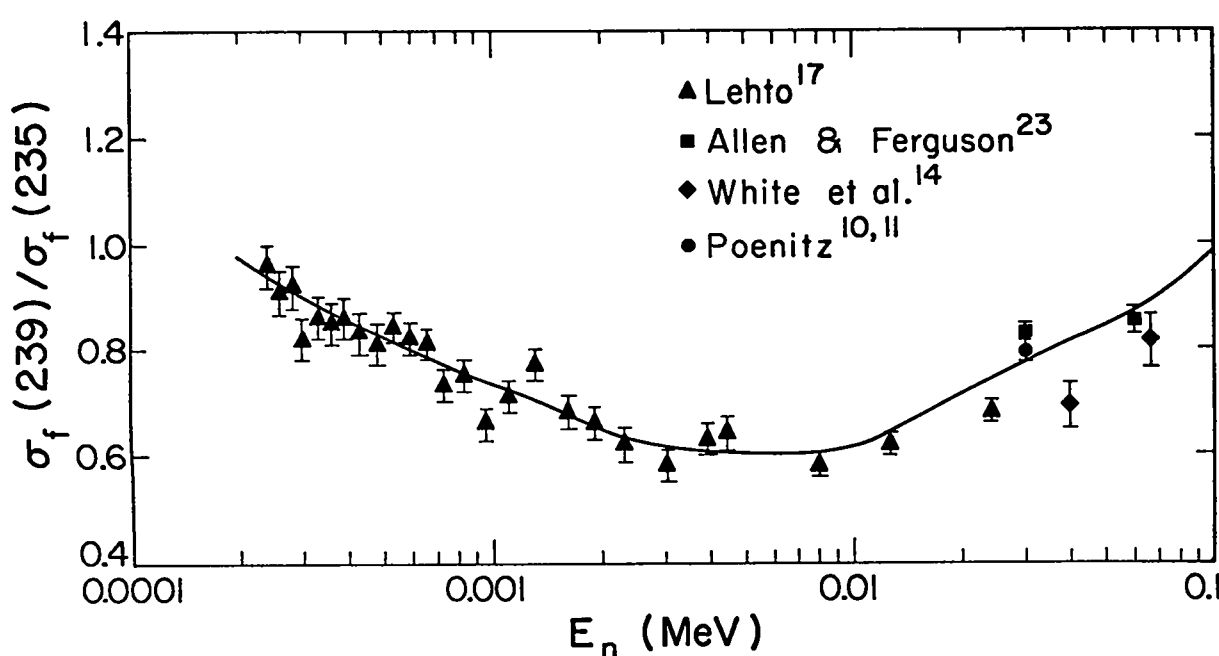


Fig. 3. Ratio of fission cross section for  $^{239}\text{Pu}$  to that of  $^{235}\text{U}$ , for energies up to 0.1 MeV.

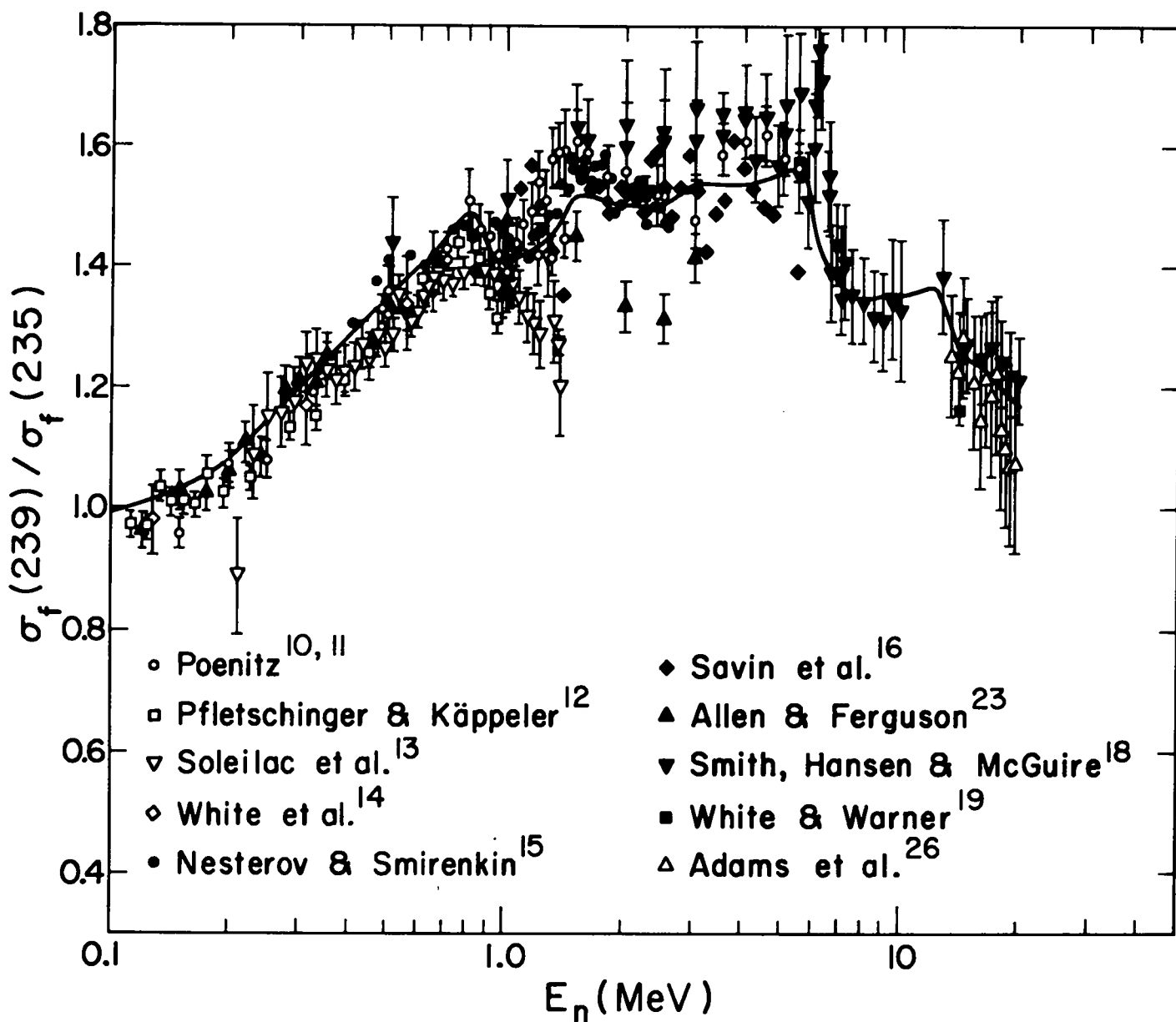


Fig. 4. Ratio of fission cross section for  $^{239}\text{Pu}$  to that for  $^{235}\text{U}$ , for energies above 0.1 MeV.

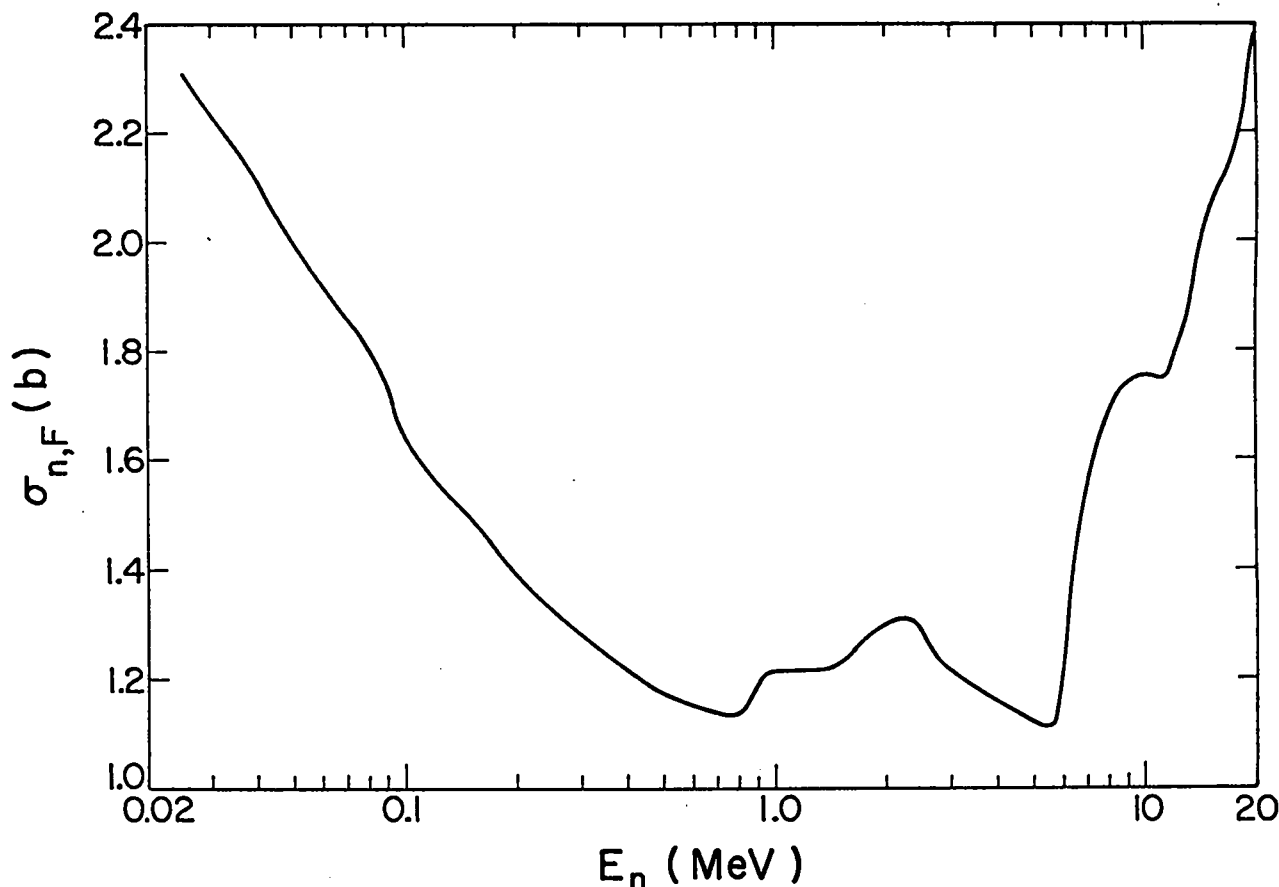


Fig. 5. Fission cross section for  $^{235}\text{U}$  used as reference.

$$\sigma_{n,F} = \sigma_{n,f} + \sigma_{n,n'f} + \sigma_{n,2nf} + \sigma_{n,3nf} + \dots , \quad (1)$$

where  $\sigma_{n,F}$  is the total fission cross section.  $\sigma_{n,f}$  refers to the process whereby fission occurs directly. In the  $n,n'f$  reaction (second-chance fission), the compound nucleus initially decays by the emission of a neutron and the residual nucleus then undergoes fission. In  $n,2nf$ , two neutrons are emitted prior to fission.

The differentiation of these processes is important because the energy distribution of the pre-fission neutrons is considerably different from that of the prompt neutrons emitted in the fission process, especially near threshold. That the pre-fission neutrons are lower in energy than fission neutrons is indicated by the threshold nature of the higher order processes and confirmed by fragmentary experimental evidence.

The  $n,n'f$  process is fundamentally an inelastic-scattering reaction, and competes in the sequential mode with the  $n,n'\gamma$  and  $n,2n$  channels rather than

the  $n,f$  channel. This is indicated by a rather sharp rise in the total fission cross section that occurs simultaneously with a sharp drop in the  $n,n'\gamma$  cross section (for those isotopes where such measurements exist). Similarly, the  $n,2nf$  process occurs in competition with the  $n,2n\gamma$  and  $n,3n$  channels.

Of course, no experimental data exist on the individual fission channels, such as  $n,n'f$ ,  $n,2nf$ , etc. The  $^{239}\text{Pu}$  fission cross section is relatively constant below the  $n,n'f$  threshold\* at about 5.5 MeV. Therefore, first-chance fission,  $\sigma_{n,f}$ , is assumed to be constant from this threshold all the way to 20 MeV. Similarly, the  $n,n'f$  cross section is assumed to be constant above the  $n,2nf$  threshold at 11.5 MeV. It is emphasized that these assumptions are based on a total lack of measurements and

\*Note that the  $n,n'f$  and  $n,2n$  thresholds are approximately the same. This is also true for the  $n,2nf$  and  $n,3n$  thresholds.

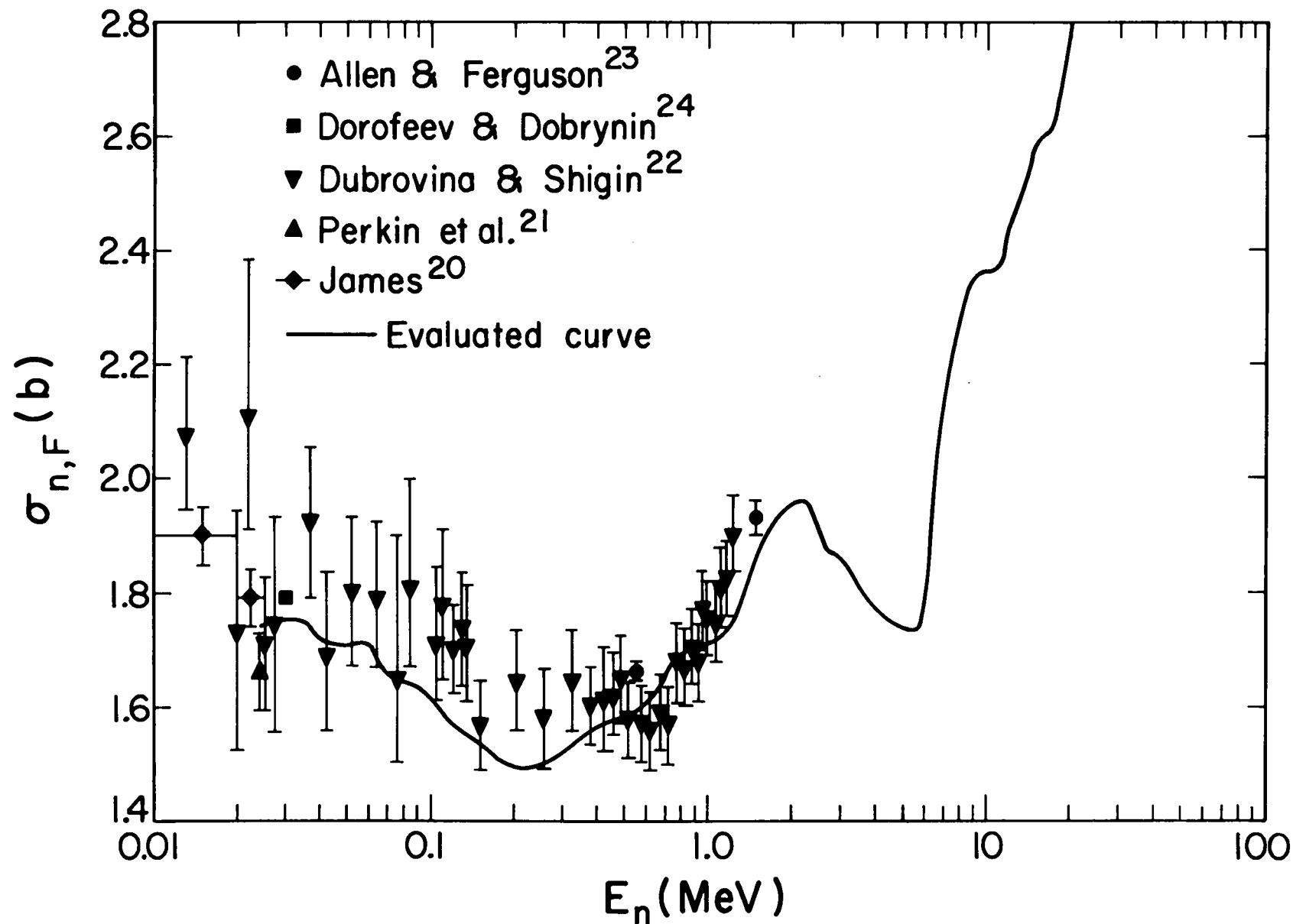


Fig. 6. Fission cross section for  $^{239}\text{Pu}$  as obtained from the ratio curve in Fig. 4 and the  $^{235}\text{U}$  fission cross-section curve in Fig. 5. Only the absolute data are plotted.

theoretical understanding. The recommended curves for  $\sigma_{n,n'f}$  and  $\sigma_{n,2nf}$  are shown in Fig. 7.

#### D. Mean Number of Prompt Neutrons per Fission

Many recent measurements on  $\bar{v}$  have been reported, so that  $\bar{v}$  vs incident neutron energy is fairly well established up to 14.4 MeV. This evaluation is based on the data of Soleilac et al.,<sup>27</sup> Hopkins and Diven,<sup>28</sup> Mather et al.,<sup>29</sup> Colvin and Sowerby,<sup>30</sup> Condé et al.,<sup>31</sup> Savin et al.,<sup>32</sup> and Nesterov et al.,<sup>33</sup> plus the recommended thermal value of Hanna et al.<sup>34</sup> These data were measured with respect to the thermal spontaneous  $\bar{v}$  for  $^{252}\text{Cf}$ . The ratios obtained were then fitted with a curve that is linear over two regions:

$$\begin{aligned} \bar{v}(\text{Pu}) &= 0.7599 + 0.04009E_n, \quad 0 < E_n < 11.5 \text{ MeV} \\ \bar{v}(\text{Cf}) &= 0.8329 + 0.03374E_n, \quad 11.5 < E_n < 20 \text{ MeV}. \quad (2) \end{aligned}$$

Assuming  $\bar{v}(^{252}\text{Cf}) = 3.748$ ,

$$\begin{aligned} \bar{v}(^{239}\text{Pu}) &= 2.8480 + 0.1502E_n \text{ (MeV)}, \quad 0 < E_n < 11.5 \text{ MeV} \\ &= 3.1216 + 0.1237E_n \text{ (MeV)}, \quad 11.5 \text{ MeV} < E_n < 20.0 \text{ MeV}. \quad (3) \end{aligned}$$

No experimental data exist between 14.4 and 22.4 MeV. Above the latter energy Soleilac et al.<sup>27</sup> have reported six measurements that indicate a smaller slope; however, the curve fitted to data between 11.5 and 14.4 MeV is consistent with an intercept at 22 MeV. Therefore, the above representation is used up to 20 MeV; the results are given in Fig. 8.

#### E. Delayed Neutrons from Fission

The delayed neutron fraction, from earlier work summarized by Keepin,<sup>35</sup> appeared to be fairly constant with incident neutron energy, with a thermal value of 0.0061 neutrons/fission and a "fast fission spectrum" value of 0.0063. However, one measurement by Shpakov et al.<sup>36</sup> at 14.5 MeV indicated a significant increase at energies above the fission spectrum neutrons.

Two recent measurements have shown strong indications that the delayed neutron fraction decreases

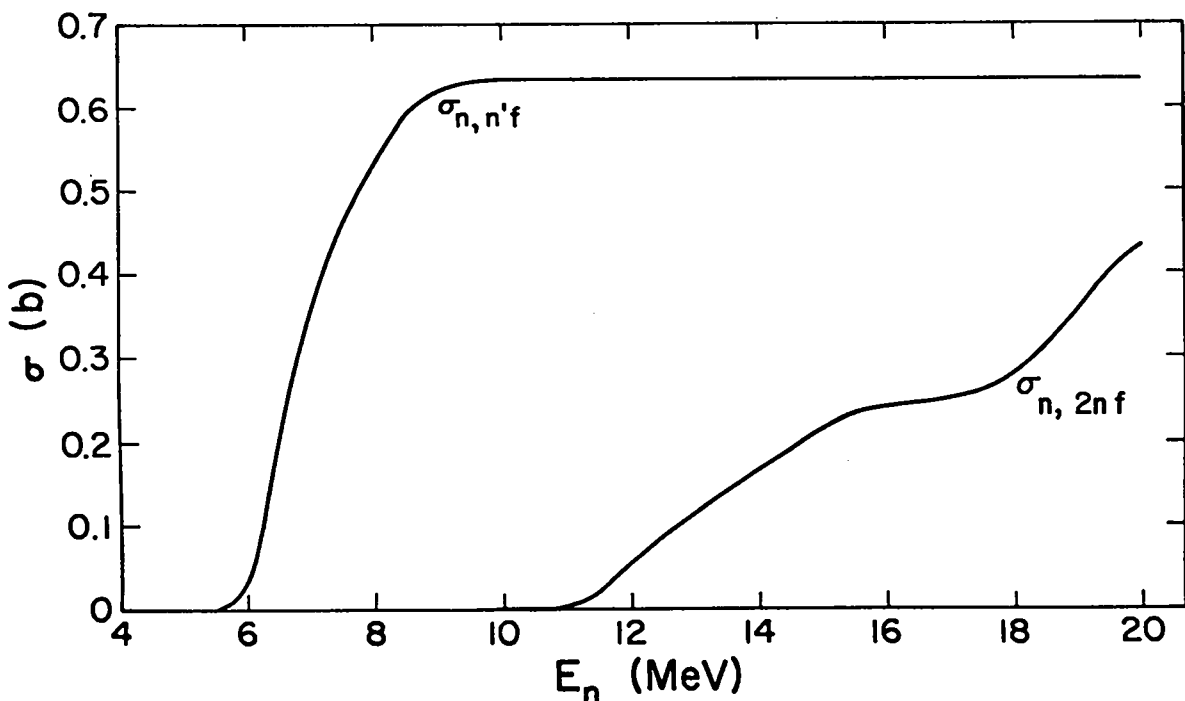


Fig. 7.  $\sigma_{n,n'f}$  and  $\sigma_{n,2nf}$  for  $^{239}\text{Pu}$ .

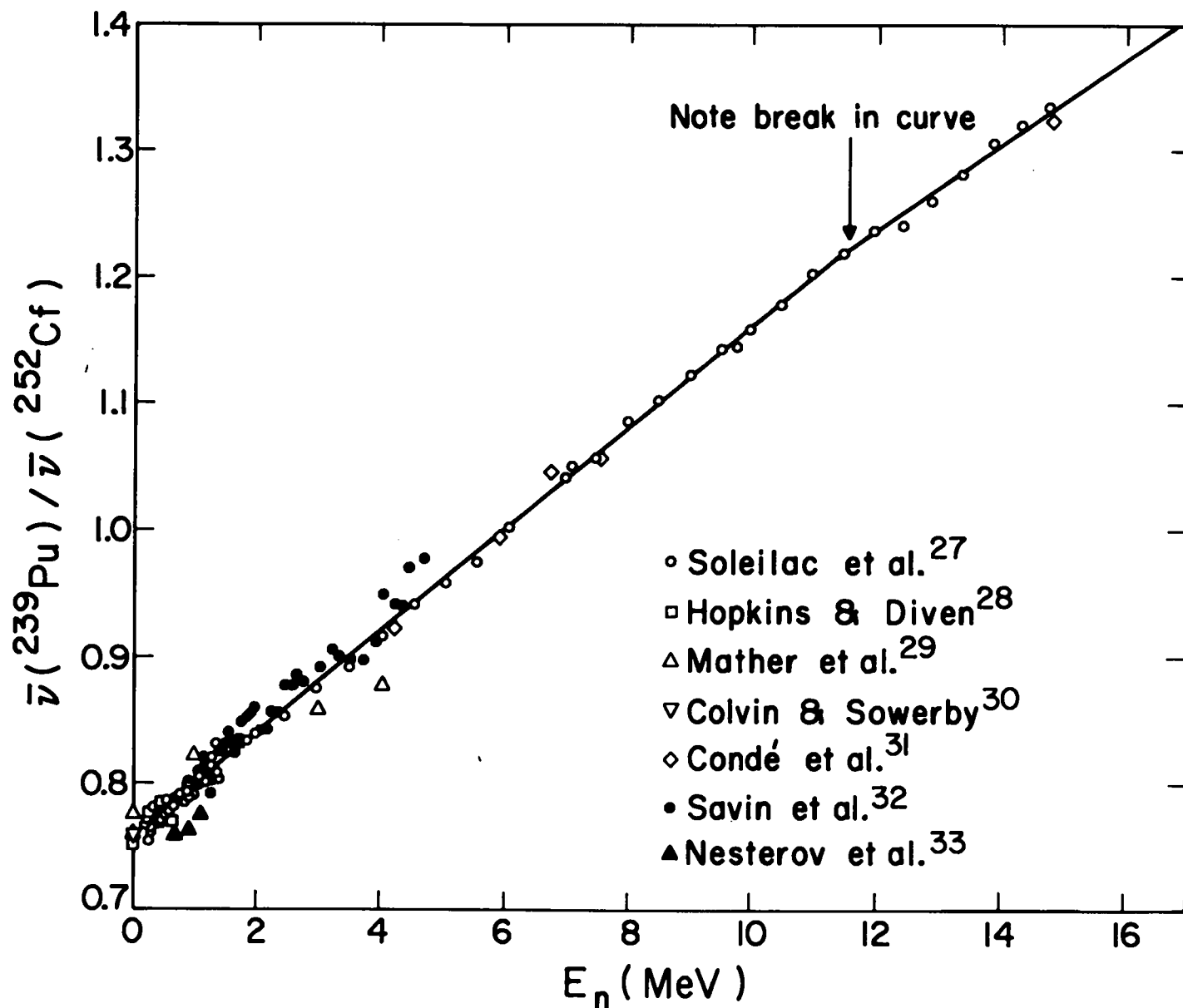


Fig. 8. Ratio of mean number of prompt neutrons per fission for  $^{239}\text{Pu}$  to the spontaneous fission for  $^{252}\text{Cf}$ .

at higher energies. Evans et al.<sup>37</sup> found a rather abrupt drop in the curve for several isotopes\* around 5 MeV, and Masters et al.<sup>38</sup> found a much lower value at 14.9 MeV. The evaluated curve follows the data of Evans et al.<sup>37</sup> and Masters et al.,<sup>38</sup> using the shape of the curve of Evans et al. for  $^{235}\text{U}$  to interpolate between 3.1 and 14.9 MeV. In the absence of data above 14.9 MeV, it is assumed that the curve is flat between 14.9 and 20.0 MeV.

\*They did not measure the delayed fraction for  $^{239}\text{Pu}$  above 1.8 MeV.

The value at thermal was derived from measurements of Keepin<sup>35</sup> and of Conant and Palmedo.<sup>39</sup> An average of these results agrees well with an extrapolation of the data of Evans et al.<sup>37</sup> The recommended curve is shown in Fig. 9.

The energy distribution of the delayed neutrons is taken from the review by Keepin,<sup>35</sup> who integrated all data over all groups. The recommended curve is shown in Fig. 10.

#### F. Fission Neutron Energy Distribution

The conventional way to represent the energy distribution of prompt fission neutrons is by a

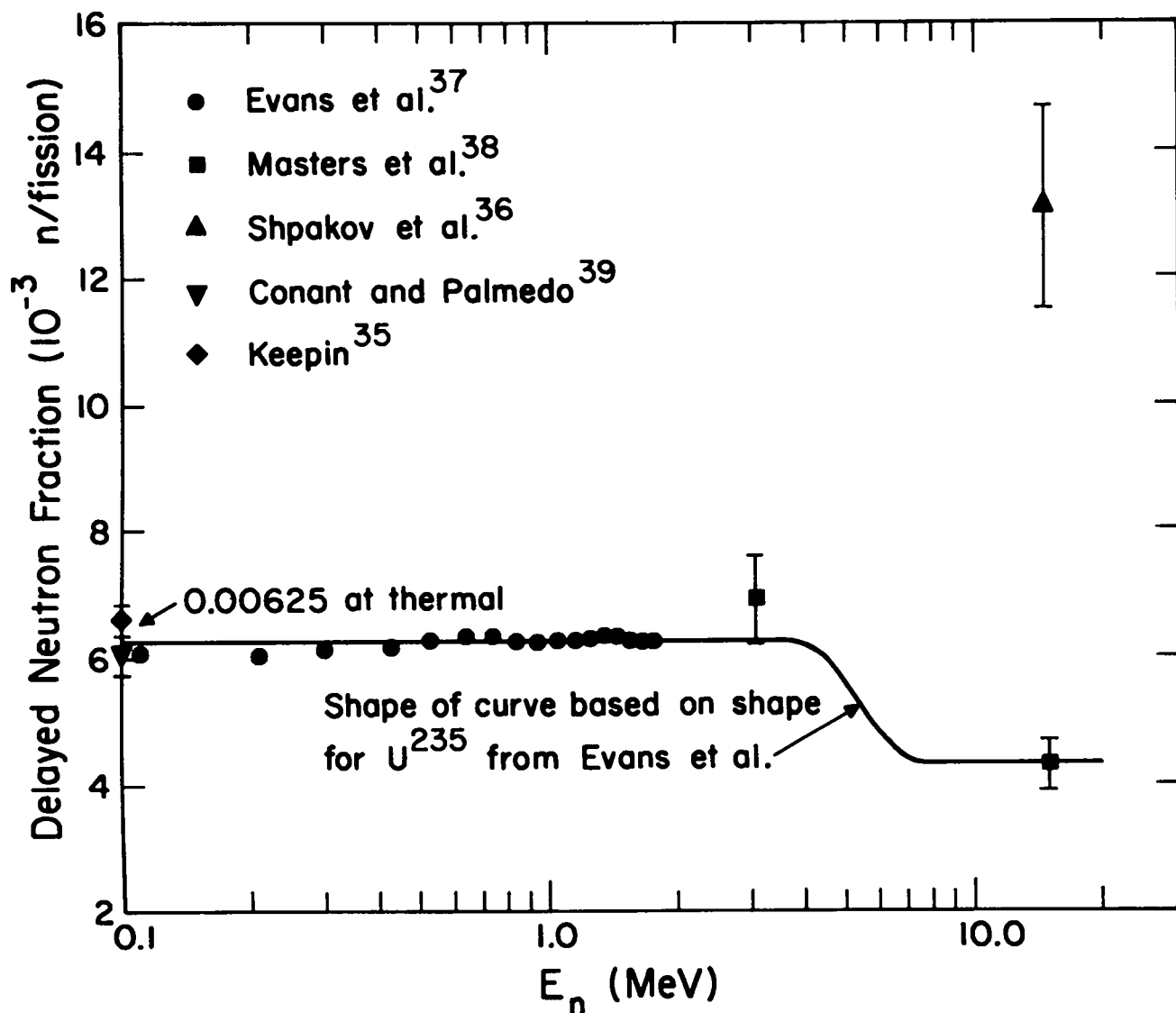


Fig. 9. Delayed neutron fraction for  $^{239}\text{Pu}$ . Data of Conant and Palmedo and of Keepin at thermal are plotted at 0.1 MeV, the lowest energy point on the graph.

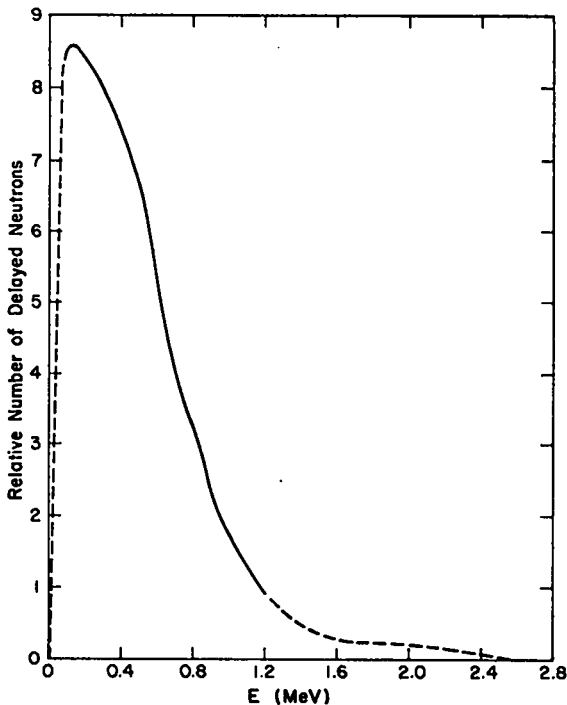


Fig. 10. Relative number of delayed neutron vs final-state neutron energy for  $^{239}\text{Pu}$ .

Maxwellian distribution,

$$F(E) = N E^{1/2} \exp(-E/T_f) , \quad (4)$$

where  $E$  is the emitted neutron energy,  $N$  is the normalization factor, and  $T_f$  is the nuclear temperature. The latter is related to the mean secondary neutron energy by the equation,

$$\bar{E} = \frac{3}{2} T_f . \quad (5)$$

Therefore, the evaluation of the energy distribution consists of evaluating the measurements of  $T_f$  as a function of the incident neutron energy,  $E_n$ .

Values of  $T_f$  are given by Barnard et al.,<sup>40</sup> Belov et al.,<sup>41</sup> Zamyatnin et al.,<sup>42</sup> Condé and During,<sup>43</sup> Smirenkin,<sup>44</sup> Coppola and Knitter,<sup>8</sup> and Bertrand and Voignier.<sup>45</sup> Smith<sup>46</sup> found the ratio of  $T_f(^{239}\text{Pu})/T_f(^{235}\text{U})$  to be 1.075 at energies of 35-400 keV. Based on the evaluation by Barnard et al.<sup>40</sup> of  $T_f(^{235}\text{U}) = 1.297$  MeV, this gives  $T_f = 1.394$  MeV for  $^{239}\text{Pu}$ . The data are tabulated in Table I.

The evaluated temperatures are  $T_f = 1.39$  MeV at thermal energy and  $T_f = 1.58$  MeV at  $E = 14.0$  MeV with

TABLE I  
FISSION NEUTRON TEMPERATURES

Energy (MeV)	Temperature (MeV)	References
Th	1.35 $\pm$ 0.04	Belov et al.
Th	1.39 $\pm$ 0.01	Average of several experiments as referenced by Barnard et al.
0.04	1.34 $\pm$ 0.04	Condé & During
0.130	1.407 $\pm$ 0.020	Barnard et al.
0.035 - 0.400	1.394 $\pm$ 0.028	Smith
1.5	1.41 $\pm$ 0.05	Coppola & Knitter
1.9	1.45 $\pm$ 0.04	Coppola & Knitter
2.3	1.52 $\pm$ 0.04	Coppola & Knitter
3.9	1.42 $\pm$ 0.03	Smirenkin
4.0	1.51 $\pm$ 0.07	Coppola & Knitter
4.5	1.69 $\pm$ 0.06	Coppola & Knitter
5.0	1.61 $\pm$ 0.07	Coppola & Knitter
5.5	1.61 $\pm$ 0.05	Coppola & Knitter
14.0	1.58 $\pm$ 0.08	Zamyatnin et al.
14.1	1.44 $\pm$ 0.15	Bertrand & Voignier

values at other energies obtained from a fit to the curve,

$$T_f(E) = A + B[\bar{v}(E) + 1]^{1/2} . \quad (6)$$

This effectively ignores the higher points of Coppola and Knitter in favor of the lower (and older) points of Zamyatnin et al. and Smirenkin.

If the form of Eq. (6) is ignored, the data of Coppola and Knitter and of Zamyatnin can be reconciled by a curve which rises rapidly up to about 4-5 MeV, then flattens out to intersect the error bars in the measurement of Zamyatnin. The recommended curve is shown in Fig. 11.

The energy distribution for pre-fission neutrons from the  $n,n'$  and  $n,2n$  processes is based on the energy distribution for  $n,n'$  neutrons (see Sec. II-H).

#### G. Radiative Capture Cross Section

The radiative capture cross section is determined almost exclusively from measurements of the ratio,  $\alpha$ , with respect to the fission cross sections. This evaluation is based on the measurements of Hopkins and Diven<sup>47</sup> and de Saussure et al.,<sup>48</sup> covering the range above 25 keV. Many measurements have been made in the energy range below 30 keV, the region covered by the resonance parameter representation taken from ENDF/B-III.

The capture cross section was obtained by multiplying pointwise the evaluated curves for  $\alpha$  and

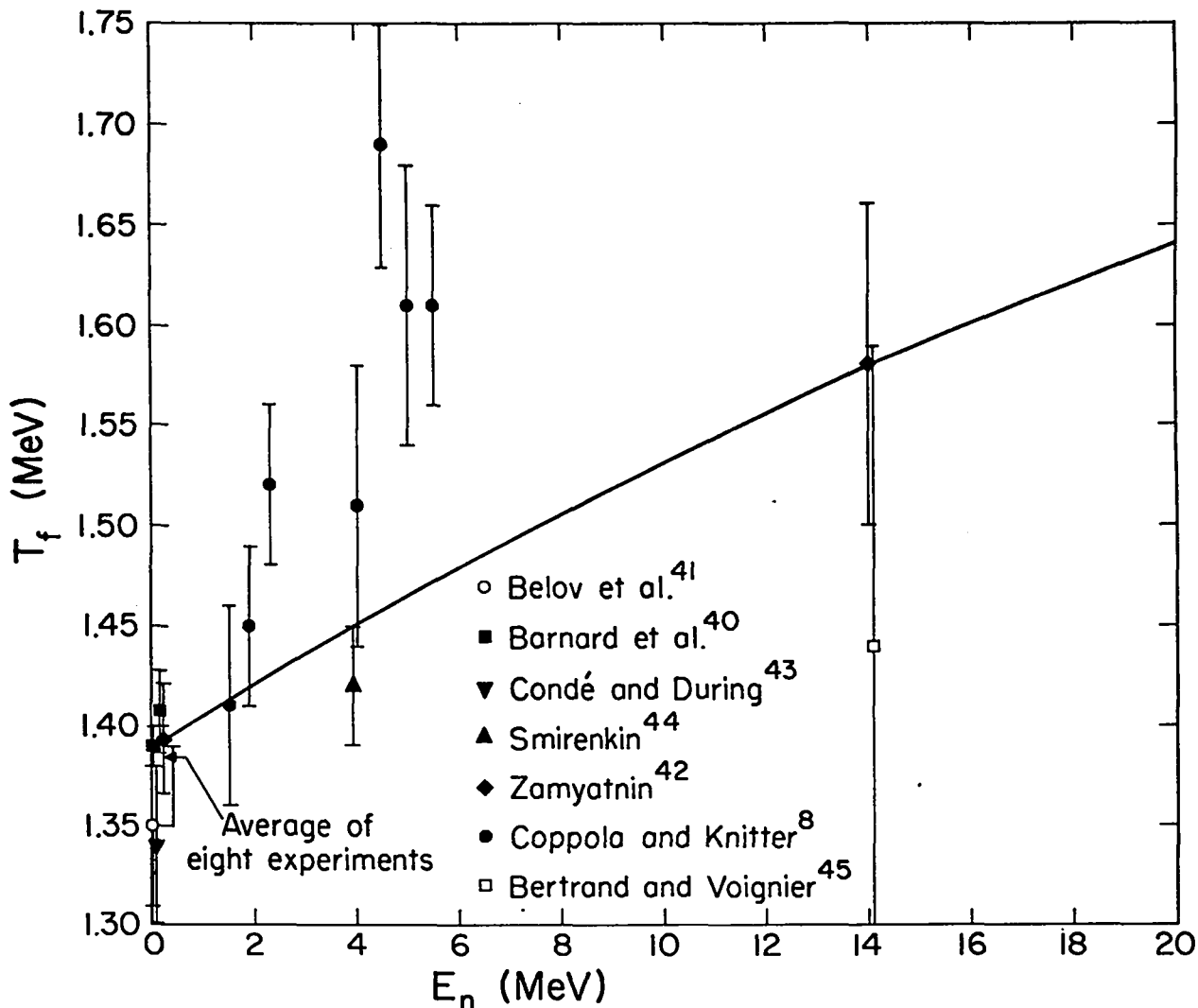


Fig. 11. Fission temperature for  $^{239}\text{Pu}$ .

$\sigma_{n,F}$ . The recommended curves for  $\alpha$  and  $\sigma_{n,\gamma}$  are shown in Figs. 12 and 13, respectively.

#### H. Inelastic Scattering Cross Section

The inelastic scattering cross section at lower energies was obtained by adding the cross sections for exciting the individual energy levels. No measurements of these level cross sections are available, so those curves were specifically drawn to resemble in shape the curve for energy-level cross sections for other nuclides. The general shapes of the total inelastic cross section and the shapes for the low-energy levels, were based roughly on the evaluation of Hunter et al.<sup>49</sup> The energies of the various excited levels were taken from Lederer et al.<sup>50</sup>

Above the 556-keV level, few levels have been identified. Therefore, above this energy a continuum was introduced which was assumed to give the total inelastic curve in a smooth fashion as a function of energy. At 556 keV, the average final-state energy of the inelastically scattered neutrons was calculated, yielding a value of 0.33 MeV. Thus,  $T_i = 0.166$  MeV was used for the continuum energy-distribution function at 556 keV.

The energy-distribution data of Andreev<sup>51</sup> and Cranberg<sup>52</sup> at about 1.2 and 2.0 MeV can be fitted with temperatures of 0.35 and 0.38 MeV, using the distribution function which describes evaporation processes ( $\sigma_{n,n'}$ ,  $2\sigma_{n,2n}$ ,  $3\sigma_{n,3n}$ ,  $\sigma_{n,n'f}$ , and  $2\sigma_{n,2nf}$ ):

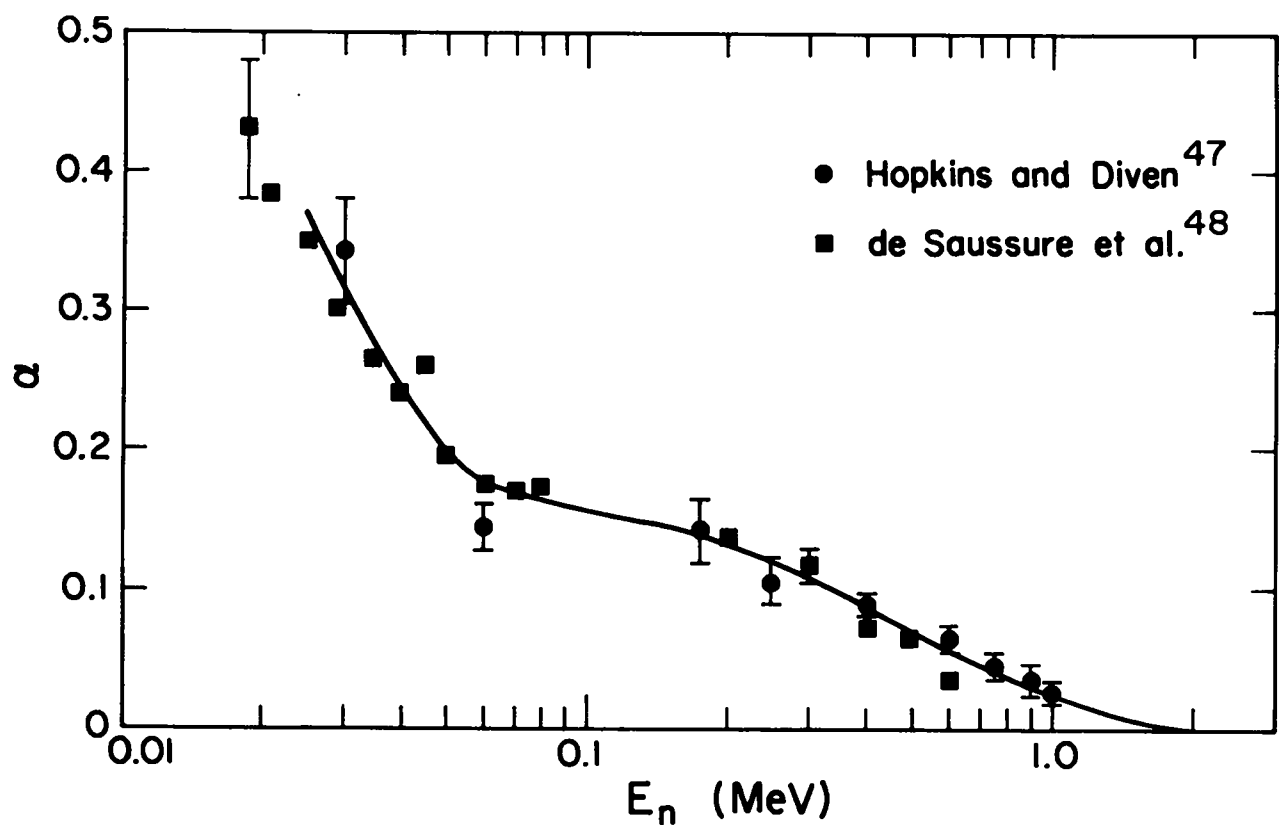


Fig. 12. Ratio of radiative capture cross section to fission cross section ( $\alpha$ ) for  $^{239}\text{Pu}$ .

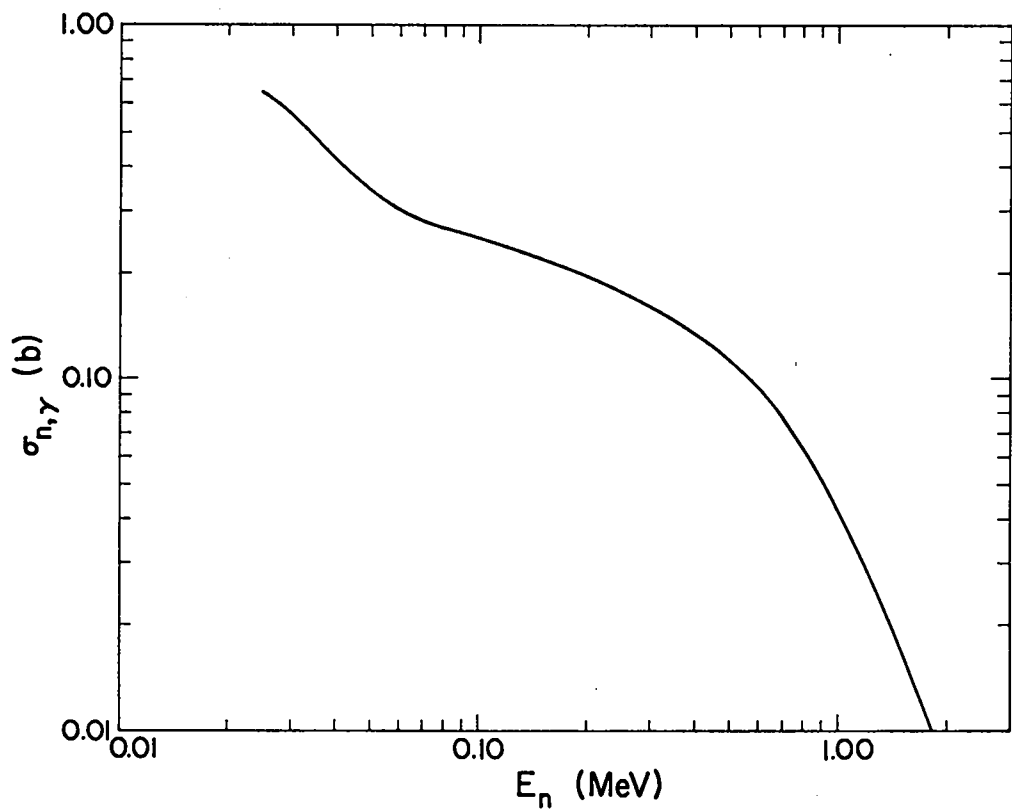


Fig. 13. Radiative capture cross section for  $^{239}\text{Pu}$ .

$$F(E) = NE \exp(-E/T_1) . \quad (7)$$

At an incident-neutron energy of 14 MeV Zamyatnin et al.<sup>42</sup> measured the neutron energy distribution of all secondary neutrons, including  $\sigma_{n,n'}$ ,  $2\sigma_{n,2n}$  and  $3\sigma_{n,3n}$ , as well as  $\bar{v}\sigma_{n,F}$  neutrons. From these measurements, they derived the spectrum of all evaporation neutrons which was then fitted with a temperature of 0.53 MeV. Coppola and Knitter<sup>8</sup> derived the inelastic energy distribution at incident energies of 1.5-5.5 MeV, by subtracting the fission component from their measured spectra. With their data, a curve of  $T_1$  vs  $E_n$  (shown in Fig. 14) was obtained. This energy-dependent temperature was used for all evaporation processes, with appropriate modification in the behavior as each energy threshold is reached.

At high energies, inelastic scattering certainly occurs via direct interaction; that is, the incident neutron collides with a nucleon and is scattered, leaving behind a part of its initial energy. Two features are characteristic of such a process. First, the energy loss of the scattered neutron is small compared to the incident energy. Second, the angular distribution of the scattered neutron is predominantly forward-peaked.

This process is displayed in the data of Kammerdiener<sup>53</sup> who measured the angular distribution of inelastically-scattered neutrons at 14 MeV, using ring geometry. According to the usual representation of fission, these high-energy, forward-peaked neutrons can occur only through direct inelastic scattering.

Five levels were arbitrarily introduced (at 1.0, 1.5, 2.0, 2.5, and 3.0 MeV), with cross sections rising to a total of 200 mb at 14 MeV. Each level is associated with an angular distribution that is forward-peaked.\* With appropriate threshold modifications the cross sections for each level are taken to be the same above a few MeV. The curves for the various individual levels, the continuum, and the total inelastic cross section are given in Figs. 15 and 16.

#### I. $\sigma_{n,2n}$ and $\sigma_{n,3n}$

These cross sections are based largely on the evaluation<sup>\*\*</sup> of Hunter et al.,<sup>49</sup> with thresholds

\* See Sec. II-J.

\*\* The final-state energy distribution would perhaps be more physically represented by a different temperature representation for successive neutron emission. This will be taken into account in future evaluations.

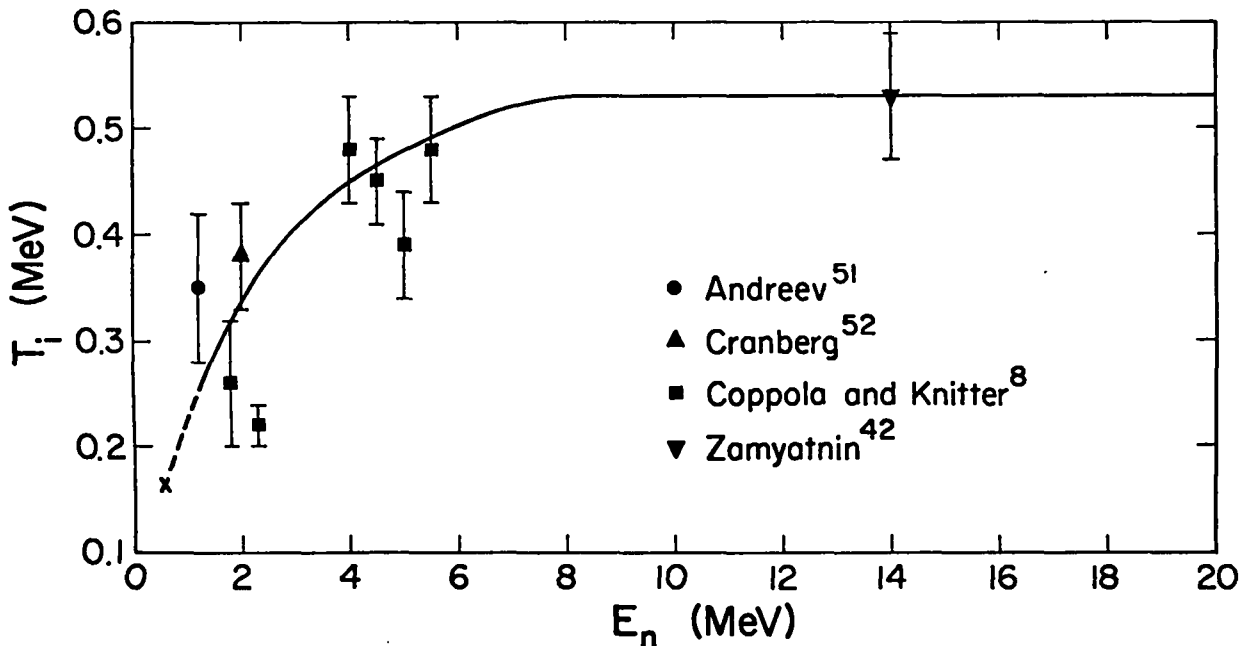


Fig. 14. Inelastic-scattering energy-dependent temperature for  $^{239}\text{Pu}$ .

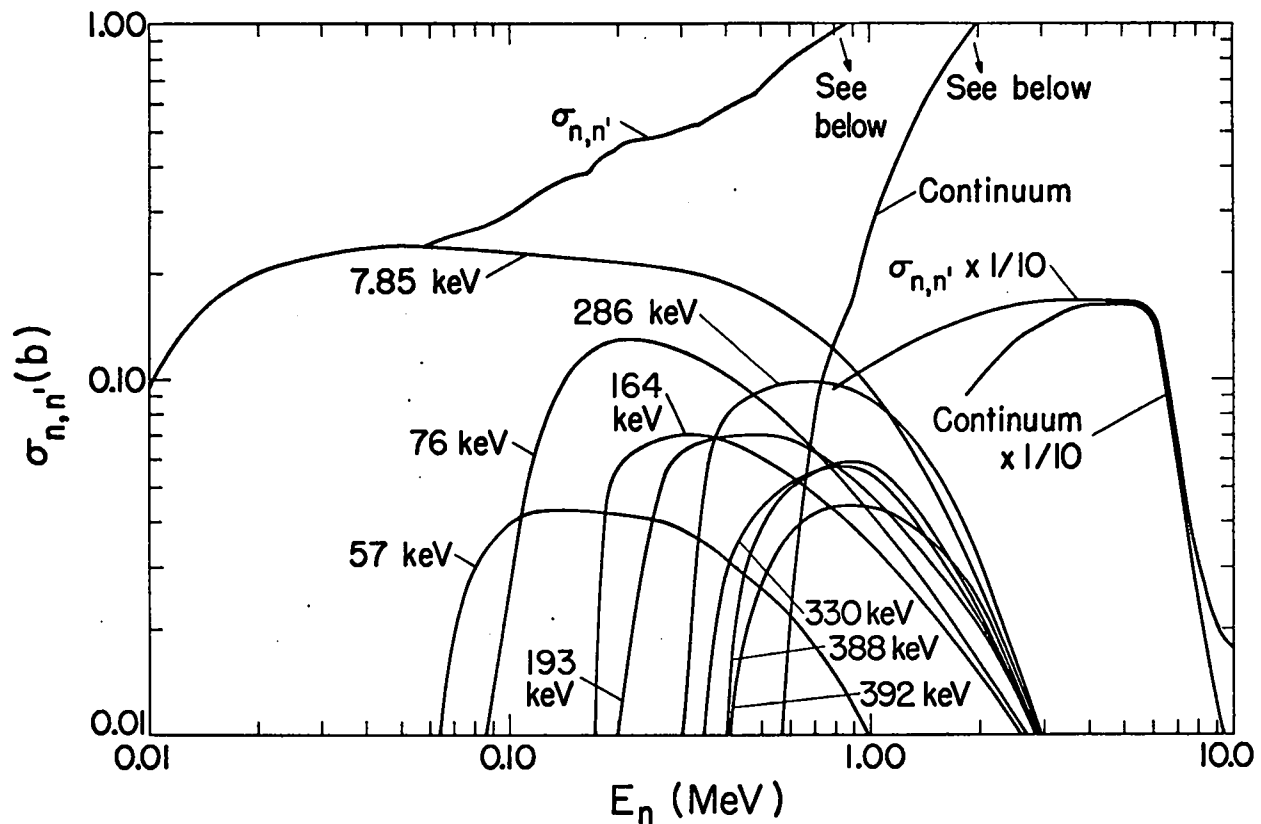


Fig. 15. Inelastic-scattering cross section and continuum cross section, and energy-level cross sections for  $^{239}\text{Pu}$ .

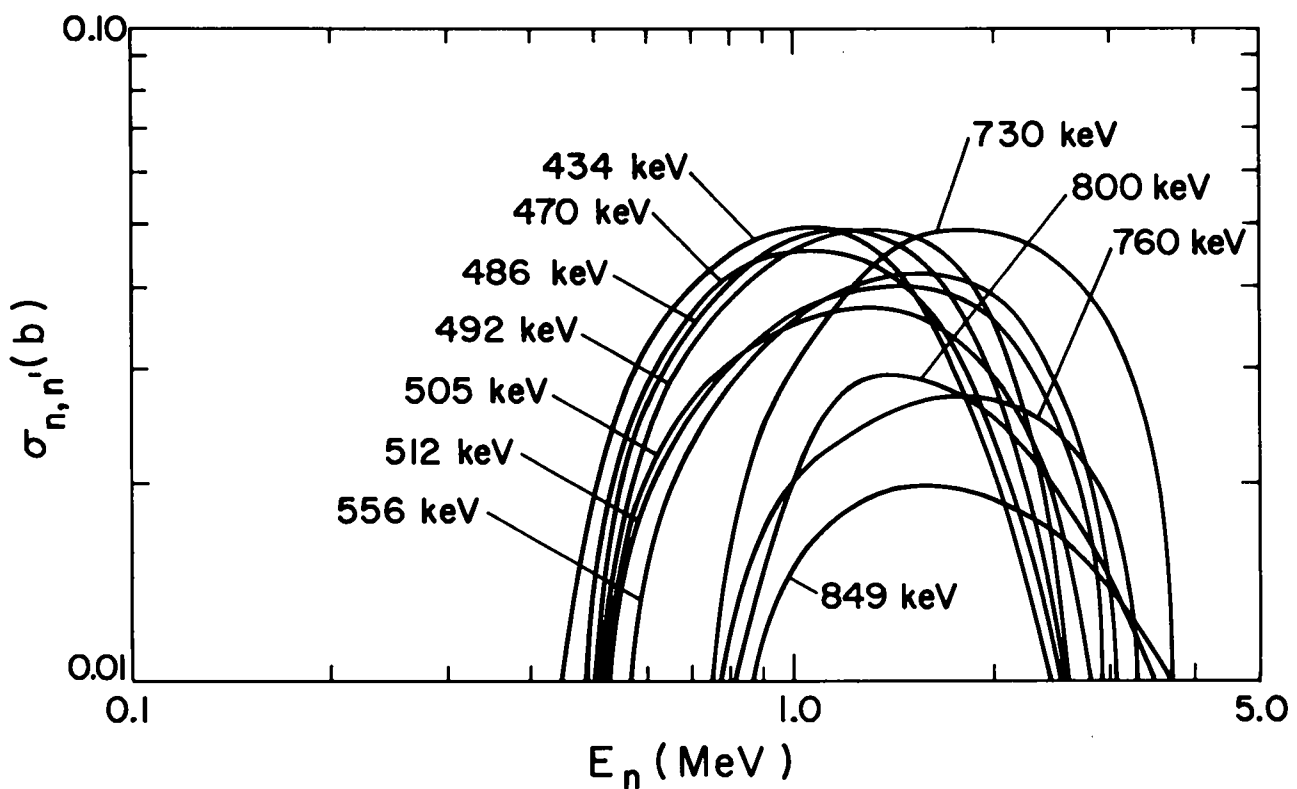


Fig. 16. Energy-level cross sections for  $^{239}\text{Pu}$ .

obtained from Wapstra and Gove.<sup>54</sup> The higher-energy end of  $\sigma_{n,2n}$  was based on calculations by Whalen and Worlton.<sup>55</sup> The recommended curves<sup>\*</sup> are given in Fig. 17.

#### J. Angular Distributions

The elastic-scattering angular distribution for  $^{239}\text{Pu}$  has been measured by Knitter and Coppola,<sup>7</sup> Coppola and Knitter,<sup>8</sup> Allen et al.,<sup>9</sup> Cranberg,<sup>52</sup> and Kammerdiener.<sup>53</sup> These distributions were fitted by the Legendre expansion,

$$\frac{d\sigma}{d\Omega}(E_n, \theta) = \frac{\sigma_{n,n}(E_n)}{2\pi} \sum_{\ell=0}^L \left[ \frac{2\ell+1}{2} a_\ell(E_n) P_\ell(\cos \theta) \right] , \quad (8)$$

where  $\sigma_{n,n}$  is the elastic-scattering cross section and  $P_\ell(\cos \theta)$  is the  $\ell$ th Legendre polynomial,  $a_0(E_n) \equiv 1.0$ . The value of  $L$  is determined at each energy by the fit to experimental data, subject to the constraints that  $L$  must be even, and the energy-dependent coefficients must extrapolate smoothly over the energy range. The angular distributions at energies between 0.19 and 14 MeV are shown in Figs. 18-35. The graphs of the Legendre coefficients as a function of  $E_n$  are given in Figs. 36-39. No attempt was made to remove inelastic contributions from the experimental data.

The Legendre coefficients plotted in Figs. 36-39 were obtained from the initial best fits to the experimental data in Figs. 18-35. These points were then fit with a smooth curve, yielding the final recommended set of Legendre coefficients.

\*The  $n,2n$  and  $n,3n$  measurements of Mather et al. (D. S. Mather, P. F. Bampton, R. E. Coles, G. James, and P. J. Nind, "Measurement of  $(n,2n)$  Cross Sections for Incident Energies Between 6 and 14 MeV," Atomic Weapons Research Establishment report AWRE O 72/72 and EANDC (UK) 142-AL, November 1972) were received about the time this evaluation was completed. These measurements do not agree with this evaluation. Since their data on  $^{238}\text{U}$  indicate serious discrepancies both in shape and magnitude with earlier experiments, it was decided that these data would not be incorporated in the present evaluation. Furthermore, the  $^{239}\text{Pu}$  measurements were not borne out by integral calculations of Whalen and Worlton, which were factors of two to three lower for  $\sigma_{n,2n}$ .

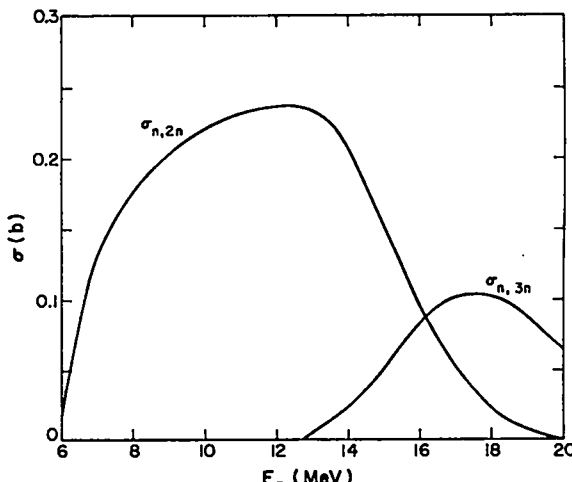


Fig. 17.  $\sigma_{n,2n}$  and  $\sigma_{n,3n}$  for  $^{239}\text{Pu}$ .

These coefficients were used in turn to calculate the angular distributions which are plotted in Figs. 18-35. Thus, the curves shown in Figs. 18-35 are the final recommended angular distributions, not the initial best fits to the experimental data.

The inelastic angular distributions for the constructed direct-interaction levels were based on the elastic distributions at energies below about 2 MeV.

The curves of the Legendre coefficients for the direct-interaction levels as a function of  $E_n$  are shown in Fig. 40.

#### K. Charged-Particle Cross Sections

Cross sections for the  $n,\alpha$ ;  $n,t$ ;  $n,p$ ; and  $n,d$  reactions are taken directly from the ENDF/B-III evaluation. The curves are shown in Fig. 41.

#### L. Tabulated Cross Sections

The recommended cross sections are tabulated in Table II. The tabulated values for the various inelastic levels are given in Table III.

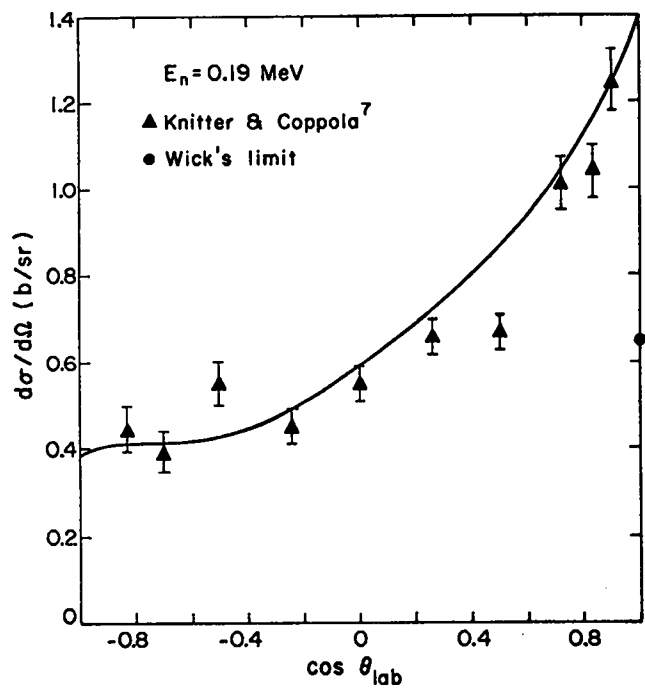


Fig. 18

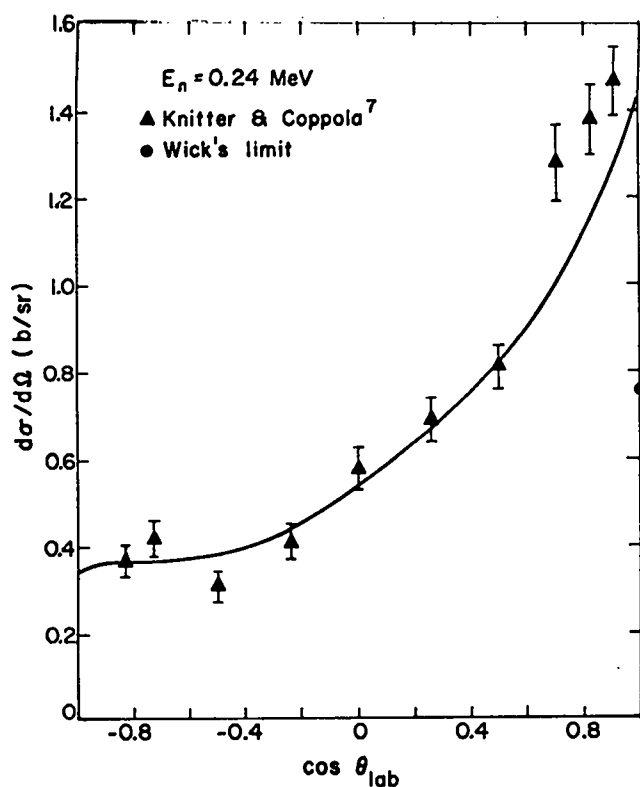


Fig. 19

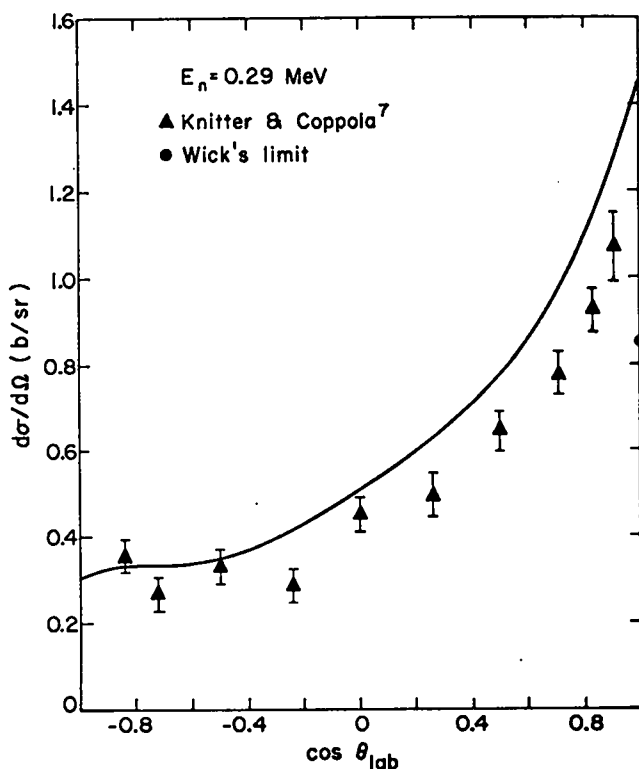


Fig. 20

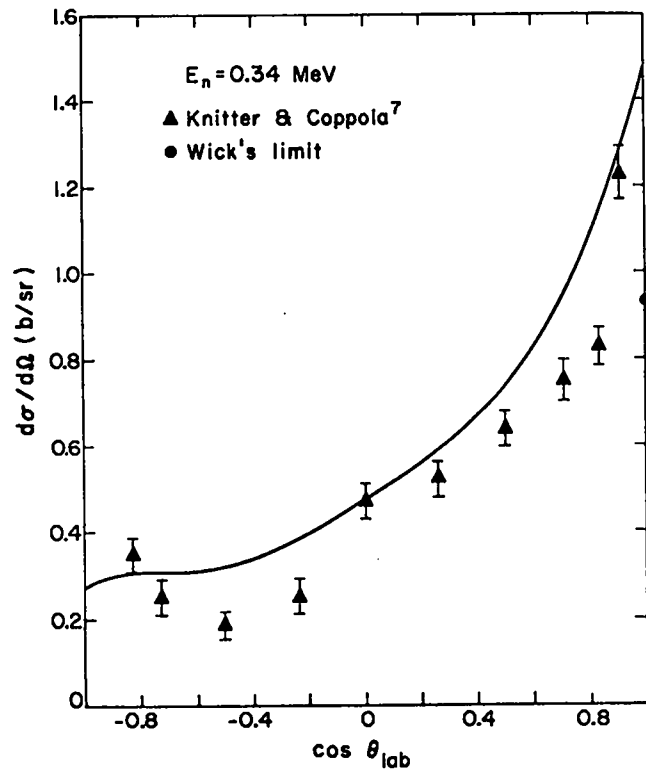


Fig. 21

Figs. 18-21. Elastic-scattering angular distribution for  $^{239}\text{Pu}$  at 0.19, 0.24, 0.29, and 0.34 MeV, respectively.

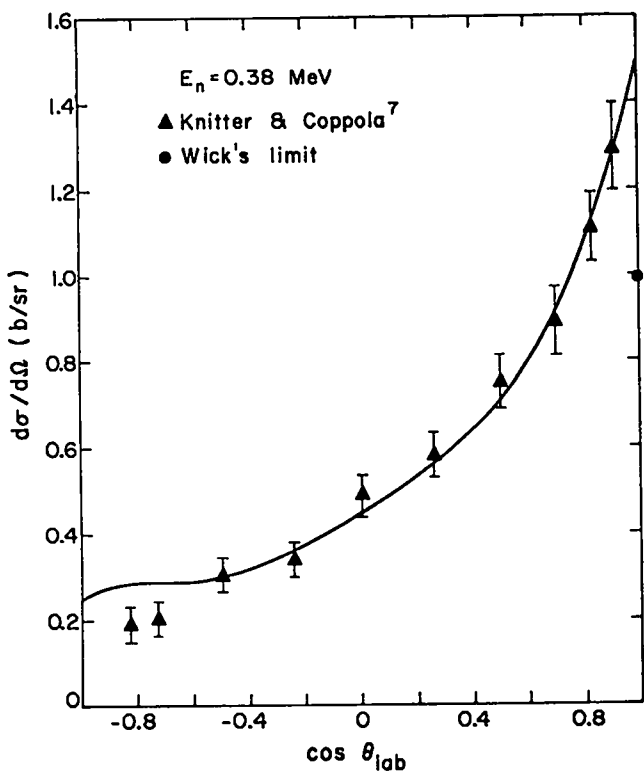


Fig. 22

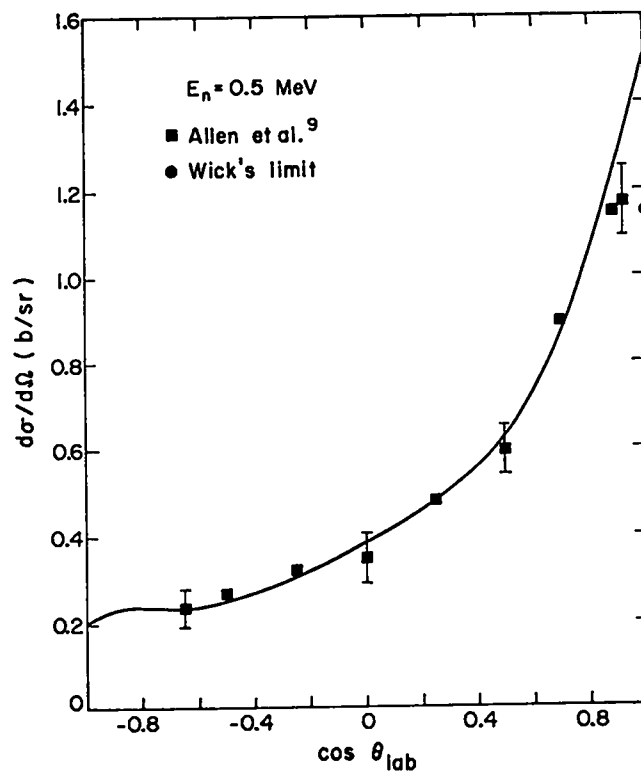


Fig. 23

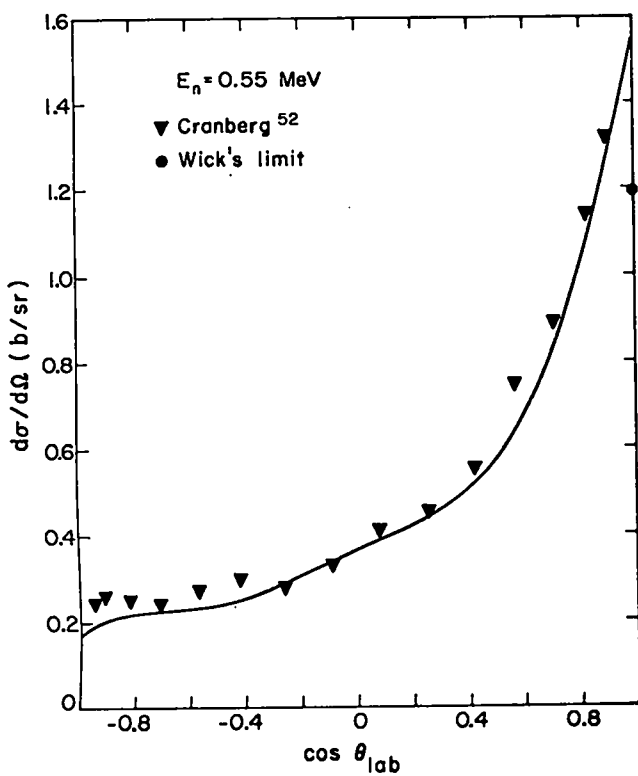


Fig. 24

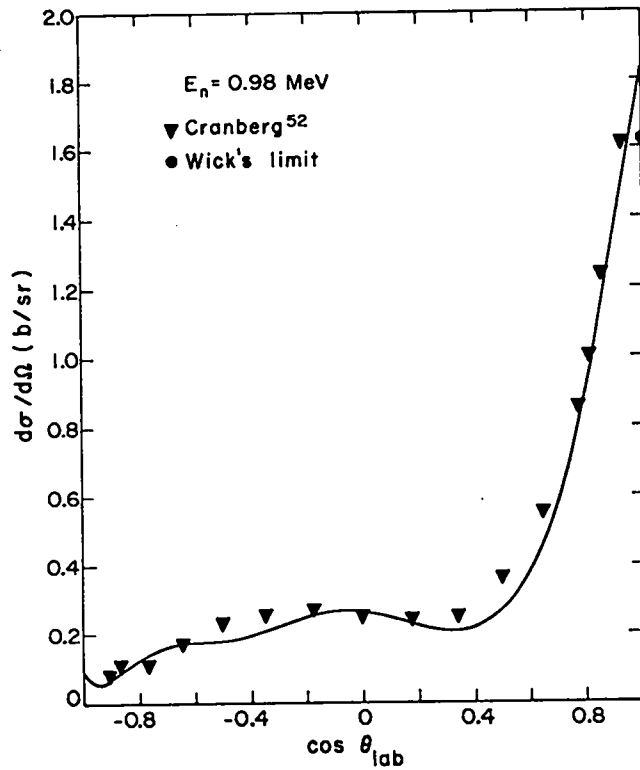


Fig. 25

Figs. 22-25. Elastic-scattering angular distribution for  $^{239}\text{Pu}$  at 0.38, 0.5, 0.55, and 0.98 MeV, respectively.

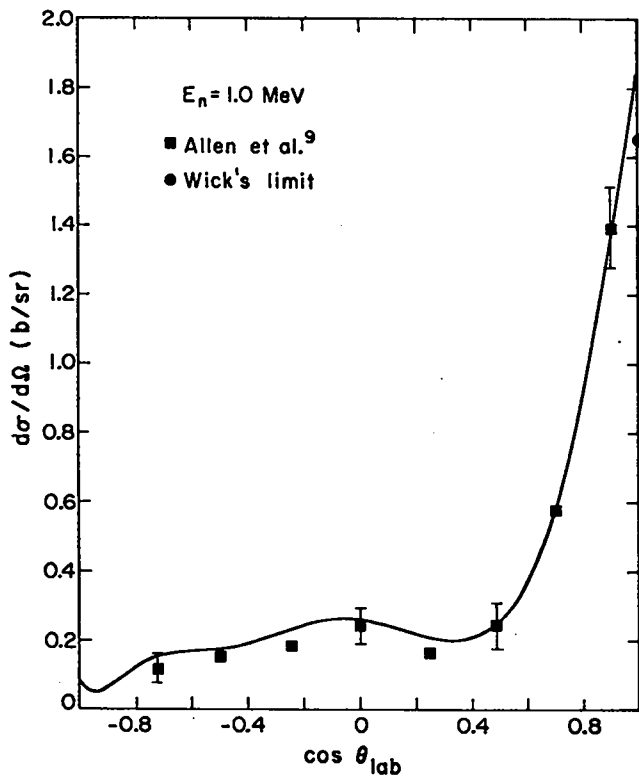


Fig. 26

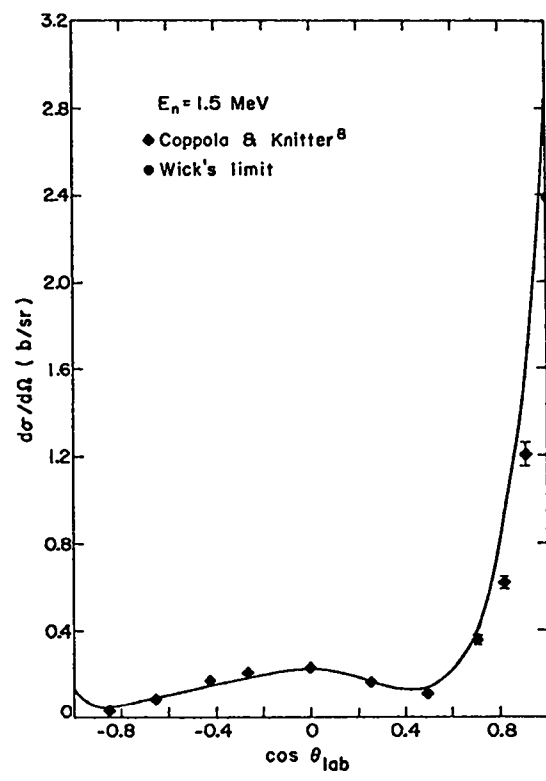


Fig. 27

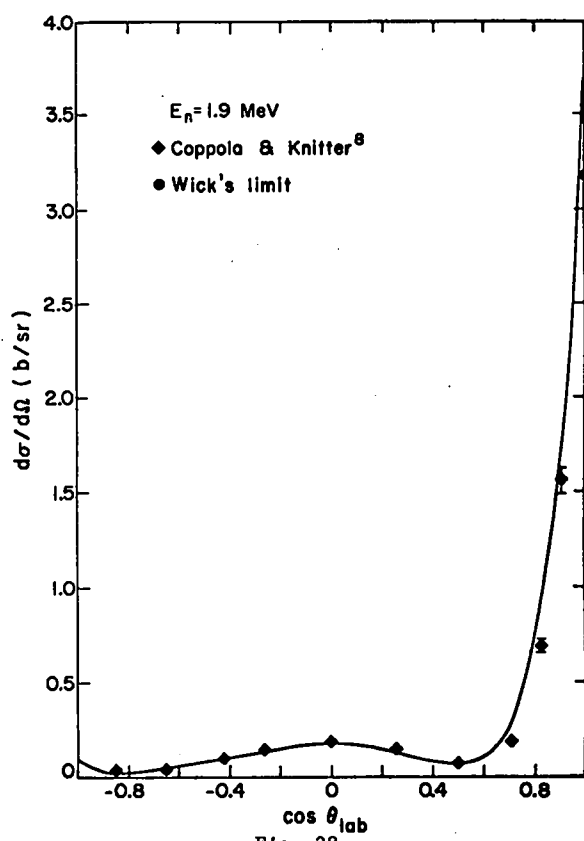


Fig. 28

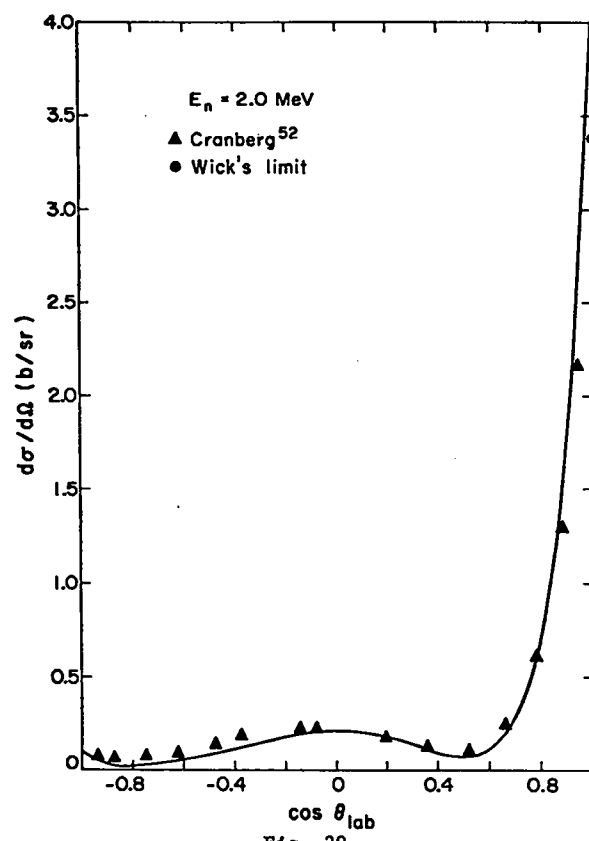


Fig. 29

Figs. 26-29. Elastic-scattering angular distribution for  $^{239}\text{Pu}$  at 1.0, 1.5, 1.9, and 2.0 MeV, respectively.

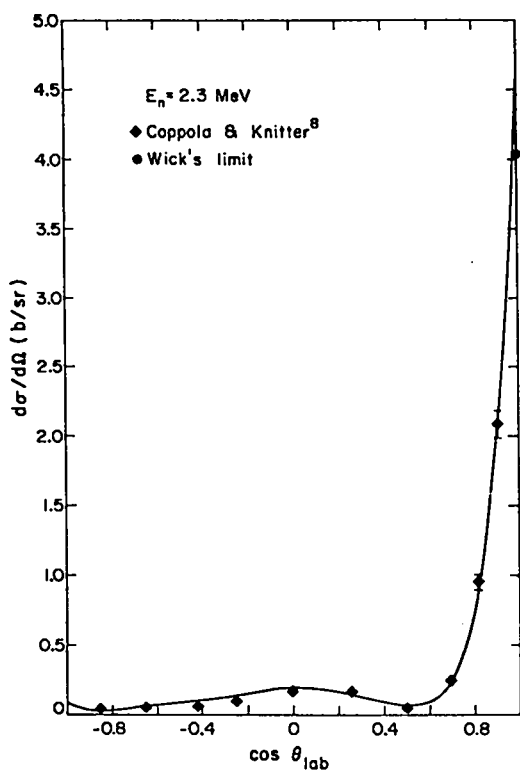


Fig. 30

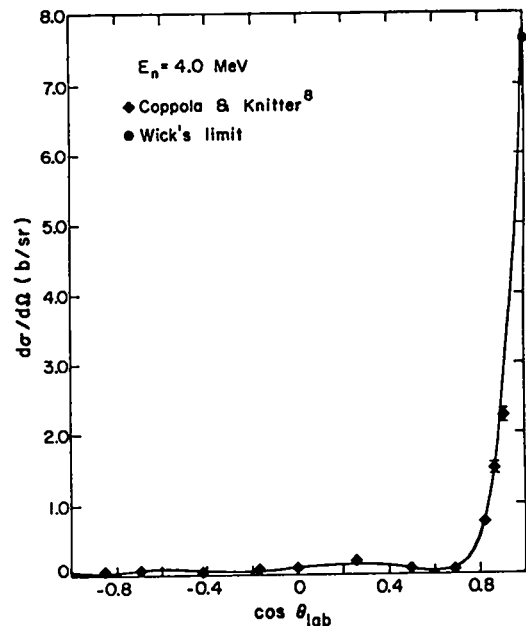


Fig. 31

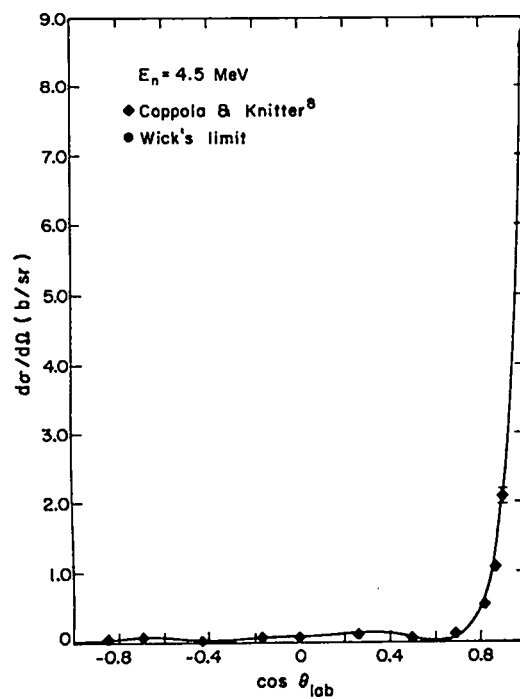


Fig. 32

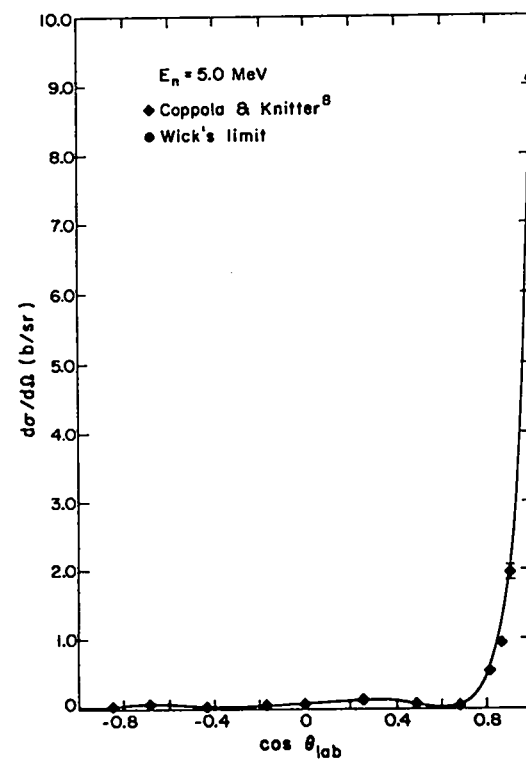


Fig. 33

Figs. 30-33. Elastic-scattering angular distribution for  $^{239}\text{Pu}$  at 2.3, 4.0, 4.5, and 5.0 MeV, respectively.

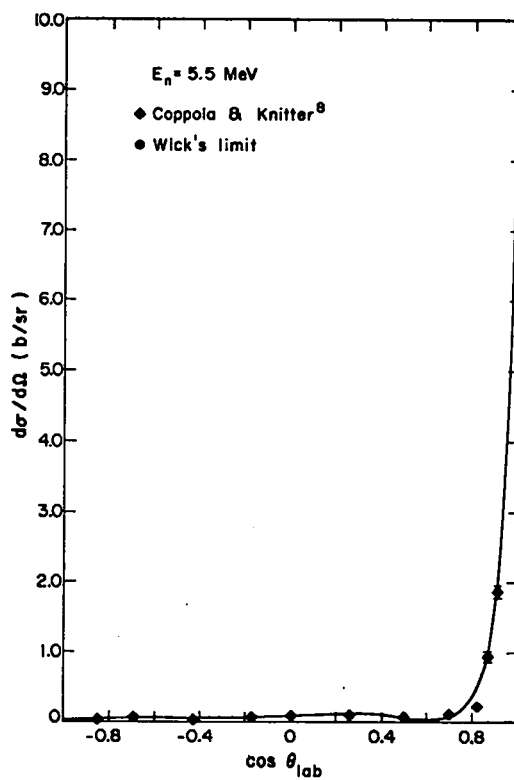


Fig. 34. Elastic-scattering angular distribution for  $^{239}\text{Pu}$  at 5.5 MeV.

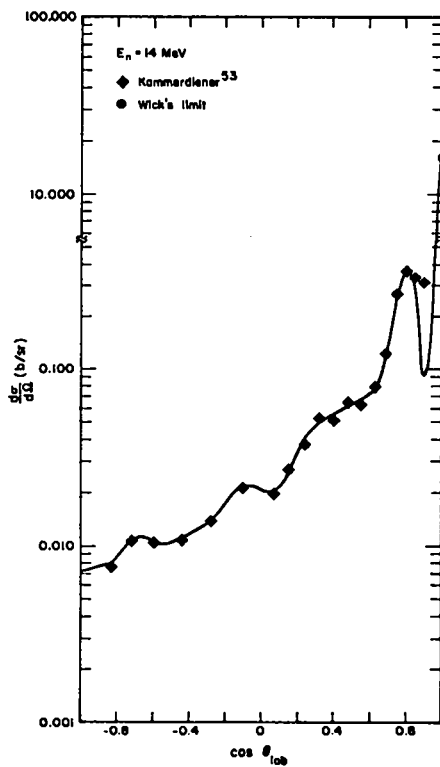


Fig. 35. Elastic-scattering angular distribution for  $^{239}\text{Pu}$  at 14 MeV.

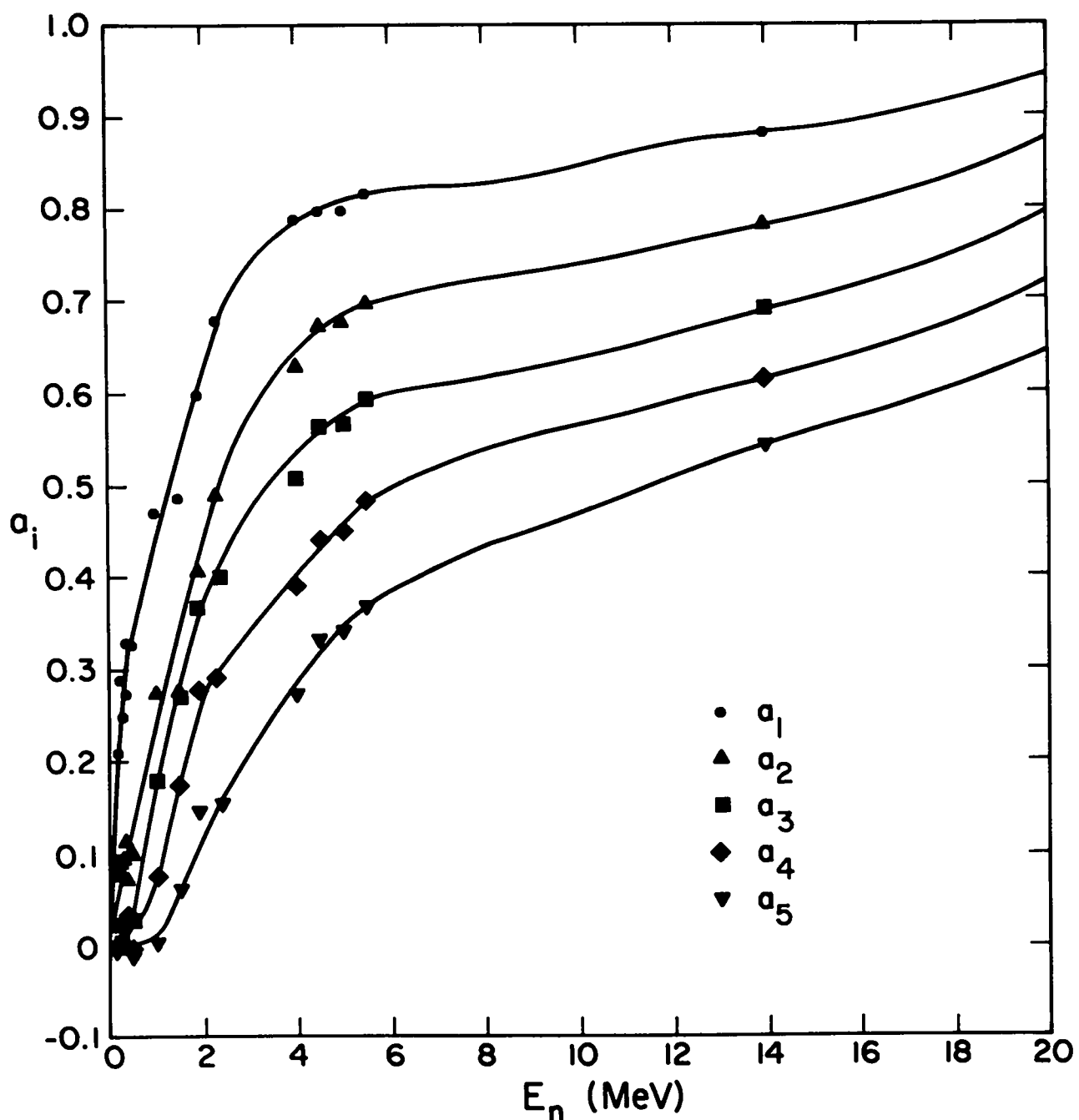


Fig. 36. Legendre polynomial coefficients for elastic-scattering angular distributions for  $^{239}\text{Pu}$ .

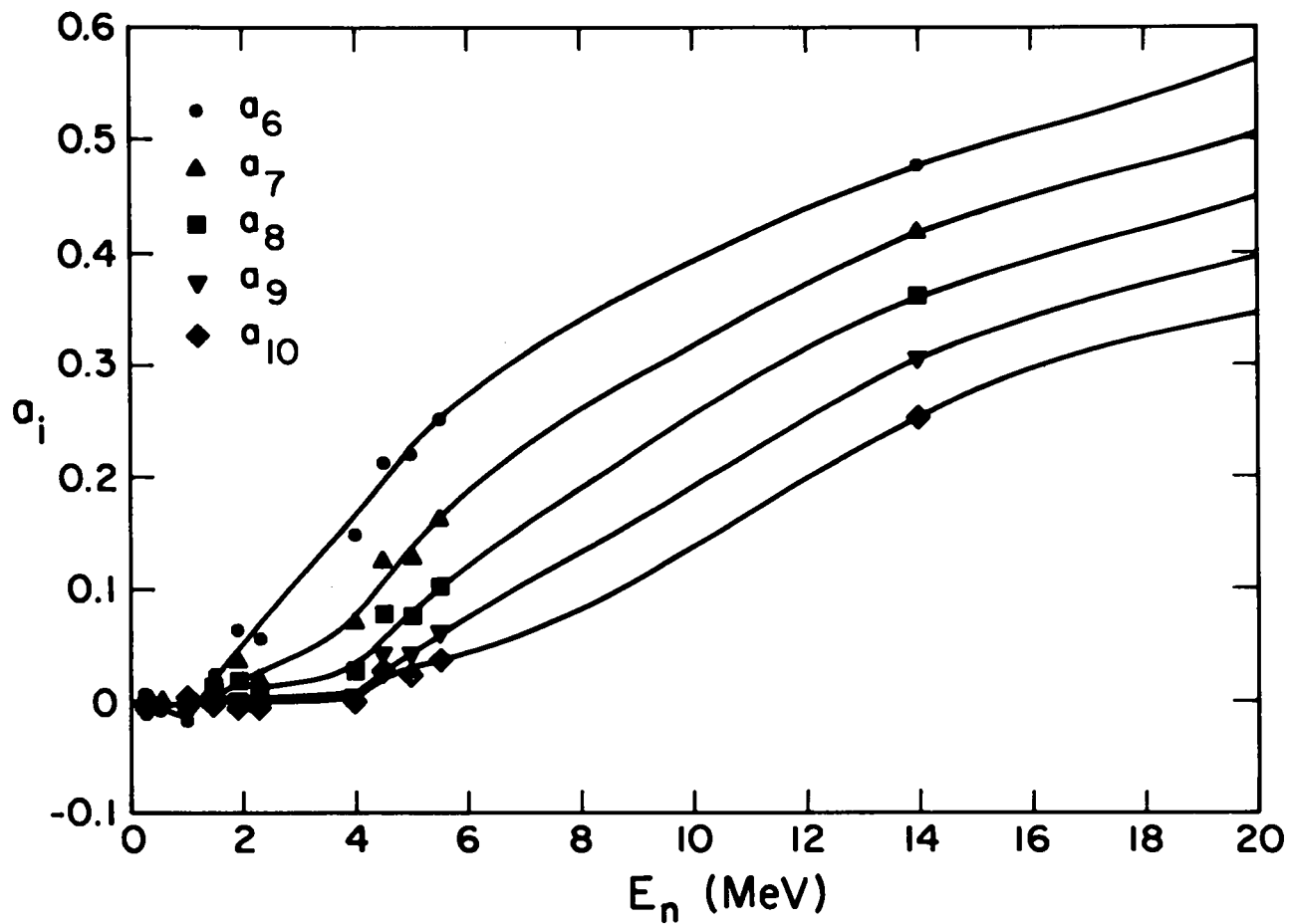


Fig. 37. Legendre Polynomial coefficients for elastic-scattering angular distributions for  $^{239}\text{Pu}$ .

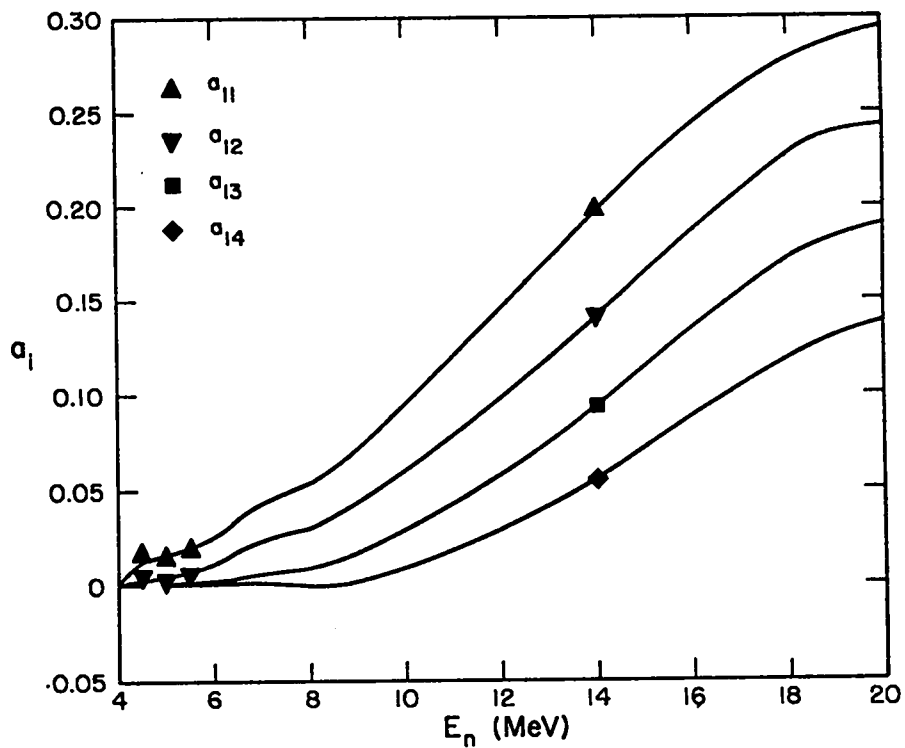


Fig. 38. Legendre polynomial coefficients for elastic-scattering angular distributions for  $^{239}\text{Pu}$ .

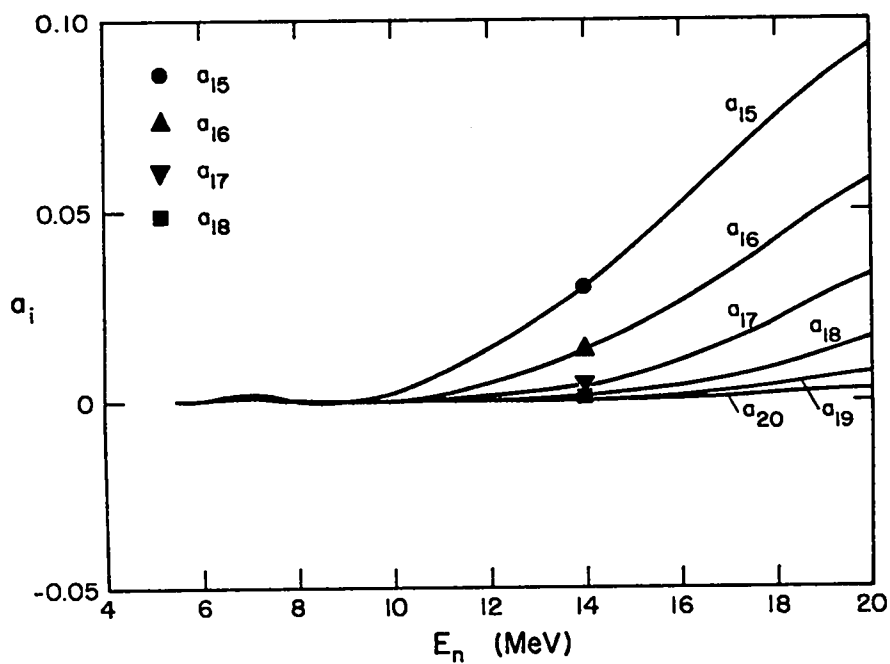


Fig. 39. Legendre polynomial coefficients for elastic-scattering angular distributions for  $^{239}\text{Pu}$ .

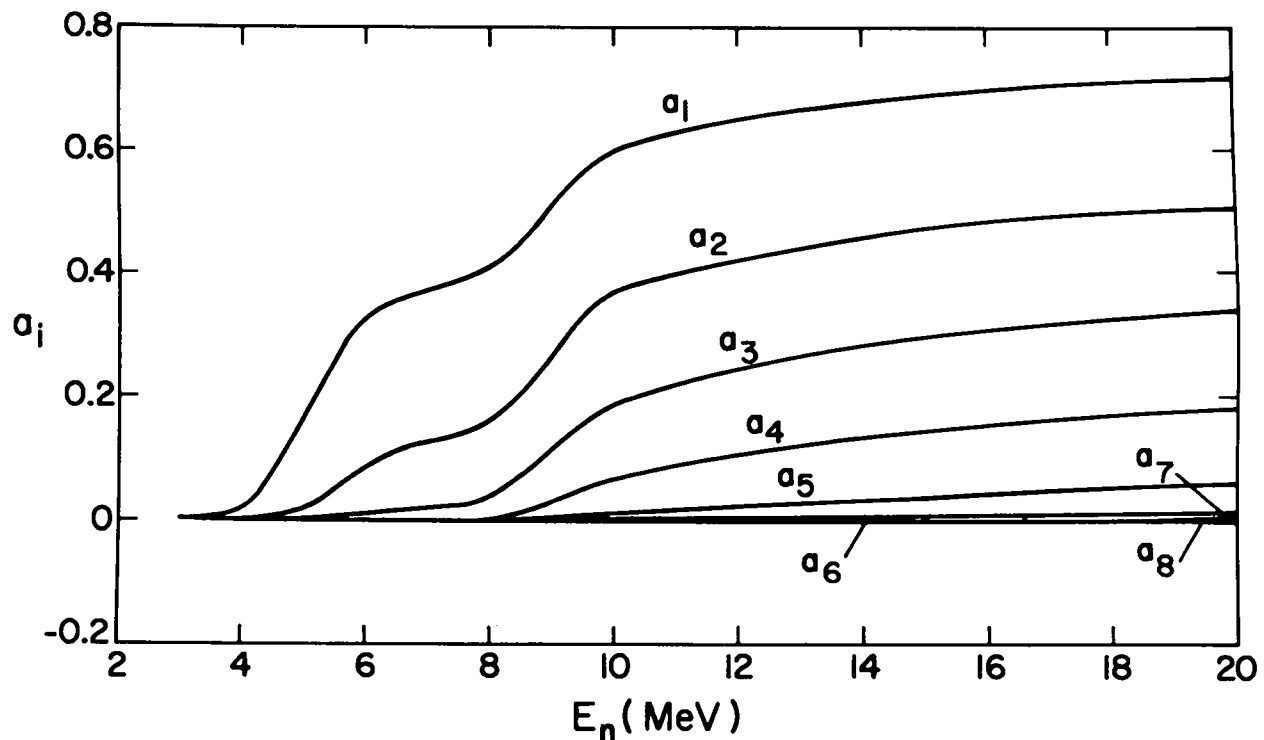


Fig. 40. Legendre polynomial coefficients for direct-interaction inelastic-scattering angular distributions for  $^{239}\text{Pu}$ .

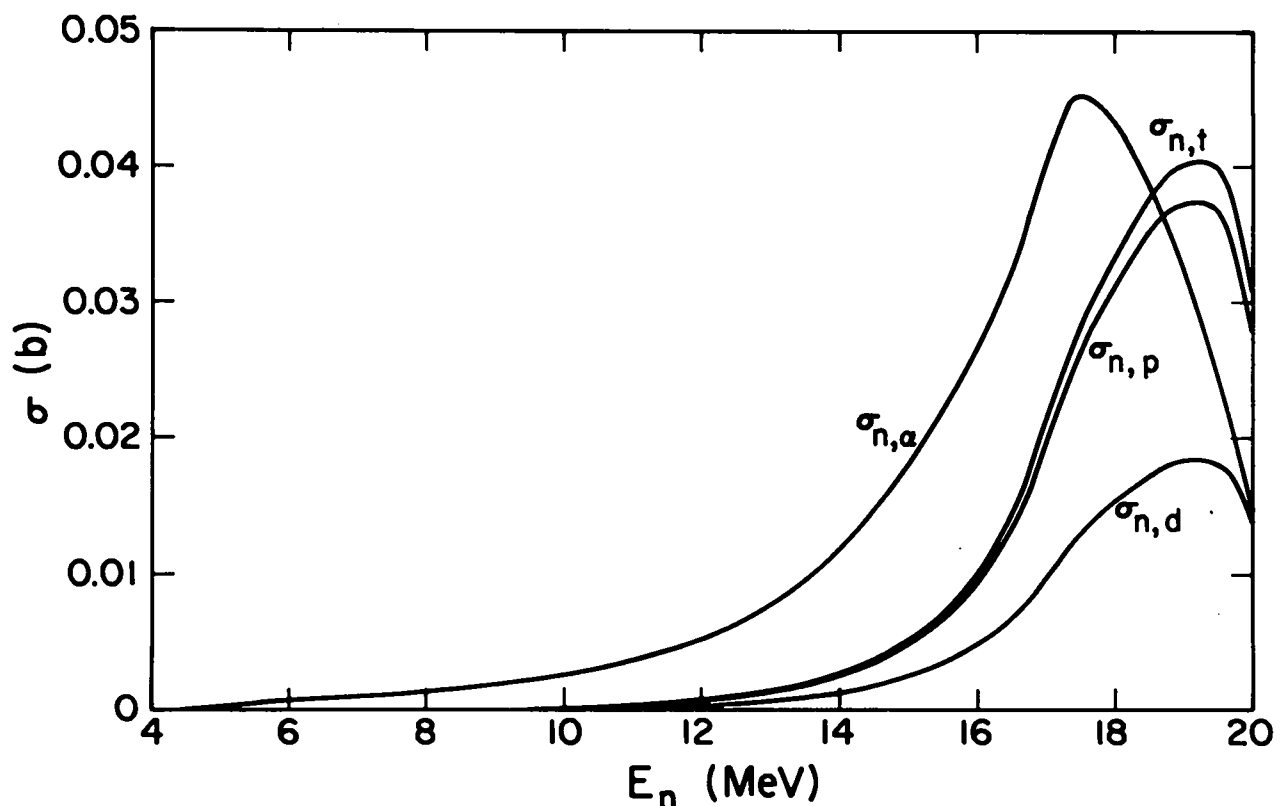


Fig. 41.  $\sigma_{n,\alpha}$ ,  $\sigma_{n,t}$ ,  $\sigma_{n,d}$ , and  $\sigma_{n,p}$  for  $^{239}\text{Pu}$ .

TABLE II  
NEUTRON CROSS SECTIONS FOR Pu-239 (IN BARNS)

<u>E(MeV)</u>	<u><math>\sigma_{n,T}</math></u>	<u><math>\sigma_{n,n}</math></u>	<u><math>\sigma_{n,Y}</math></u>	<u><math>\sigma_{n,F}</math></u>	<u><math>\sigma_{n,n'}</math></u>	<u><math>\sigma_{n,2n}</math></u>	<u><math>\sigma_{n,3n}</math></u>	<u><math>\sigma_{n,f}</math></u>	<u><math>\sigma_{n,n'f}</math></u>	<u><math>\sigma_{n,2nf}</math></u>	<u><math>\sigma_{n,a}</math></u>	<u><math>\sigma_{n,p}</math></u>	<u><math>\sigma_{n,d}</math></u>	<u><math>\sigma_{n,t}</math></u>
0.007883					0.000									
0.0080					0.005									
0.0085					0.027									
0.0090					0.056									
0.0095					0.082									
0.010					0.095									
0.011					0.116									
0.012					0.130									
0.013					0.142									
0.014					0.155									
0.015					0.165									
0.016					0.176									
0.017					0.184									
0.018					0.192									
0.019					0.197									
0.020					0.202									
0.025	13.820	11.216	0.645	1.743	0.216									
0.030	13.640	11.105	0.560	1.750	0.225									
0.035	13.470	11.006	0.484	1.748	0.232									
0.040	13.320	10.950	0.417	1.716	0.237									
0.045	13.170	10.852	0.371	1.708	0.239									
0.050	13.040	10.758	0.339	1.703	0.240									
0.055	12.900	10.633	0.318	1.709	0.240									
0.057239	12.849	10.589	0.311	1.709	0.240									
0.060	12.780	10.524	0.304	1.708	0.244									
0.070	12.530	10.335	0.282	1.656	0.257									
0.076319	12.383	10.199	0.274	1.648	0.262									
0.080	12.300	10.123	0.269	1.642	0.266									
0.090	12.090	9.914	0.261	1.634	0.281									
0.100	11.890	9.728	0.252	1.614	0.296									
0.110	11.733	9.582	0.246	1.589	0.316									
0.120	11.540	9.399	0.241	1.564	0.336									
0.130	11.380	9.241	0.233	1.555	0.351									
0.140	11.240	9.106	0.227	1.542	0.365									
0.150	11.095	8.965	0.221	1.534	0.375									
0.160	10.980	8.859	0.217	1.522	0.382									
0.164689	10.920	8.805	0.214	1.518	0.383									
0.170	10.838	8.720	0.212	1.511	0.395									
0.180	10.740	8.611	0.206	1.502	0.421									
0.193811	10.592	8.454	0.200	1.495	0.443									
0.200	10.530	8.388	0.197	1.489	0.456									
0.250	10.080	7.924	0.179	1.495	0.482									
0.287201	9.805	7.632	0.166	1.506	0.501									
0.300	9.720	7.535	0.162	1.514	0.509									
0.331386	9.513	7.304	0.154	1.534	0.521									
0.389630	9.182	6.914	0.138	1.560	0.570									
0.393646	9.163	6.892	0.136	1.561	0.574									
0.400	9.130	6.854	0.134	1.562	0.580									
0.435823	8.981	6.678	0.126	1.570	0.607									
0.471974	8.780	6.457	0.117	1.578	0.628									
0.488041	8.720	6.383	0.114	1.579	0.644									
0.494066	8.707	6.362	0.113	1.580	0.652									
0.500	8.655	6.298	0.112	1.581	0.664									
0.507121	8.600	6.238	0.111	1.582	0.669									
0.514150	8.565	6.190	0.109	1.583	0.683									
0.558335	8.406	5.981	0.101	1.592	0.732									
0.600	8.258	5.774	0.093	1.603	0.788									
0.650	8.085	5.553	0.084	1.618	0.830									
0.700	7.927	5.334	0.077	1.641	0.875									
0.733051	7.860	5.223	0.073	1.664	0.900									
0.763177	7.765	5.086	0.070	1.679	0.930									
0.803344	7.690	4.977	0.066	1.687	0.960									
0.852549	7.590	4.840	0.060	1.697	0.993									
0.900	7.500	4.717	0.053	1.700	1.030									
0.950	7.420	4.599	0.048	1.703	1.070									

TABLE II (Cont'd)

E(MeV)	$\sigma_{n,T}$	$\sigma_{n,n}$	$\sigma_{n,\gamma}$	$\sigma_{n,F}$	$\sigma_{n,n'}$	$\sigma_{n,2n}$	$\sigma_{n,3n}$	$\sigma_{n,f}$	$\sigma_{n,n'f}$	$\sigma_{n,2nf}$	$\sigma_{n,a}$	$\sigma_{n,p}$	$\sigma_{n,d}$	$\sigma_{n,t}$
1.00418	7.350	4.492	0.043	1.705	1.110									
1.2	7.230	4.245	0.028	1.729	1.228									
1.4	7.220	4.077	0.020	1.801	1.322									
1.50627	7.240	4.000	0.0167	1.860	1.3633									
1.6	7.260	3.955	0.014	1.885	1.406									
1.8	7.340	3.942	0.010	1.925	1.463									
2.00836	7.450	3.979	0.006	1.950	1.515									
2.25	7.560	4.027	0.002	1.960	1.571									
2.51045	7.680	4.144	0.000	1.920	1.616									
2.75	7.795	4.287	-	1.866	1.642									
3.01254	7.895	4.379	-	1.860	1.656									
3.25	7.982	4.488	-	1.834	1.660									
3.50	8.018	4.551	-	1.806	1.661									
3.75	8.040	4.592	-	1.787	1.661									
4.00	8.017	4.587	-	1.769	1.661									
4.25	7.985	4.571	-	1.753	1.661									
4.50	7.900	4.491	-	1.748	1.661									
4.75	7.833	4.431	-	1.741	1.661									
5.00	7.7221	4.325	-	1.736	1.661									
5.25	7.5933	4.206	-	1.733	1.654									
5.50	7.5125	4.141	-	1.730	1.641				1.730	0.00		0.0005		
5.67965	7.4336	4.092	-	1.731	1.610	0.000			1.730	0.001		0.0006		
5.75	7.4137	4.079	-	1.735	1.597	0.002			1.730	0.005		0.0007		
6.00	7.3017	4.017	-	1.768	1.501	0.015			1.730	0.038		0.0007		
6.25	7.0908	3.957	-	1.837	1.250	0.046			1.730	0.107		0.0008		
6.50	6.9408	3.910	-	1.930	1.020	0.080			1.730	0.200		0.0008		
6.75	6.8549	3.890	-	2.013	0.841	0.110			1.730	0.283		0.0009		
7.00	6.7629	3.842	-	2.090	0.700	0.130			1.730	0.360		0.0009		
7.5	6.4811	3.724	-	2.190	0.410	0.156			1.730	0.460		0.0011		
8.0	6.3523	3.606	-	2.263	0.307	0.175			1.730	0.533		0.0013		
8.5	6.2559	3.5064	-	2.319	0.239	0.190			1.730	0.589		0.0015		
9.0	6.1059	3.3521	-	2.349	0.200	0.203			1.730	0.619		0.0018		
9.5	6.0196	3.2615	-	2.360	0.183	0.213			1.730	0.630		0.0021	0.00	0.00
10.0	5.9608	3.1980	-	2.363	0.176	0.221			1.730	0.633		0.0025	0.0001	0.0002
10.5	5.8824	3.1149	-	2.363	0.174	0.227			1.730	0.633	0.000	0.0030	0.0002	0.00
11.0	5.8524	3.0710	-	2.367	0.178	0.232	-		1.730	0.633	0.004	0.0036	0.0003	0.0001
11.5	5.8431	3.0356	-	2.384	0.183	0.235	-		1.730	0.633	0.021	0.0043	0.0005	0.0002
12.0	5.8333	2.9764	-	2.422	0.191	0.237	-		1.730	0.633	0.059	0.0052	0.0007	0.0003
12.5	5.8420	2.9393	-	2.454	0.202	0.238	-		1.730	0.633	0.091	0.0063	0.0009	0.0010
12.7069	5.8580	2.9421	-	2.463	0.206	0.237	0.0		1.730	0.633	0.100	0.0070	0.0011	0.0006
13.0	5.8922	2.9471	-	2.482	0.213	0.234	0.005	1.730	0.633	0.119	0.0077	0.0013	0.0007	0.0014
13.5	5.9562	2.9781	-	2.503	0.221	0.226	0.014	1.730	0.633	0.140	0.0095	0.0018	0.0009	0.0019
14.0	5.9981	2.9990	-	2.529	0.225	0.205	0.022	1.730	0.633	0.166	0.0117	0.0025	0.0013	0.0026
14.5	6.0310	3.0155	-	2.553	0.223	0.180	0.036	1.730	0.633	0.190	0.0145	0.0035	0.0018	0.0037
15.0	6.0700	3.0356	-	2.580	0.221	0.152	0.051	1.730	0.633	0.217	0.0179	0.0049	0.0025	0.0051
15.5	6.1050	3.0577	-	2.597	0.219	0.124	0.068	1.730	0.633	0.234	0.0220	0.0068	0.0034	0.0071
16.0	6.1300	3.0802	-	2.603	0.218	0.095	0.083	1.730	0.633	0.240	0.0267	0.0094	0.0048	0.0099
16.5	6.1600	3.1027	-	2.608	0.2165	0.072	0.095	1.730	0.633	0.245	0.0322	0.0131	0.0066	0.0139
17.0	6.1900	3.1176	-	2.613	0.215	0.052	0.102	1.730	0.633	0.250	0.0403	0.0195	0.0097	0.0209
17.5	6.2150	3.1243	-	2.624	0.214	0.036	0.104	1.730	0.633	0.261	0.0452	0.0263	0.0131	0.0281
18.0	6.2350	3.1325	-	2.642	0.213	0.022	0.103	1.730	0.633	0.279	0.0433	0.0310	0.0153	0.0329
18.5	6.2600	3.1367	-	2.673	0.212	0.013	0.097	1.730	0.633	0.310	0.0388	0.0350	0.0172	0.0373
19.0	6.3052	3.1526	-	2.719	0.2112	0.007	0.087	1.730	0.633	0.356	0.0325	0.0373	0.0184	0.0402
19.5	6.3452	3.1726	-	2.764	0.2105	0.003	0.076	1.730	0.633	0.401	0.0245	0.0367	0.0181	0.0398
20.0	6.3610	3.2005	-	2.797	0.210	0.0	0.066	1.730	0.633	0.434	0.0146	0.0281	0.0139	0.0309

TABLE III  
CROSS SECTIONS FOR INELASTIC LEVELS OF Pu-239 (IN BARNS)

<u>E(keV)</u>	<u>7.85</u>	<u>57</u>	<u>76</u>	<u>164</u>	<u>193</u>	<u>286</u>	<u>330</u>	<u>388</u>	<u>392</u>	<u>434</u>	<u>470</u>	<u>486</u>	<u>492</u>
7.883	0.000												
8.0	0.005												
8.5	0.027												
9.0	0.056												
9.5	0.082												
10.0	0.095												
11.0	0.116												
12.0	0.130												
13.0	0.142												
14.0	0.155												
15.0	0.165												
16.0	0.176												
17.0	0.184												
18.0	0.192												
19.0	0.197												
20.0	0.202												
25.0	0.216												
30.0	0.225												
35.0	0.232												
40.0	0.237												
45.0	0.239												
50.0	0.240												
57.239	0.240	0.000											
60.0	0.239	0.005											
70.0	0.237	0.020											
76.319	0.235	0.027	0.000										
80.0	0.234	0.0295	0.0025										
90.0	0.232	0.036	0.013										
100.0	0.230	0.040	0.026										
110.0	0.228	0.042	0.046										
120.0	0.227	0.043	0.066										
130.0	0.225	0.043	0.083										
140.0	0.224	0.043	0.098										
150.0	0.223	0.043	0.109										
160.0	0.222	0.043	0.117										
164.689	0.221	0.043	0.119	0.000									
170.0	0.220	0.043	0.123	0.009									
180.0	0.219	0.043	0.127	0.032									
193.811	0.218	0.042	0.129	0.054	0.000								
200.0	0.217	0.042	0.130	0.057	0.010								
250.0	0.211	0.040	0.128	0.067	0.036								
287.201	0.207	0.039	0.124	0.070	0.061	0.000							
300.0	0.206	0.038	0.122	0.070	0.063	0.010							
331.386	0.200	0.036	0.115	0.070	0.066	0.034	0.000						
389.630	0.191	0.032	0.106	0.068	0.070	0.076	0.027	0.000					
393.646	0.190	0.032	0.104	0.068	0.070	0.078	0.028	0.004	0.000				
400.0	0.188	0.031	0.103	0.067	0.070	0.079	0.030	0.010	0.002				
435.823	0.182	0.029	0.097	0.064	0.071	0.087	0.036	0.025	0.016	0.000			
471.974	0.175	0.027	0.091	0.062	0.071	0.091	0.041	0.034	0.0215	0.0145	0.000		
488.041	0.172	0.0264	0.089	0.061	0.071	0.093	0.0423	0.037	0.024	0.0173	0.011	0.000	
494.066	0.171	0.026	0.088	0.0605	0.0707	0.0935	0.043	0.038	0.025	0.0185	0.0123	0.0055	0.000
500.0	0.169	0.0258	0.087	0.060	0.0704	0.094	0.044	0.039	0.0258	0.0196	0.0138	0.010	0.0056
507.121	0.168	0.0255	0.086	0.0597	0.0702	0.0944	0.0443	0.0396	0.0267	0.0204	0.0152	0.0110	0.008
514.150	0.167	0.025	0.085	0.059	0.070	0.095	0.045	0.041	0.028	0.0215	0.0175	0.0126	0.0107
558.335	0.1585	0.023	0.0793	0.0563	0.0694	0.097	0.0482	0.0458	0.0335	0.0276	0.023	0.021	0.0182
600.00	0.151	0.0215	0.0741	0.0538	0.068	0.098	0.051	0.0492	0.037	0.0322	0.0276	0.0257	0.0233
650.0	0.143	0.0195	0.069	0.0508	0.0655	0.098	0.0536	0.0524	0.0404	0.036	0.0326	0.0305	0.0282
700.0	0.136	0.0178	0.0641	0.0483	0.063	0.098	0.0553	0.055	0.0423	0.040	0.036	0.0344	0.032
733.051	0.131	0.0167	0.061	0.0466	0.0615	0.098	0.0561	0.0562	0.0433	0.0415	0.0381	0.0371	0.0342
763.177	0.126	0.0157	0.0591	0.045	0.0595	0.098	0.0568	0.0575	0.0438	0.0432	0.0401	0.0385	0.0363
803.344	0.121	0.0144	0.0557	0.0434	0.0575	0.097	0.057	0.0581	0.0442	0.045	0.042	0.041	0.0384
852.549	0.113	0.0132	0.052	0.0412	0.055	0.0955	0.057	0.0587	0.0445	0.0468	0.0432	0.043	0.0406
900.0	0.107	0.012	0.0487	0.039	0.0523	0.093	0.057	0.059	0.0446	0.048	0.044	0.045	0.0425
950.0	0.101	0.0107	0.046	0.0373	0.0496	0.0905	0.056	0.0584	0.0444	0.0486	0.0446	0.0463	0.0442

505    512    556    730    760    800    849    Continuum    (MeV) 1.0    1.5    2.0    2.5    3.0

0.000												
0.0057	0.000											
0.0162	0.015	0.000										0.000
0.0204	0.019	0.0152										0.021
0.0238	0.0224	0.0193										0.045
0.0266	0.0254	0.0228										0.078
0.028	0.027	0.0247	0.000									0.099
0.0293	0.0285	0.0262	0.0115	0.000								0.115
0.0304	0.0302	0.0285	0.0162	0.012	0.000							0.128
0.0316	0.032	0.0305	0.0205	0.0146	0.0121	0.000						0.148
0.0329	0.0337	0.0332	0.0245	0.017	0.015	0.0116						0.170
0.0337	0.0352	0.034	0.0275	0.0188	0.0177	0.0135	0.212					

TABLE III (Cont'd)

<u>E(MeV)</u>	<u>7.85</u>	<u>57</u>	<u>76</u>	<u>164</u>	<u>193</u>	<u>286</u>	<u>330</u>	<u>388</u>	<u>392</u>	<u>434</u>	<u>470</u>	<u>486</u>	<u>492</u>
1.00418	0.094	0.009	0.043	0.0352	0.0473	0.058	0.054	0.0575	0.044	0.049	0.045	0.0473	0.0451
1.2	0.073	0.0	0.034	0.0295	0.0393	0.076	0.0454	0.0496	0.041	0.0485	0.045	0.049	0.048
1.4	0.046	-	0.0276	0.0246	0.033	0.063	0.0373	0.0412	0.037	0.0436	0.0415	0.0468	0.0484
1.50627	0.049	-	0.0246	0.0223	0.0297	0.0562	0.0339	0.0370	0.0347	0.0391	0.0391	0.0448	0.0479
1.6	0.044	-	0.0225	0.0206	0.0277	0.051	0.0311	0.034	0.0328	0.0355	0.037	0.0427	0.0464
1.8	0.034	-	0.0189	0.0176	0.0235	0.0404	0.0258	0.0275	0.0285	0.0275	0.030	0.036	0.0417
2.00836	0.027	-	0.0162	0.0152	0.020	0.031	0.0213	0.0225	0.0238	0.0210	0.023	0.0282	0.0351
2.25	0.020	-	0.0134	0.0126	0.0165	0.0222	0.0176	0.0166	0.0184	0.0135	0.0161	0.0191	0.0242
2.51045	0.015	-	0.0112	0.0106	0.0135	0.0168	0.0136	0.0136	0.0142	0.0090	0.0103	0.0115	0.0138
2.75	0.0115	-	0.0096	0.0090	0.0110	0.0126	0.0110	0.0110	0.0111	0.0075	0.0090	0.0095	0.0090
3.01254	0.008	-	0.008	0.007	0.008	0.0097	0.008	0.008	0.008	0.005	0.007	0.008	0.006
3.25	0.005	-	0.005	0.004	0.005	0.006	0.005	0.005	0.005	0.0020	0.0040	0.0050	0.0030
3.5	0.002	-	0.002	0.001	0.002	0.0034	0.002	0.002	0.002	0.0	0.001	0.002	0.001
3.75	0.000	-	0.000	0.000	0.000	0.000	0.000	0.000	0.000	-	0.000	0.000	0.000
4.0	-	-	-	-	-	-	-	-	-	-	-	-	-
4.25	-	-	-	-	-	-	-	-	-	-	-	-	-
4.5	-	-	-	-	-	-	-	-	-	-	-	-	-
4.75	-	-	-	-	-	-	-	-	-	-	-	-	-
5.0	-	-	-	-	-	-	-	-	-	-	-	-	-
5.25	-	-	-	-	-	-	-	-	-	-	-	-	-
5.5	-	-	-	-	-	-	-	-	-	-	-	-	-

\*Above this energy, the cross sections for these levels are identical.

<u>E(MeV)</u>	<u>Continuum</u>	<u>Direct Interaction</u>		<u>E(MeV)</u>	<u>Continuum</u>	<u>Direct Interaction</u>		<u>E(MeV)</u>	<u>Continuum</u>	<u>Direct Interaction</u>	
		<u>Continuum</u>	<u>Interaction</u>			<u>Continuum</u>	<u>Interaction</u>			<u>Continuum</u>	<u>Interaction</u>
5.67965	1.581	0.029		11.5	0.045	0.138		18.5	0.012	0.200	
5.75	1.567	0.030		12.0	0.039	0.152		19.0	0.0112	0.200	
6.00	1.467	0.034		12.5	0.035	0.167		19.5	0.0105	0.200	
6.25	1.212	0.038		12.7069	0.033	0.173		20.0	0.0100	0.200	
6.50	0.978	0.042		13.0	0.031	0.182					
6.75	0.795	0.046		13.5	0.028	0.193					
7.00	0.650	0.050		14.0	0.025	0.200					
7.5	0.353	0.057		14.5	0.023	0.200					
8.0	0.242	0.065		15.0	0.021	0.200					
8.5	0.166	0.073		15.5	0.019	0.200					
9.0	0.119	0.081		16.0	0.018	0.200					
9.5	0.093	0.090		16.5	0.0165	0.200					
10.0	0.076	0.100		17.0	0.015	0.200					
10.5	0.062	0.112		17.5	0.014	0.200					
11.0	0.053	0.125		18.0	0.013	0.200					

<u>505</u>	<u>512</u>	<u>556</u>	<u>730</u>	<u>760</u>	<u>800</u>	<u>849</u>	<u>Continuum</u>	(MeV)	<u>1.0</u>	<u>1.5</u>	<u>2.0</u>	<u>2.5</u>	<u>3.0</u>
0.0345	0.0363	0.0354	0.030	0.0202	0.0202	0.015	0.260	0.000					
0.0368	0.039	0.0397	0.0385	0.0235	0.0277	0.0181	0.4255	0.0005					
0.037	0.040	0.0416	0.0452	0.0256	0.0291	0.0195	0.5825	0.0015					
0.0360	0.0400	0.0416	0.0471	0.0264	0.0289	0.0197	0.6633	0.002	0.000				
0.0352	0.0398	0.0416	0.0481	0.0267	0.0284	0.0199	0.738	0.0025	0.0005				
0.0325	0.038	0.0407	0.0489	0.027	0.027	0.0195	0.874	0.0003	0.001				
0.0292	0.0356	0.0388	0.0482	0.0268	0.0252	0.0189	1.003	0.0035	0.0015	0.000			
0.0244	0.0304	0.0343	0.0465	0.0257	0.0224	0.0178	1.1533	0.0037	0.0018	0.0005			
0.0185	0.0245	0.0275	0.0436	0.0239	0.0192	0.0167	1.282	0.004	0.002	0.001	0.000		
0.0110	0.0175	0.0209	0.0396	0.0213	0.0166	0.0152	1.3706	0.0041	0.0021	0.0012	0.0001		
0.008	0.007	0.0132	0.035	0.0179	0.0144	0.0138	1.448	0.0042	0.0022	0.0013	0.0003	0.000	
0.0050	0.0040	0.0080	0.0280	0.0110	0.0119	0.0123	1.5163	0.0042	0.0025	0.0015	0.0007	0.0006	
0.002	0.001	0.004	0.0216	0.006	0.0100	0.0110	1.574	0.0043	0.0028	0.0017	0.0012	0.0010	
0.000	0.000	0.000	0.0090	0.0030	0.0070	0.0090	1.6208	0.0044	0.0031	0.0020	0.0015	0.0012	
-	-	-	0.0	0.000	0.004	0.008	1.6355	0.0045	0.0035	0.0023	0.0017	0.0015	
-	-	-	-	-	0.0010	0.0050	1.6403	0.0046	0.0037	0.0026	0.0020	0.0018	
-	-	-	-	-	0.0	0.002	1.643	0.0047	0.0040	0.0030	0.0023	0.0020	
-	-	-	-	-	-	0.000	1.643	0.0048	0.0043	0.0035	0.0029	0.0025	
-	-	-	-	-	-	-	1.641	0.0050	0.0045	0.0040	0.0035	0.0030	
-	-	-	-	-	-	-	1.631	0.0050	0.0049	0.0046	0.0044	0.0041	
-	-	-	-	-	-	-	1.614	0.0054*	0.0054*	0.0054*	0.0054*	0.0054*	

### III. PLUTONIUM-240

#### A. Total Cross Section

The only reported measurements of the total cross section are those by Smith et al.<sup>56</sup> Above 1.5 MeV, the total is taken to be the sum of the partial cross sections, following the shape of the curve for the total cross sections of  $^{238}\text{U}$  and for  $^{239}\text{Pu}$ . The results are shown in Fig. 42.

#### B. Elastic-Scattering Cross Sections

Elastic-scattering cross sections obtained by integrating the differential elastic cross section over all angles are given by Smith et al.<sup>56</sup> The evaluated curve follows the experiments closely up to about 1 MeV, where the scatter in the data becomes quite large. Above 1-1.5 MeV, the elastic-scattering cross section was obtained by subtracting the nonelastic cross section from the total. The recommended curve is shown in Fig. 43.

Smith et al.<sup>56</sup> measured the angular distribution for elastic scattering plus some inelastic contributions. However, the results are presented in terms of Legendre polynomial coefficients, obtained from fitting each measurement. A 5th-order fit was made at each energy, a limit that is both too low (in comparison with the results for neighboring nuclides) and odd, in violation of physical principles and ENDF/B procedures. In the absence of the original data (in units of mb/sr) a refitting procedure could not be performed; hence, these data were not used in this evaluation. On the basis of nuclear systematics, the angular distributions for  $^{239}\text{Pu}$  were used for  $^{240}\text{Pu}$ .

#### C. Fission Cross Section

Measurements of the fission cross section of  $^{240}\text{Pu}$  have been reported by White and Warner,<sup>19</sup> Savin et al.,<sup>16,57</sup> Dorofeev and Dobrynnin,<sup>24</sup> Perkin et al.,<sup>21</sup> Ruddick and White,<sup>58</sup> Smith et al.,<sup>18</sup> Nesterov and Smirenkin,<sup>59</sup> and Gilboy and Knoll.<sup>60</sup> Some of these measurements were ratios of the fission cross section of  $^{240}\text{Pu}$  relative to that of  $^{235}\text{U}$ ; all of them, however, have been reduced to absolute cross sections by multiplying by the appropriate fission cross sections as described in the evaluation of the neutron cross sections of  $^{239}\text{Pu}$  (Sec. II-C).

The evaluated curve follows the experimental average up to about 400 keV. Above that energy, the

experimental measurements do not show good agreement, although the spread is not extreme. The recommended curve tends to follow the measurements of Savin et al.<sup>57</sup> above 500 keV.

The point of White and Warner<sup>19</sup> at 14.1 MeV establishes the absolute value of the curve in the high-energy region; the general shape of the curve above about 5 MeV was taken from the curve for  $^{239}\text{Pu}$ . The recommended curves are shown in Figs. 44 and 45.

#### D. Mean Number of Prompt Neutrons from Fission

Measurements of  $\bar{v}$  are given by Savin et al.,<sup>16</sup> Kuzminov,<sup>61</sup> and de Vroey et al.<sup>62</sup> These were reduced to ratios of  $\bar{v}$  for  $^{240}\text{Pu}$  to the spontaneous fission  $\bar{v}$  for  $^{252}\text{Cf}$ . A fit to the data of Savin et al. and de Vroey et al. below 4 MeV yields a straight line that is inconsistent with the measurements of Kuzminov, especially near 15 MeV. In view of the above inconsistency and the difficulty of establishing a two-segment linear fit without measurements between 4 and 15 MeV, this evaluation is based only on the data of Savin et al. and de Vroey et al., although it is questionable to disregard the only high-energy measurement available. The ratio of  $\bar{v}$  for  $^{240}\text{Pu}$  to that of  $^{252}\text{Cf}$  is given by

$$\frac{\bar{v}(\text{Pu})}{\bar{v}(\text{Cf})} = 0.773 + 0.0382E_n \text{ (MeV)} , \quad 0 < E_n < 20 \text{ MeV} . \quad (9)$$

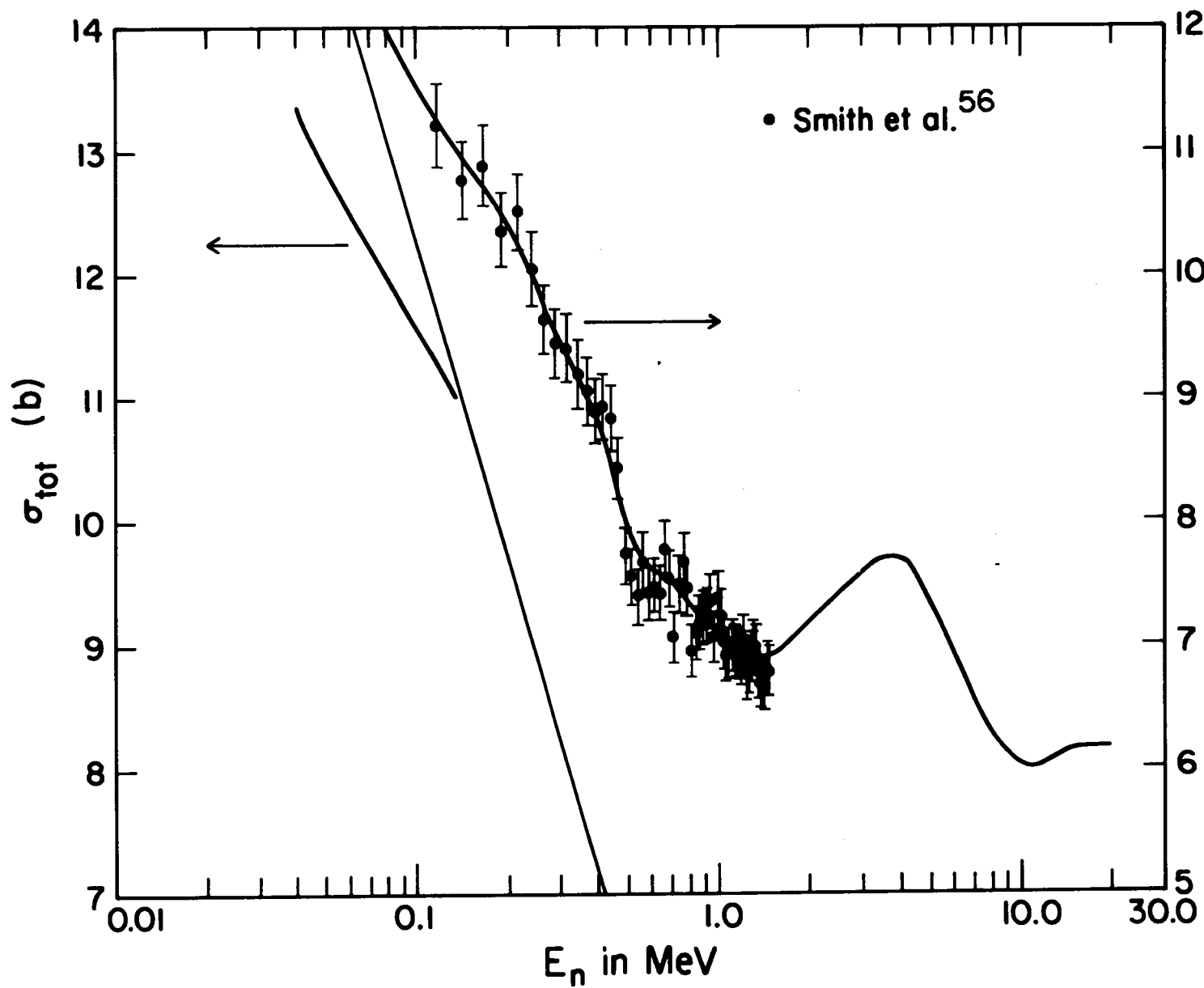
Based on  $\bar{v}$  for  $^{252}\text{Cf}$  of 3.748,

$$\bar{v}(\text{Pu}) = 2.897 + 0.143E_n \text{ (MeV)} . \quad (10)$$

The recommended curve is shown in Fig. 46.

#### E. Delayed Neutrons from Fission

Keepin<sup>35</sup> gives a value of 0.0088 for the delayed neutron fraction in the fission spectrum. In the absence of data to the contrary, the shape of the curve for the delayed neutron fraction as a function of energy is taken to be the same as that for  $^{239}\text{Pu}$  (see Fig. 9). The final-state energy distribution given by Keepin is essentially the same as that for  $^{239}\text{Pu}$  (see Fig. 10).



#### F. Fission Neutron Energy Distribution

Because there are no measurements of the energy distributions for neutron-induced fission of  $^{240}\text{Pu}$ , the nuclear temperature for various incident-neutron energies was calculated from the relation given by Terrell:<sup>63</sup>

$$T_f(E_n) \approx 0.50 + 0.43 (\bar{v} + 1)^{1/2}, \quad (11)$$

where  $\bar{v}$  as a function of  $E_n$  is given by Eq. 10. Equation (11) gives, for example,  $T_f(0) = 1.355$  MeV,  $T_f(14$  MeV) = 1.547 MeV, and  $T_f(20$  MeV) = 1.619 MeV. The curve of  $T_f$  vs  $E_n$  is shown in Fig. 47.

Again, the fission process is represented by the relation,

$$\sigma_{n,F} = \sigma_{n,f} + \sigma_{n,n'f} + \sigma_{n,2nf} + \dots \quad (12)$$

The prefission neutron energy distributions are taken to be the same as those for inelastic scattering (see Sec. III-G), with appropriate threshold modifications.

#### G. Inelastic Scattering

The level energies for  $^{240}\text{Pu}$  were taken from Lederer et al.<sup>50</sup> Measurements of the cross sections for exciting levels in the ranges  $42 \pm 5$ ,  $140 \pm 10$ ,  $300 \pm 20$ ,  $600 \pm 20$ , and  $900 \pm 50$  keV were reported by Smith et al.<sup>56</sup> These measurements give results for the energy levels at 43, 142, 296, and 599 keV, and provide a check on the sum of the levels at 863, 903, and 945 keV.

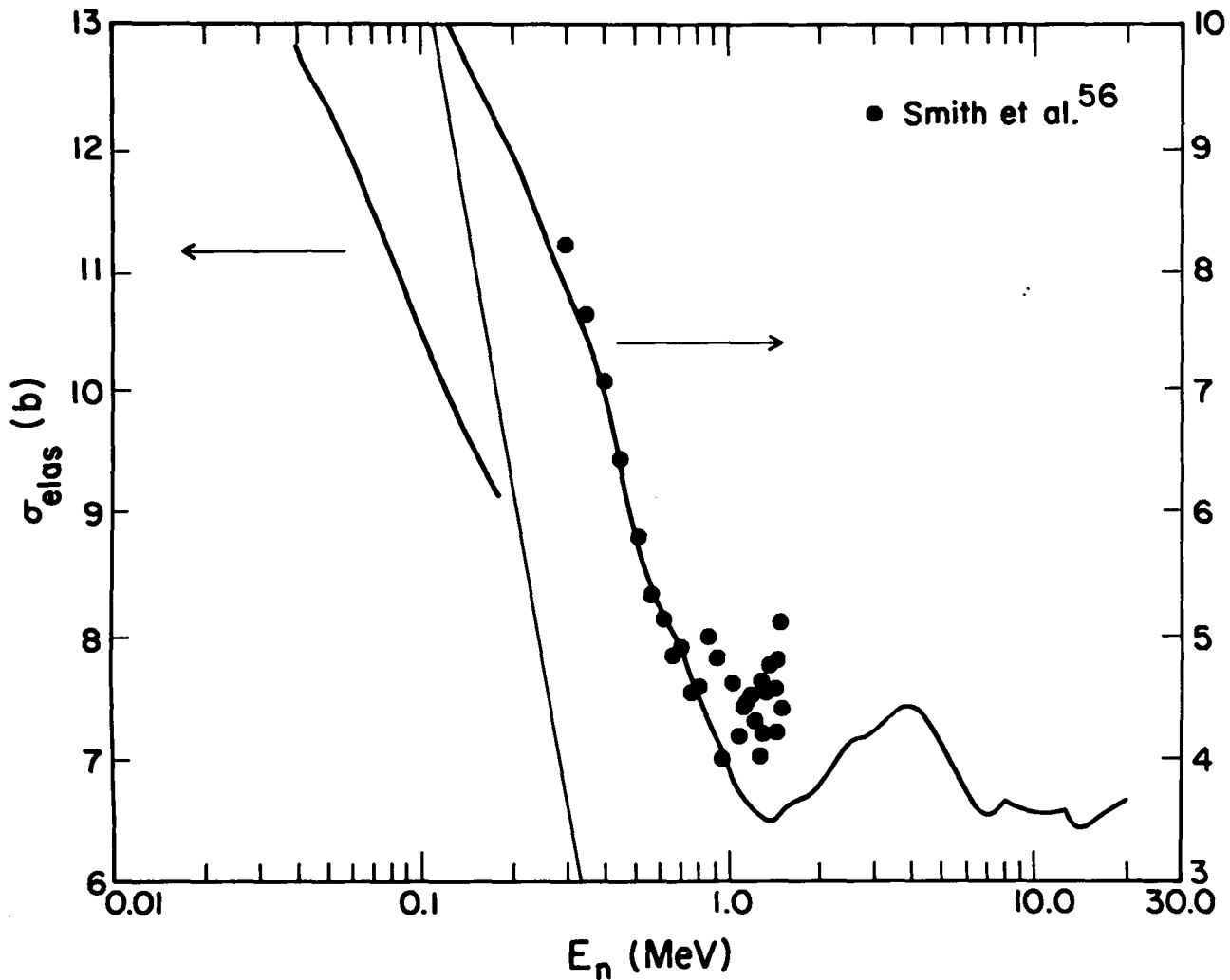


Fig. 43. Elastic-scattering cross section for  $^{240}\text{Pu}$ .

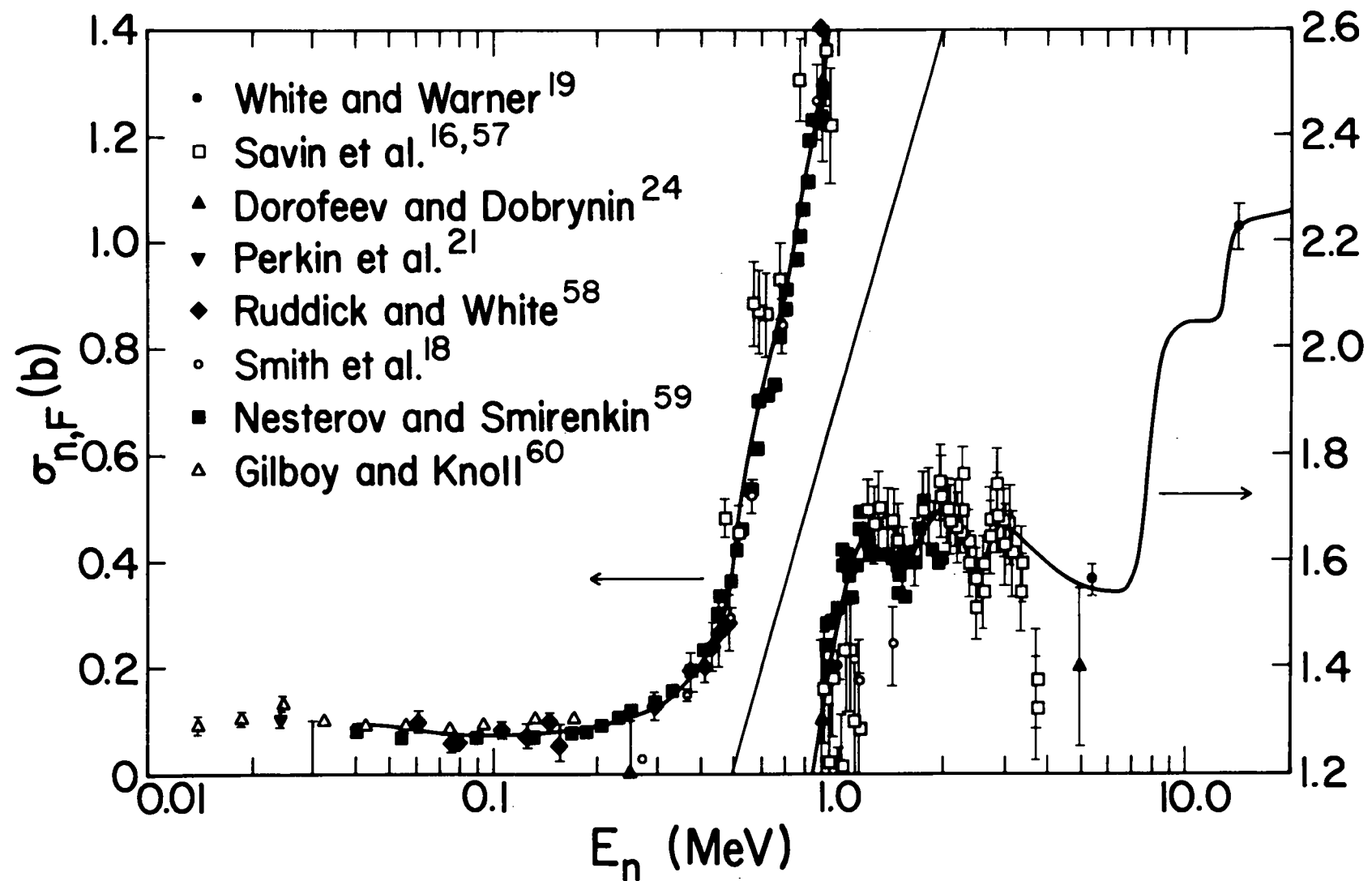


Fig. 44. Fission cross section for  $^{240}\text{Pu}$ . All measurements made relative to other cross sections have been reduced to fission cross sections by means of appropriate ratio curves.

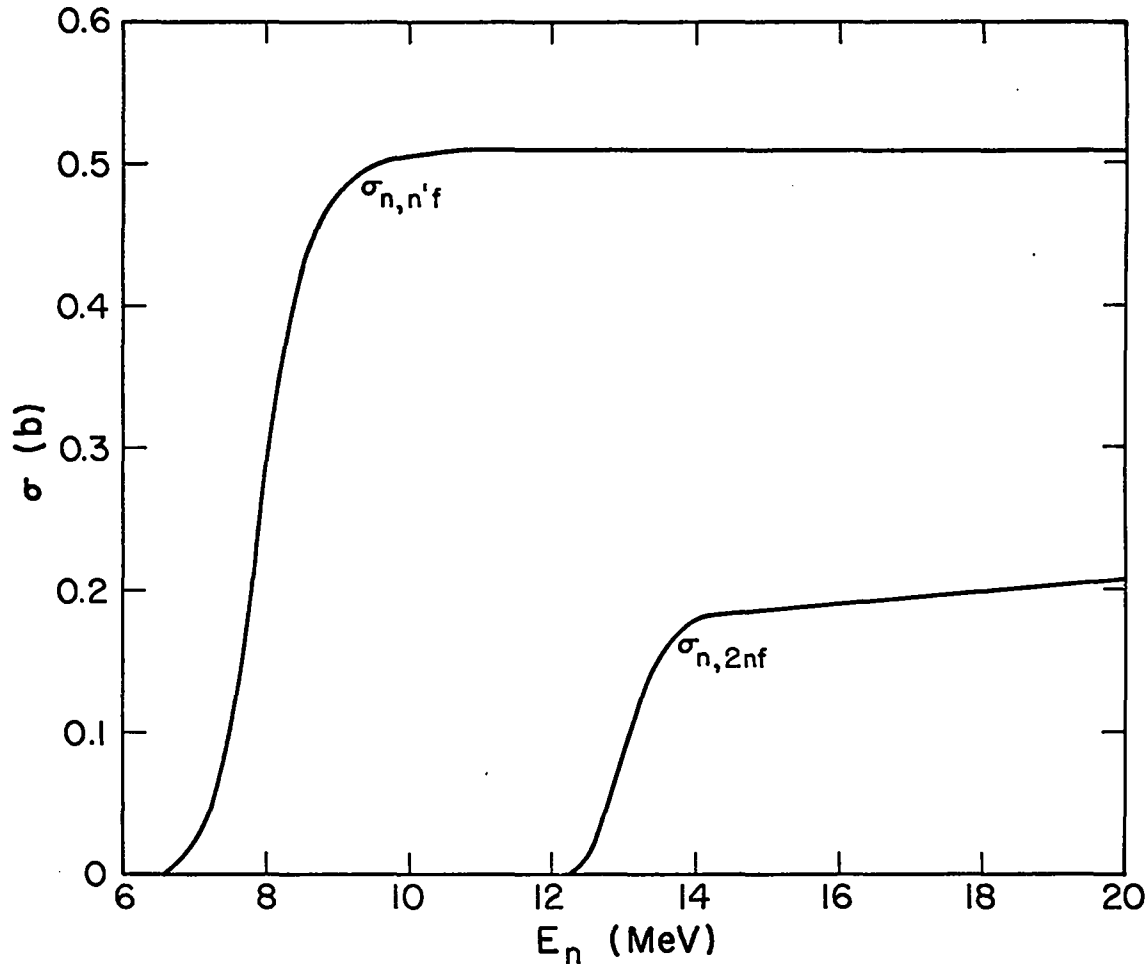


Fig. 45.  $\sigma_{n,n'f}$  and  $\sigma_{n,2nf}$  for  $^{240}\text{Pu}$ .

A continuum was introduced along with the level at 945 keV to account for the unresolved energy levels above that energy. At an incident energy of 940 keV, the average neutron energy obtained from the levels is 760 keV. Thus, the temperature for the continuum distribution was taken to be 380 keV at that energy. The curve at high energies was based on the curve for  $^{239}\text{Pu}$ ; the results are shown in Fig. 48.

Following the procedure used for  $^{239}\text{Pu}$ , levels were introduced at 2, 3, 4, and 5 MeV to represent direct-interaction inelastic scattering. Angular distributions for those levels were assumed as they were for  $^{239}\text{Pu}$ . The cross sections for the various excited levels, the continuum, and the total inelastic are shown in Figs. 49-51.

#### H. Radiative Capture Cross Section

The radiative capture cross section for  $^{240}\text{Pu}$  was evaluated by Pitterle and Yamamoto<sup>64</sup> for inclusion in the ENDF/B-III evaluation (MAT 1105). In the absence of experimental measurements in the energy region of interest, their evaluation<sup>\*</sup> was used, without modification, in this work. The curve is reproduced in Fig. 52.

#### I. $\sigma_{n,2n}$ and $\sigma_{n,3n}$

In the absence of experimental measurements, these cross sections are assumed to be similar to the cross sections for  $^{239}\text{Pu}$ , with appropriate changes in threshold (see Fig. 53). If the dominant factor in these processes should be the even-odd

\* This evaluation is based on calculations, using parameters obtained from resonance-region measurements.

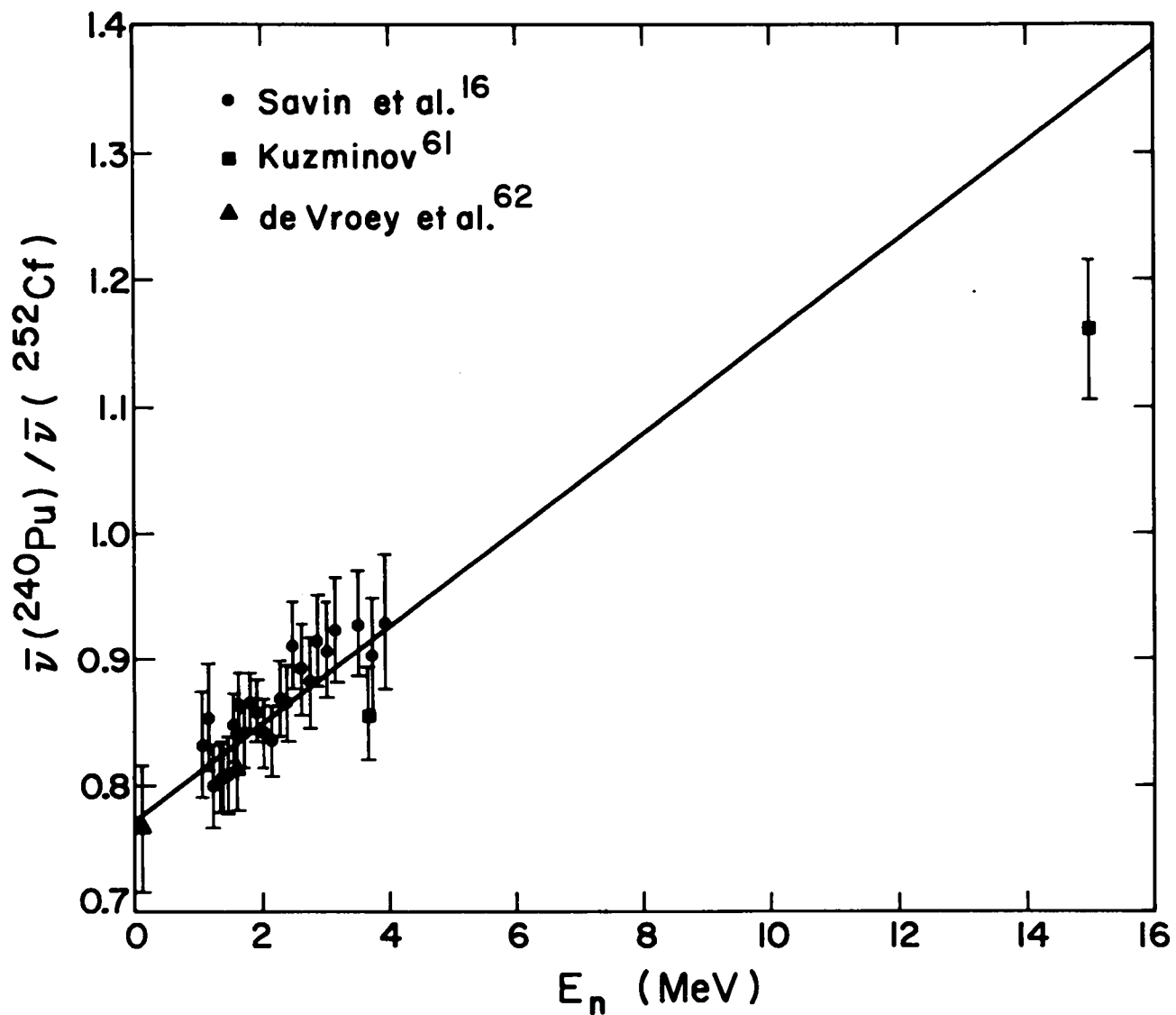


Fig. 46. Ratio of mean number of prompt neutrons per fission for  $^{240}\text{Pu}$  to the spontaneous value for  $^{252}\text{Cf}$ .

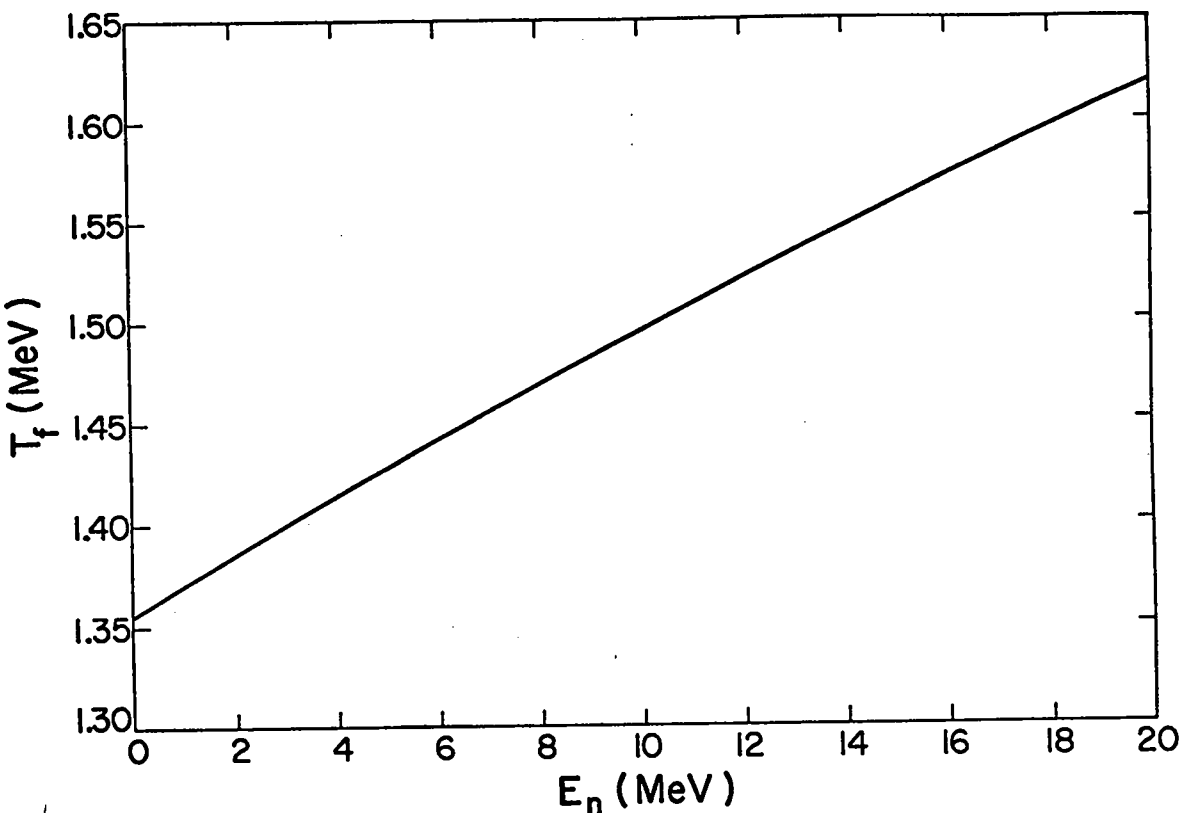


Fig. 47. Fission temperature for  $^{240}\text{Pu}$ .

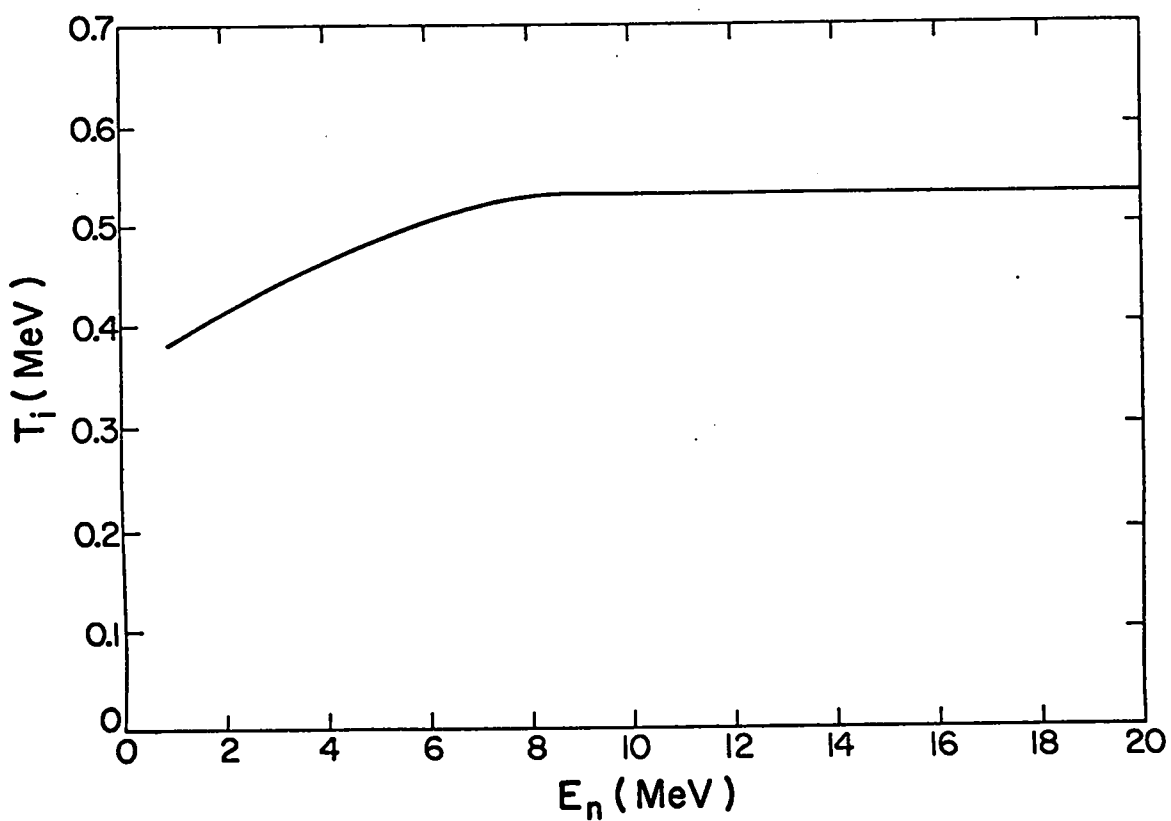


Fig. 48. Inelastic-scattering nuclear temperature for  $^{240}\text{Pu}$ .

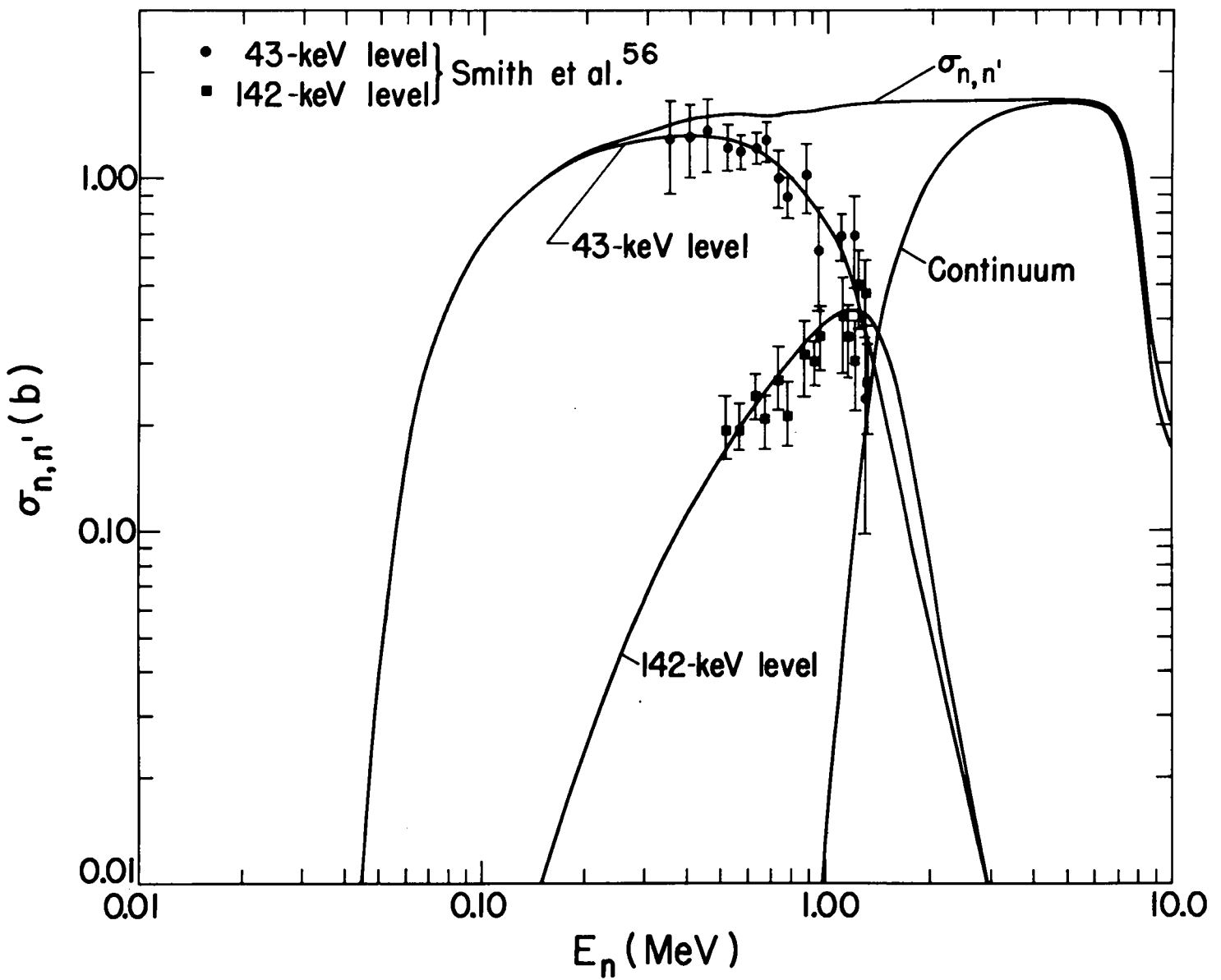


Fig. 49. Inelastic-scattering cross section, continuum cross section and energy-level cross sections for  $^{240}\text{Pu}$ .

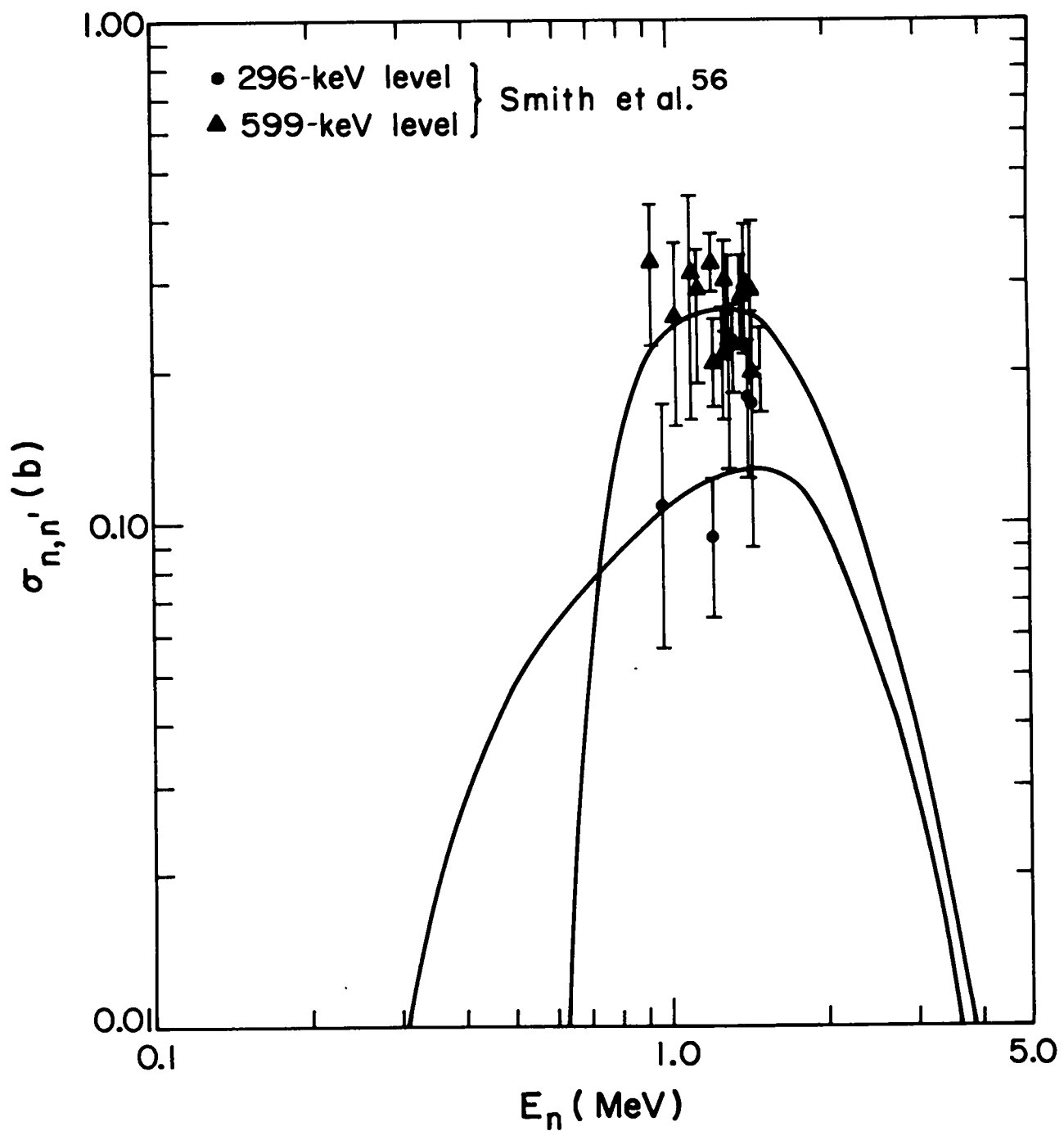


Fig. 50. Energy-level cross sections for  $^{240}\text{Pu}$ .

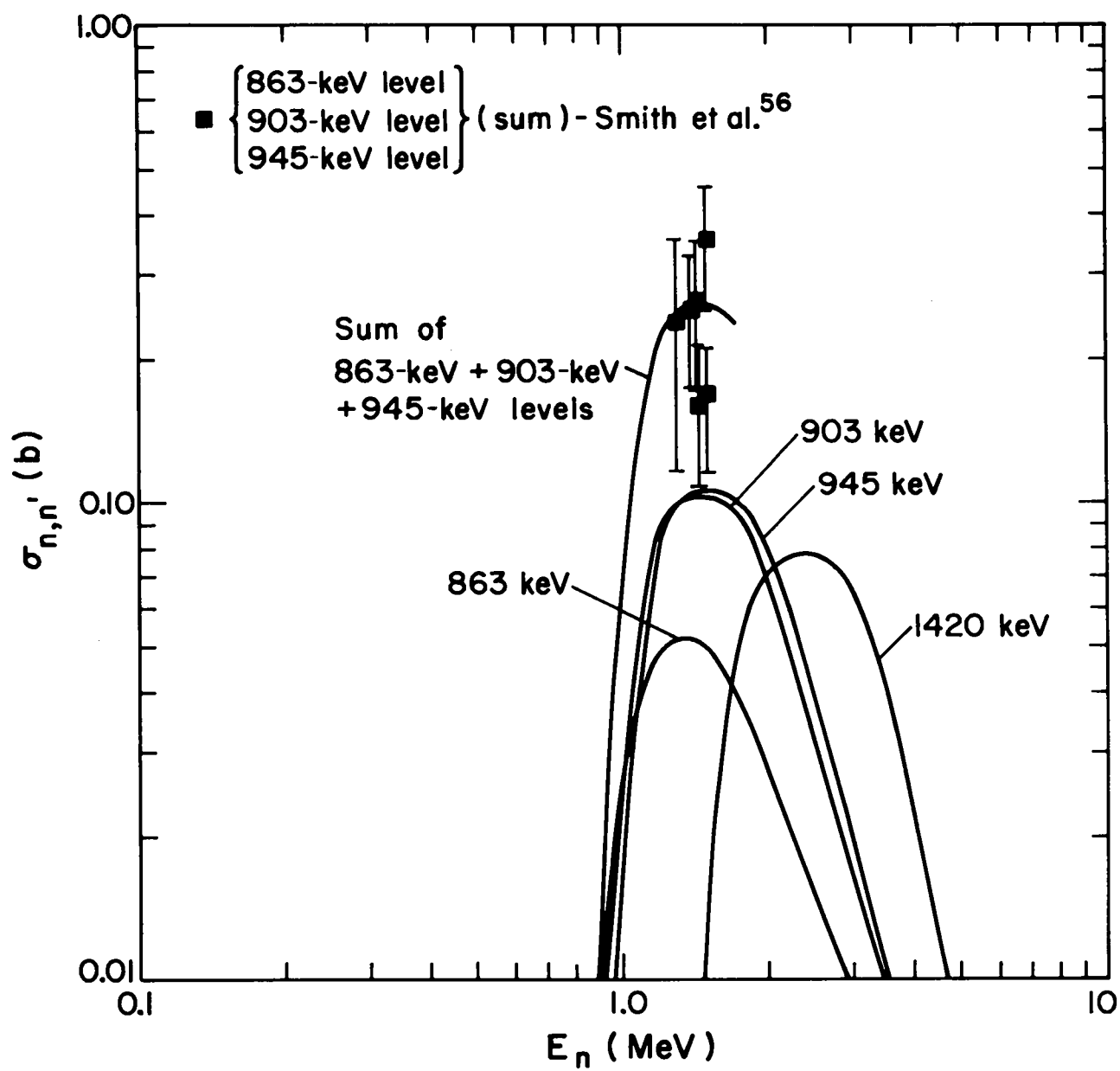


Fig. 51. Energy-level cross sections for  $^{240}\text{Pu}$ .

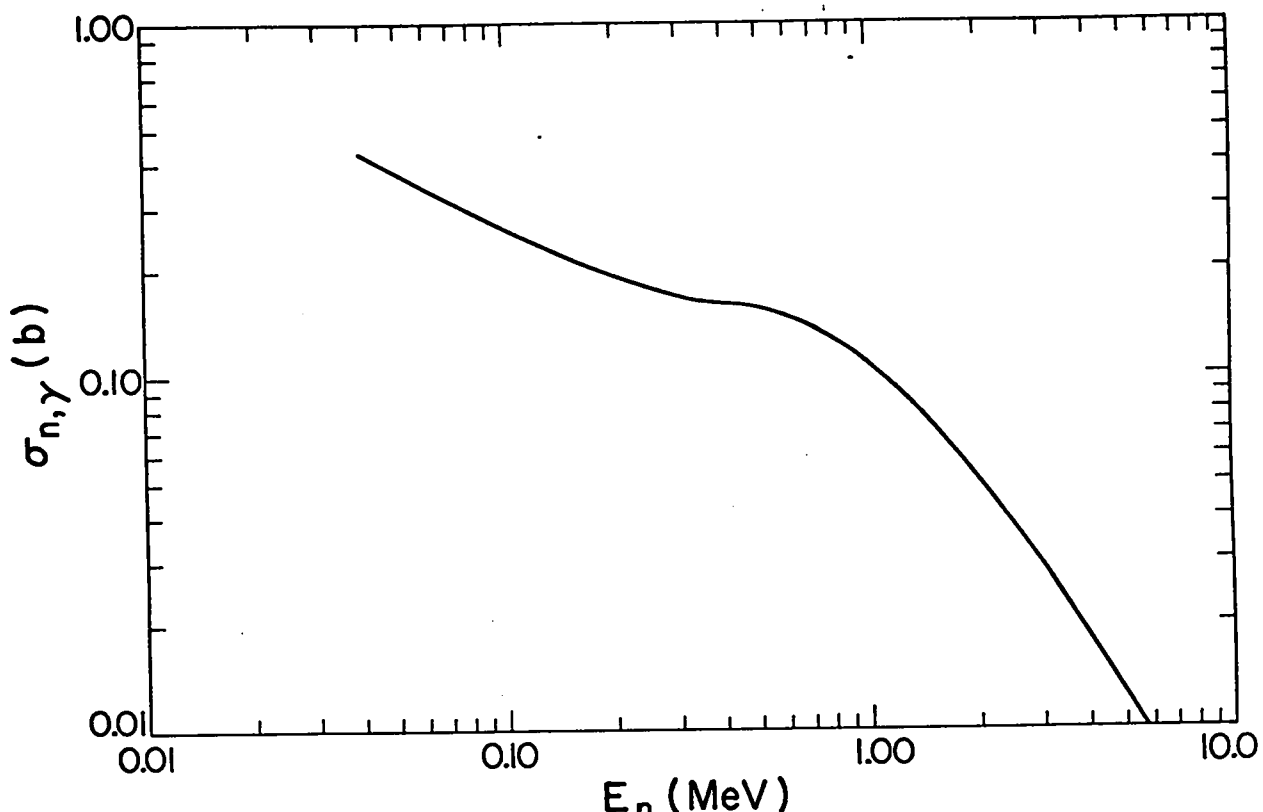


Fig. 52. Radiative-capture cross section for  $^{240}\text{Pu}$ .

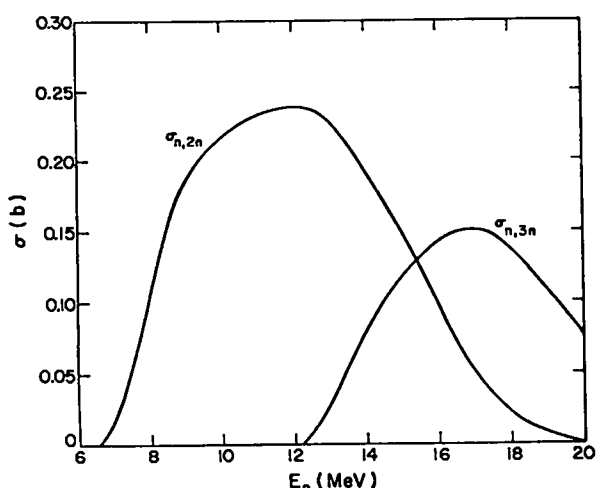


Fig. 53.  $\sigma_{n,2n}$  and  $\sigma_{n,3n}$  for  $^{240}\text{Pu}$ .

nature of the mass number, then  $^{238}\text{U}$  might prove to be the better choice.

#### J. Tabulated Cross Sections

The tabulated values of the cross sections are given in Table IV, while values for the inelastic levels are given in Table V.

TABLE IV  
NEUTRON CROSS SECTIONS FOR  $^{240}\text{Pu}$  (IN BARNS)

<u><math>E_n</math> (MeV)</u>	<u><math>\sigma_{n,T}</math></u>	<u><math>\sigma_{n,n}</math></u>	<u><math>\sigma_{n,\gamma}</math></u>	<u><math>\sigma_{n,F}</math></u>	<u><math>\sigma_{n,n'}</math></u>	<u><math>\sigma_{n,2n}</math></u>	<u><math>\sigma_{n,3n}</math></u>	<u><math>\sigma_{n,f}</math></u>	<u><math>\sigma_{n,n'f}</math></u>	<u><math>\sigma_{n,2nf}</math></u>
0.040	13.356	12.8315	0.430	0.0945						
0.043172	13.1323	12.630	0.410	0.0923	0.000					
0.050	12.851	12.3424	0.380	0.0912	0.0374					
0.055	12.664	12.132	0.362	0.0880	0.0820					
0.060	12.507	11.920	0.343	0.083	0.161					
0.065	12.361	11.710	0.330	0.080	0.241					
0.070	12.209	11.494	0.318	0.079	0.318					
0.075	12.096	11.330	0.306	0.078	0.382					
0.080	11.991	11.175	0.297	0.076	0.443					
0.085	11.858	10.992	0.288	0.074	0.504					
0.090	11.742	10.827	0.278	0.072	0.565					
0.100	11.505	10.505	0.265	0.071	0.664					
0.110	11.338	10.274	0.252	0.070	0.742					
0.120	11.193	10.066	0.242	0.071	0.814					
0.130	11.059	9.875	0.233	0.073	0.878					
0.140	10.944	9.709	0.224	0.075	0.936					
0.142596	10.916	9.666	0.223	0.076	0.951					
0.150	10.831	9.533	0.218	0.078	1.002					
0.160	10.747	9.4168	0.212	0.080	1.0382					
0.170	10.654	9.2849	0.206	0.082	1.0811					
0.180	10.558	9.1449	0.202	0.084	1.1271					
0.190	10.461	9.0228	0.198	0.087	1.1532					
0.200	10.392	8.9224	0.194	0.091	1.1846					
0.22	10.211	8.6972	0.188	0.098	1.2278					
0.24	10.006	8.4573	0.183	0.104	1.2617					
0.26	9.807	8.2281	0.179	0.111	1.2889					
0.28	9.611	8.0042	0.175	0.118	1.3138					
0.297243	9.498	7.8665	0.173	0.123	1.3355					
0.30	9.466	7.8239	0.172	0.128	1.3421					
0.35	9.149	7.4307	0.164	0.158	1.3963					
0.40	8.801	6.9910	0.161	0.198	1.4510					
0.45	8.331	6.4211	0.162	0.261	1.4869					
0.50	7.908	5.8400	0.159	0.403	1.5060					
0.55	7.723	5.4706	0.153	0.585	1.5144					
0.601516	7.578	5.2225	0.1485	0.704	1.5030					
0.65	7.531	5.0801	0.144	0.807	1.4999					
0.70	7.510	4.9682	0.139	0.904	1.4988					
0.75	7.398	4.7370	0.133	1.012	1.516					
0.80	7.309	4.536	0.128	1.107	1.538					
0.85	7.254	4.384	0.123	1.208	1.539					
0.866525	7.247	4.354	0.121	1.231	1.541					
0.906793	7.191	4.2255	0.117	1.308	1.5405					
0.948969	7.172	4.1003	0.112	1.406	1.5537					
1.00	7.121	3.9530	0.108	1.483	1.5770					
1.1	7.005	3.7107	0.099	1.596	1.5993					
1.2	6.942	3.5949	0.091	1.647	1.6091					
1.3	6.910	3.5260	0.085	1.679	1.620					
1.4	6.898	3.5000	0.079	1.679	1.640					
1.42596	6.901	3.5080	0.078	1.670	1.645					
1.5	6.911	3.5660	0.073	1.622	1.650					

TABLE IV (Cont'd)

<u><math>E_n</math> (MeV)</u>	<u><math>\sigma_{n,T}</math></u>	<u><math>\sigma_{n,n}</math></u>	<u><math>\sigma_{n,\gamma}</math></u>	<u><math>\sigma_{n,F}</math></u>	<u><math>\sigma_{n,n'}</math></u>	<u><math>\sigma_{n,2n}</math></u>	<u><math>\sigma_{n,3n}</math></u>	<u><math>\sigma_{n,f}</math></u>	<u><math>\sigma_{n,n'f}</math></u>	<u><math>\sigma_{n,2nf}</math></u>
1.6	6.946	3.6230	0.068	1.605	1.650					
1.7	7.015	3.6740	0.063	1.628	1.650					
1.8	7.069	3.6975	0.0595	1.662	1.650					
1.9	7.134	3.7390	0.0560	1.689	1.650					
2.00833	7.187	3.7905	0.0525	1.694	1.650					
2.2	7.292	3.9265	0.0465	1.669	1.650					
2.4	7.374	4.0770	0.0410	1.606	1.650					
2.5	7.404	4.1478	0.0392	1.567	1.650					
2.6	7.439	4.1728	0.0372	1.579	1.650					
2.8	7.528	4.1968	0.0332	1.648	1.650					
3.01250	7.591	4.2393	0.0297	1.672	1.650					
3.5	7.695	4.3887	0.0233	1.633	1.650					
4.01667	7.696	4.4286	0.0184	1.599	1.650					
4.5	7.553	4.3172	0.0148	1.571	1.650					
5.02083	7.309	4.0946	0.0124	1.552	1.650					
5.5	7.093	3.9092	0.0108	1.543	1.630					
6.0	6.898	3.7276	0.0094	1.541	1.620					
6.5	6.699	3.5906	0.0084	1.540	1.560					
6.56072	6.668	3.5797	0.0083	1.540	1.540	0.000				
7.0	6.519	3.5334	0.0076	1.561	1.400	0.017				
7.5	6.388	3.5881	0.0069	1.635	1.105	0.053				0.095
8.0	6.292	3.6507	0.0063	1.822	0.710	0.103				0.282
8.5	6.198	3.6192	0.0058	1.963	0.455	0.155				0.423
9.0	6.121	3.5976	0.0054	2.019	0.312	0.187				0.479
9.5	6.072	3.5819	0.0051	2.040	0.242	0.203				0.500
10.0	6.022	3.5542	0.0048	2.045	0.200	0.218				0.505
10.5	6.004	3.5539	0.0045	2.048	0.1716	0.226				0.508
11.0	6.006	3.5608	0.0042	2.050	0.1590	0.232				0.510
11.5	6.012	3.5667	0.0039	2.050	0.1554	0.236				
12.0	6.026	3.5738	0.0036	2.050	0.1606	0.238				
12.2398	6.039	3.5833	0.0035	2.050	0.1642	0.238	0.000			0.000
12.5	6.058	3.5791	0.0033	2.062	0.1686	0.236	0.009	1.540	0.510	0.012
13.0	6.069	3.4994	0.0030	2.135	0.1766	0.227	0.028	1.540	0.510	0.085
13.5	6.100	3.4469	0.0027	2.202	0.1824	0.211	0.055			0.152
14.0	6.117	3.4286	0.0024	2.230	0.1850	0.192	0.079			0.180
14.5	6.136	3.4429	0.0021	2.235	0.1830	0.173	0.100			0.185
15.0	6.147	3.4562	0.0018	2.239	0.1810	0.152	0.117			0.189
15.5	6.158	3.4805	0.0015	2.241	0.1790	0.124	0.132			0.191
16.0	6.167	3.5088	0.0012	2.243	0.1780	0.095	0.141			0.193
16.5	6.172	3.5296	0.0009	2.245	0.1765	0.072	0.148			0.195
17.0	6.175	3.5504	0.0006	2.247	0.1750	0.052	0.150			0.197
17.5	6.177	3.5707	0.0003	2.249	0.1740	0.036	0.147			0.199
18.0	6.178	3.5950	0.0000	2.251	0.1730	0.022	0.137			0.201
18.5	6.178	3.6180	-	2.253	0.1720	0.013	0.122			0.203
19.0	6.178	3.6338	-	2.255	0.1712	0.007	0.111			0.205
19.5	6.178	3.6535	-	2.257	0.1705	0.003	0.094			0.207
20.0	6.178	3.6750	-	2.258	0.1700	0.000	0.075	1.540	0.510	0.208

Same as  $\sigma_{n,F}$  below 6.56072 MeV

TABLE V  
CROSS SECTIONS FOR INELASTIC LEVELS OF  $^{240}\text{Pu}$  (IN BARNS)

$E_n$ (MeV)	43	142	296	599	863	903	945	1420	2000	3000	4000	5000	Continuum	
0.043172	0.000													
0.050		0.0374												
0.055		0.082												
0.060		0.161												
0.065		0.241												
0.070		0.318												
0.075		0.382												
0.080		0.443												
0.085		0.504												
0.090		0.565												
0.100		0.664												
0.110		0.742												
0.120		0.814												
0.130		0.878												
0.140		0.936												
0.142596	0.951	0.000												
0.150	0.992	0.0100												
0.160	1.026	0.0122												
0.170	1.066	0.0151												
0.180	1.109	0.0181												
0.190	1.132	0.0212												
0.200	1.160	0.0246												
0.22	1.196	0.0318												
0.24	1.223	0.0387												
0.26	1.242	0.0469												
0.28	1.259	0.0548												
0.297243	1.273	0.0625	0.000											
0.30	1.274	0.0641	0.0040											
0.35	1.290	0.088	0.0183											
0.40	1.310	0.112	0.0290											
0.45	1.310	0.138	0.0389											
0.50	1.295	0.163	0.0480											
0.55	1.270	0.189	0.0554											
0.601516	1.224	0.215	0.0640	0.000										
0.65	1.173	0.238	0.0704	0.0185										
0.70	1.110	0.263	0.0768	0.0490										
0.75	1.045	0.286	0.083	0.102										
0.80	0.998	0.310	0.089	0.141										
0.85	0.931	0.333	0.094	0.181										
0.866525	0.914	0.341	0.096	0.190	0.000									
0.906793	0.860	0.358	0.100	0.211	0.0115	0.000								
0.948969	0.817	0.375	0.104	0.227	0.0172	0.0135	0.000					0.000		
1.0	0.760	0.393	0.108	0.239	0.0245	0.0243	0.0164					0.0118		
1.1	0.634	0.417	0.115	0.256	0.0390	0.0580	0.0455					0.0348		
1.2	0.498	0.423	0.121	0.263	0.0491	0.0890	0.0810					0.0850		
1.3	0.369	0.410	0.126	0.266	0.0520	0.0995	0.1005					0.1970		
1.4	0.279	0.369	0.127	0.262	0.0519	0.1020	0.1050					0.3441		
1.42596	0.252	0.356	0.1273	0.261	0.0513	0.1022	0.1057	0.000					0.3895	
1.5	0.202	0.312	0.127	0.254	0.0499	0.1018	0.1060	0.0142					0.4831	
1.6	0.151	0.251	0.126	0.237	0.0461	0.1004	0.1055	0.0284					0.6046	
1.7	0.115	0.194	0.123	0.215	0.0412	0.0962	0.1024	0.0448					0.7184	
1.8	0.088	0.144	0.116	0.196	0.0363	0.0880	0.0965	0.0568					0.8284	
1.9	0.070	0.107	0.110	0.174	0.0315	0.0780	0.0883	0.0650					0.9262	
2.00833	0.054	0.079	0.098	0.153	0.0277	0.0670	0.0797	0.0703	0.000				1.0213	
2.2	0.0356	0.0457	0.0777	0.120	0.0211	0.0492	0.0607	0.0775	0.0004				1.1621	
2.4	0.0257	0.0296	0.0623	0.0904	0.0170	0.0373	0.0457	0.0784	0.0008				1.2628	
2.5	0.0215	0.0244	0.0547	0.0800	0.0151	0.0322	0.0393	0.0780	0.0010				1.3038	
2.6	0.0178	0.0202	0.0484	0.0696	0.0136	0.0276	0.0346	0.0763	0.0011				1.3408	
2.8	0.0125	0.0133	0.0376	0.0519	0.0111	0.0210	0.0262	0.0718	0.0012				1.4034	
3.01250	0.0090	0.0090	0.0272	0.0380	0.0092	0.0165	0.0200	0.0643	0.0013	0.000			1.4555	

TABLE V (Cont'd)

$E_n$ (MeV)	43	142	296	599	863	903	945	1420	2000	3000	4000	5000	Continuum
3.5	0.000	0.000	0.0129	0.0180	0.0060	0.0098	0.0160	0.0403	0.0017	0.0010			1.5497
4.01667			0.0070	0.0090	0.000	0.0070	0.0070	0.0227	0.0023	0.0015	0.000		1.5935
4.5			0.000	0.000		0.000	0.000	0.0126	0.0030	0.0020	0.0010		1.6314
5.02083								0.0080	0.0040	0.0030	0.0015	0.000	1.6335
5.5								0.000	0.0054	0.0054	0.0030	0.0010	1.6152
6.0									0.0075	0.0075	0.0060	0.0040	1.5950
6.5									0.0090	0.0090	0.0080	0.0080	1.5250
6.56072									0.0092	0.0092	0.0092	0.0083	1.5041
7.0									0.0110*	0.0110*	0.0110*	0.0110*	1.3560*

\*Above this energy, the cross sections for these levels are identical.

$E_n$ (MeV)	Direct Interaction	Continuum
7.5	0.0456	1.0594
8.0	0.0520	0.6580
8.5	0.0584	0.3966
9.0	0.0648	0.2472
9.5	0.0720	0.1700
10.0	0.0800	0.1200
10.5	0.0896	0.0820
11.0	0.1000	0.0590
11.5	0.1104	0.045
12.0	0.1216	0.039
12.2398	0.1272	0.037
12.5	0.1336	0.035
13.0	0.1456	0.031
13.5	0.1544	0.0280
14.0	0.1600	0.0250
14.5	0.1600	0.0230
15.0	0.1600	0.0210
15.5	0.1600	0.0190
16.0	0.1600	0.0180
16.5	0.1600	0.0165
17.0	0.1600	0.0150
17.5	0.1600	0.0140
18.0	0.1600	0.0130
18.5	0.1600	0.0120
19.0	0.1600	0.0112
19.5	0.1600	0.0105
20.0	0.1600	0.0100

#### IV. INTEGRAL TESTING

The evaluated microscopic cross sections for  $^{239}\text{Pu}$  and  $^{240}\text{Pu}$  were processed from ENDF/B tapes by ETOG (Ref. 65) into 30-group cross-section sets. ETOG is adequate for these calculations, since the spectra lie predominantly below the preission threshold. The energy boundaries for this 30-group structure are given in Table VI. These group averaged cross sections were then used to calculate the eigenvalues of several bare and reflected plutonium

TABLE VI  
ENERGY BOUNDARIES AND LETHARGY WIDTHS  
FOR THE 30-GROUP STRUCTURE  
( $E_{\max} = 17 \text{ MeV}$ )

Group	$E_g$ (Lower Boundary)	$\Delta U_g$
1	15.0	MeV
2	13.5	
3	12.0	
4	10.0	
5	7.79	
6	6.07	
7	3.68	
8	2.865	
9	2.232	
10	1.738	
11	1.353	
12	0.823	
13	0.50	
14	0.303	
15	0.184	
16	0.0676	
17	0.0248	
18	0.00912	
19	0.00335	
20	0.001235	
21	454.0	eV
22	167.0	
23	61.4	
24	22.6	
25	8.32	
26	3.06	
27	1.13	
28	0.414	
29	0.152	
30	0.000139	

assemblies which were measured to be delayed critical. Descriptive information on these assemblies is provided in Table VII. For the calculations mentioned above, cross sections for nuclides other than  $^{239}\text{Pu}$  and  $^{240}\text{Pu}$  were taken from the LASL-TD-Division Library. This library has been discussed in References 66-69.

The eigenvalue calculations were performed with the DTF (Ref. 70) code in spherical geometry; an  $S_{16}$  angular quadrature was used. All cross sections were 30-group,  $P_1$  transport-corrected (two-table). A summary of the calculated eigenvalues is given in Table VIII. The results for all assemblies (with

TABLE VII  
CRITICAL ASSEMBLIES USED FOR INTEGRAL TESTING  
OF Pu CROSS-SECTION DATA

Assembly	Ref.	Core Mass (kg)	Reflector Material	Reflector Thickness (cm)
Jezebel	73	16.57	-	-
Dirty Jezebel	73	18.82	-	-
U - Ref. - Pu#1	74	8.48	NAT <sub>U</sub>	4.128
U - Ref. - Pu#2	74	6.28	NAT <sub>U</sub>	11.684
U - Ref. - Pu#3	74	6.06	NAT <sub>U</sub>	19.609
Be - Ref. - Pu	74	8.48	Be*	3.688
W - Ref. - Pu	74	8.48	W**	4.699
VERA - 11 - A	75	63.67	NAT <sub>U</sub> ***	43.0
ZEBRA - Core 3	75	835.7	NAT <sub>U</sub> ***	30.5

\* 2% oxygen  
\*\* 5.5% Ni, 2.5% Cu, 0.7% Zr  
\*\*\* See Ref. 75 for impurities

TABLE VIII  
CALCULATED EIGENVALUES FOR THE Pu  
CRITICAL ASSEMBLIES

Assembly	Eigenvalue ( $k_{\text{eff}}$ )
Jezebel	0.9995
Dirty Jezebel	1.0024
U - Ref. - Pu#1	0.9945
U - Ref. - Pu#2	1.0010
U - Ref. - Pu#3	0.9969
Be - Ref. - Pu	1.0009
W - Ref. - Pu	1.0022
VERA - 11A	1.0005
ZEBRA CORE-3	1.0083

the exception of ZEBRA CORE-3) are seen to fall within  $\pm 0.5\%$  of critical ( $k_{\text{eff}} = 1$ ). The eigenvalues for VERA-11A and ZEBRA CORE-3 were corrected for resonance self-shielding effects; these correction factors were described in a previous paper.<sup>67</sup>

The central-core-replacement reactivity of plutonium in the Jezebel assembly has been measured by Engle et al.,<sup>71</sup> using cylindrical samples 0.5 in. in diameter and 0.5 in. long. The sample was represented by a sphere of equal volume for calculational purposes. The plutonium central-core-replacement worth in the center of Jezebel was calculated to be 1451  $\text{c/g-mole}$ , using a calculated value of the dollar of  $\Delta k = k(\text{prompt critical}) - k(\text{delayed critical}) = 0.00197$ . Here  $k(\text{prompt critical})$  and  $k(\text{delayed critical})$  refer to the calculated reactivities of Jezebel in its prompt-critical and delayed-critical configurations. See Ref. 72 for a more detailed discussion of central-core-replacement calculations. This worth compares quite well with the measured value of 1439  $\text{c/g-mole}$ , i.e., an error of less than 1%.

## V. DISCUSSION

In any evaluation program, cut-off dates for consideration of experimental data must be assigned, otherwise it is impossible to incorporate each set of additional results without starting the program anew. For the present work, some important experimental results were received too late for proper assessment. A few unincorporated examples on  $^{239}\text{Pu}$  are: The total cross section of Schwartz et al.,<sup>6</sup> the  $n,2n$  and  $n,3n$  cross sections of Mather et al., and the correction to  $\bar{\nu}$  by Frehaut et al. Also, there are many measurements on  $^{235}\text{U}$  fission which now require a reevaluation of the primary standard cross section. Fortunately, the new measurements on  $\bar{\nu}$  for  $^{240}\text{Pu}$  are in reasonable agreement with the curve chosen here, thereby verifying that the high-energy measurement of Kuzminov<sup>61</sup> should be ignored.

Another experiment that casts some doubt on the present evaluation is described by Auchampaugh and Ragan (LASL, private communication). Their very preliminary results on the fission neutron spectra as a function of energy indicate no change in the nuclear temperature as the incident-neutron energy is increased. In addition, the temperatures found for  $^{235}\text{U}$ ,  $^{238}\text{U}$ , and  $^{239}\text{Pu}$  are not those commonly

used in evaluations today. These experiments are being continued and should be studied extensively before revisions are made to the work described here.

Other problems were encountered in this evaluation. Because both the shape and magnitude of many of the partial cross sections are "guessed" over a wide energy range, the structure produced in some of the partial cross sections is often inadvertent and has no physical meaning. While attempts were made to keep such structure to a minimum, it was not removed entirely and is especially apparent in the elastic scattering for  $^{240}\text{Pu}$ , where the elastic was obtained by subtracting the rest of the partials from the total cross section.

Also, the energy-dependent charged-particle cross sections employed in this evaluation were lifted directly from the ENDF/B-III evaluated files. These have not been verified experimentally at any energy either in shape or magnitude. Since the sum of these cross sections approaches 200 mb at 20 MeV, they make a significant contribution to  $\sigma_{\text{tot}}$  and therefore should be checked.

Insofar as the high-energy direct-interaction cross sections are concerned, a recent calculation indicates that a better "guess" would be to spread these interaction cross sections over a wider excitation energy. In the next pass, therefore, the level energies may be chosen at 1-MeV intervals rather than at the 500-keV intervals presently used.

It is obviously extremely difficult to make a realistic assessment of the probable errors to be assigned to the differential data. With very few exceptions, the differential data are not well established by experimental measurements. The section on integral calculations does include some verification that the low-energy differential data evaluation may not be as far off as the individual measurements might indicate. The estimated errors in Tables IX and X, however, are based on the microscopic data.

Integral tests, such as calculation of the reactivity of Jezebel, restrict the combined errors from Tables IX and X. For example, one cannot raise the fission cross section at all energies by the uncertainties indicated and still retain the capability of calculating the Jezebel reactivity. This restriction applies more strictly to  $\sigma_{n,F}$  and  $\bar{\nu}$  than to the other parameters listed. The uncertainties listed in these tables were obtained by considering

TABLE IX  
ESTIMATED UNCERTAINTIES IN EVALUATED CROSS SECTIONS OF  $^{239}\text{Pu}$  (IN PERCENT)

Nuclear Parameter	ENDF/B Designation	Neutron Energy (MeV)							
		0.03	0.1	0.5	1	2	10	15	20
$\sigma_{\text{TOT}}$	MF = 3, MT = 1	$\pm 5$	$\pm 5$	$\pm 4$	$\pm 5$	$\pm 4$	$\pm 2$	$\pm 3$	$\pm 4$
$\sigma_{\text{ELAS}}$	MF = 3, MT = 2	20	20	10	10	10	15	15	15
$\sigma_{n,F}$	MF = 3, MT = 18	7	4	4	7	5	5	7	10
$\sigma_{n,\gamma}$	MF = 3, MT = 102	15	10	10	10	-	-	-	-
$\sigma_{n,n'}$	MF = 3, MT = 4	30	30	30	30	30	30	30	30
$\sigma_{n,2n}$	MF = 3, MT = 16	-	-	-	-	-	20	30	30
$\sigma_{n,3n}$	MF = 3, MT = 17	-	-	-	-	-	-	$\times 2$	$\times 2$
$\bar{v}$	MF = 1, MT = 452	1.5	1.5	1.5	2.0	2.0	2.0	3.0	3.0

TABLE X  
ESTIMATED UNCERTAINTIES IN EVALUATED CROSS SECTIONS OF  $^{240}\text{Pu}$   
(IN PERCENT)

Nuclear Parameter	ENDF/B Designation	Neutron Energy (MeV)							
		0.05	0.1	0.5	1	2	10	15	20
$\sigma_{\text{TOT}}$	MF = 3, MT = 1	$\pm 20$	$\pm 4$	$\pm 4$	$\pm 4$	$\pm 5$	$\pm 20$	$\pm 20$	$\pm 20$
$\sigma_{\text{ELAS}}$	MF = 3, MT = 2	20	20	10	15	15	15	15	15
$\sigma_{n,F}$	MF = 3, MT = 18	15	20	20	10	4	15	5	15
$\sigma_{n,\gamma}$	MF = 3, MT = 102	$\times 2$	$\times 2$	$\times 2$	$\times 2$	$\times 2$	-	-	-
$\sigma_{n,n'}$	MF = 3, MT = 4	30	30	15	15	20	30	30	30
$\sigma_{n,2n}$	MF = 3, MT = 16	-	-	-	-	$\times 2$	$\times 2$	$\times 2$	$\times 2$
$\sigma_{n,3n}$	MF = 3, MT = 17	-	-	-	-	-	$\times 2$	$\times 2$	$\times 2$
$\bar{v}$	MF = 1, MT = 452	2.0	2.0	2.0	2.0	2.0	7.0	10.0	15.0

each parameter individually. These integral tests, therefore, give some indication that the cross sections below 3-4 MeV may be less uncertain than indicated above. It is recognized, however, that integral checks cannot uniquely reduce the microscopic uncertainties.

#### ACKNOWLEDGMENTS

We gratefully acknowledge the contributions of R. J. LaBauve, D. G. Foster, Jr., N. L. Whittemore, W. J. Krauser, P. P. Whalen, and D. R. Worlton to the various aspects of this evaluation. We also thank C. C. Cremer, D. R. Harris, P. G. Young, and

J. L. Kammerdiener for their many helpful comments on the evaluation and the formal presentation of the results.

#### REFERENCES

1. C. T. Hibdon and A. Langsdorf, "Total Neutron Cross Sections in the keV Region," in "Physics Division Supplement to Quarterly Report, September, October, and November 1953," Argonne National Laboratory report ANL-5175 (1954).
2. R. E. Meads, Atomic Energy Research Establishment report AERE-NP/R-1643 (1955).
3. A. Bratenahl, J. M. Peterson, and J. P. Stoerling, "Neutron Total Cross Sections in the 7- to 14-MeV Region," Phys. Rev. 110, 927-936 (1958).

4. J. M. Peterson, A. Bratenahl, and J. P. Stoering, "Neutron Total Cross Sections in the 17- to 29-MeV Region," Phys. Rev. 120, 521-526 (1960).
5. D. G. Foster, Jr., and D. W. Glasgow, "Neutron Total Cross Sections, 2.5-15 MeV. I. Experimental," Phys. Rev. C3, 576-603 (1971).
6. R. B. Schwartz et al., National Bureau of Standards, private communication, 1972.
7. H.-H. Knitter and M. Coppola, "Elastic Neutron Scattering Measurements on  $^{239}\text{Pu}$  in the Energy Range between 0.19 and 0.38 MeV," Z. Physik 228, 286-294 (1969).
8. M. Coppola and H.-H. Knitter, "Interactions of Neutrons with  $^{239}\text{Pu}$  in the Energy Range between 1.5 and 5.5 MeV," Z. Physik 232, 286-302 (1970).
9. R. C. Allen, R. B. Walton, R. B. Perkins, R. A. Olson, and R. F. Taschek, "Interaction of 0.5- and 1.0-MeV Neutrons with Some Heavy Elements," Phys. Rev. 104, 731-735 (1956).
10. W. P. Poenitz, "Measurement of the Ratios of Capture and Fission Neutron Cross Sections of  $^{235}\text{U}$ ,  $^{238}\text{U}$ , and  $^{239}\text{Pu}$  at 130 to 1400 keV," Nucl. Sci. Eng. 40, 383-388 (1970).
11. W. P. Poenitz, "Additional Measurements of the Ratio of the Fission Cross Sections of Plutonium-239 and Uranium-235," Nucl. Sci. Eng. 47, 228-230 (1972).
12. E. Pfletschinger and F. Käppeler, "A Measurement of the Fission Cross Sections of  $^{239}\text{Pu}$  and  $^{233}\text{U}$  Relative to  $^{235}\text{U}$ ," Nucl. Sci. Eng. 40, 375-382 (1970).
13. M. Soleilac, J. Frehaut, J. Gauriau, G. Mosinski, "Mean Number of Prompt Neutrons and Relative Cross-Sections for the Fission of  $^{235}\text{U}$  and  $^{239}\text{Pu}$  between 0.3 and 1.4 MeV," Proc. 2nd Intern. Conf. Nuclear Data for Reactors, Helsinki, June 15-19, 1970 (IAEA, Vienna, 1970), 2, 145-156.
14. P. H. White, J. G. Hodgkinson, and G. J. Wall, "Measurement of Fission Cross-Sections for Neutrons of Energies in the Range 40-500 keV," Proc. Symp. Physics and Chemistry of Fission, Salzburg, March 22-26, 1965 (IAEA, Vienna, 1965), 1, 219-233.
15. V. G. Nesterov and G. N. Smirenkin, "Cross Section Ratios for Fission of  $^{233}\text{U}$ ,  $^{235}\text{U}$ , and  $^{239}\text{Pu}$  by Fast Neutrons," Atomnaya Energiya (Eng. Trans.) 24, 224-226 (1968); Atomnaya Energiya 24, 185-187 (1968).
16. M. V. Savin, Yu. A. Khokhlov, Yu. S. Zamyatnin, and I. N. Paramonova, "Ratios of Fast Fission Cross Sections of  $^{235}\text{U}$ ,  $^{239}\text{Pu}$ , and  $^{240}\text{Pu}$ ," Atomnaya Energiya (Eng. Trans.) 29, 938-940 (1970); Atomnaya Energiya 29, 218-220 (1970).
17. W. K. Lehto, "Fission Cross-Section Ratio Measurements of  $^{239}\text{Pu}$  and  $^{233}\text{U}$  to  $^{235}\text{U}$  from 0.24 to 24 keV," Nucl. Sci. Eng. 39, 361-367 (1970).
18. R. K. Smith, G. Hansen, and S. McGuire, "Fission Cross Sections of  $^{233}\text{U}$ ,  $^{235}\text{U}$ ,  $^{238}\text{U}$ ,  $^{239}\text{Pu}$ ,  $^{240}\text{Pu}$ , and  $^{241}\text{Pu}$ ," in "Reports to the AEC Nuclear Cross Sections Advisory Committee," Atomic Energy Commission report WASH-1124 (1968), p. 110.
19. P. H. White and G. P. Warner, "The Fission Cross Sections of  $^{233}\text{U}$ ,  $^{234}\text{U}$ ,  $^{236}\text{U}$ ,  $^{238}\text{U}$ ,  $^{237}\text{Np}$ ,  $^{239}\text{Pu}$ ,  $^{240}\text{Pu}$ , and  $^{241}\text{Pu}$  Relative to that of  $^{235}\text{U}$  for Neutrons in the Energy Range 1-14 MeV," J. Nucl. Energy 21, 671-679 (1967).
20. G. D. James, "Fission Cross Section Measurements of  $^{233}\text{U}$ ,  $^{235}\text{U}$ ,  $^{239}\text{Pu}$ , and  $^{241}\text{Pu}$  in the Energy Range from 1 to 25 keV," Proc. Intern. Conf. Fast Critical Experiments and their Analysis, Argonne National Laboratory, Oct. 10-13, 1966, Argonne National Laboratory report ANL-7320 (1966).
21. J. L. Perkin, P. H. White, P. Fieldhouse, E. J. Axton, P. Cross, and J. C. Robertson, "The Fission Cross Sections of  $^{233}\text{U}$ ,  $^{234}\text{U}$ ,  $^{235}\text{U}$ ,  $^{236}\text{U}$ ,  $^{237}\text{Np}$ ,  $^{239}\text{Pu}$ ,  $^{240}\text{Pu}$  and  $^{241}\text{Pu}$  for 24 keV Neutrons," J. Nucl. Energy 19, 423-437 (1965).
22. S. M. Dubrovina and V. A. Shigin, "Neutron Fission Cross Sections of  $\text{Pa}^{231}$  and  $\text{Pu}^{239}$  in the 1.5 to 1500 keV Energy Range," Soviet Physics--Doklady 9, 579-580 (1965); Dokl. Akad. Nauk SSSR 157, 561-562 (1964).
23. W. D. Allen and A. T. G. Ferguson, "The Fission Cross Sections of  $^{233}\text{U}$ ,  $^{235}\text{U}$ ,  $^{238}\text{U}$  and  $^{239}\text{Pu}$  for Neutrons in the Energy Range 0.030 MeV to 3.0 MeV," Proc. Phys. Soc. (London) 70A, 573 (1957).
24. G. A. Dorofeev and Yu. P. Dobrynin, "Effective Cross Sections for Fission of  $^{233}\text{U}$ ,  $^{235}\text{U}$ ,  $^{239}\text{Pu}$  and  $^{240}\text{Pu}$  by Neutrons with Energies from 30 keV to 5 MeV," Atomnaya Energiya (Eng. Trans.) 2, 9-16 (1957); Atomnaya Energiya 2, 10 (1957); J. Nucl. Energy 5, 217-225 (1957).
25. T. A. Pitterle, L. Stewart, and R. E. Hunter, private communication (LASL Groups TD-2 and T-2), 1971.
26. B. Adams, R. Batchelor, and T. S. Green, "The Energy Dependence of the Fission Cross-Sections of  $^{238}\text{U}$ ,  $^{235}\text{U}$ , and  $^{239}\text{Pu}$  for Neutrons in the Energy Range 12.6 to 20 MeV," J. Nucl. Energy 14, 85-90 (1961).
27. M. Soleilac, J. Frehaut and J. Gauriau, "Energy Dependence of  $v_p$  for Neutron-Induced Fission of  $^{235}\text{U}$ ,  $^{238}\text{U}$ , and  $^{239}\text{Pu}$  from 1.3 to 15 MeV," J. Nucl. Energy 23, 257-282 (1969); plus values given in the compilation of Konshin and Manero (V. A. Konshin and F. Manero, "Energy Dependent  $v$  Values for  $^{235}\text{U}$ ,  $^{239}\text{Pu}$ ,  $^{233}\text{U}$ ,  $^{240}\text{Pu}$ ,  $^{241}\text{Pu}$ , and the Status of  $\bar{v}$  for Spontaneous Fission Isotopes," International Nuclear Data Committee report INDC(NDS)-19/N (1970)).
28. J. C. Hopkins and B. C. Diven, "Prompt Neutrons from Fission," Nucl. Phys. 48, 433-442 (1963).

29. D. S. Mather, P. Fieldhouse, and A. Moat, "Measurement of Prompt  $\bar{V}$  for the Neutron-Induced Fission of  $\text{Th}^{232}$ ,  $\text{U}^{233}$ ,  $\text{U}^{234}$ ,  $\text{U}^{238}$ , and  $\text{Pu}^{239}$ ," *Nucl. Phys.* 66, 149-160 (1965).
30. D. W. Colvin and M. G. Sowerby, "Boron Pile  $\bar{V}$  Measurements," Proc. Symp. Physics and Chemistry of Fission, Salzburg, March 22-26, 1965 (IAEA, Vienna, 1965), 2, 25-37.
31. H. Condé, J. Hansén, and M. Holmberg, "Prompt  $\bar{V}$  in Neutron-Induced Fission of  $^{239}\text{Pu}$  and  $^{241}\text{Pu}$ ," *J. Nucl. Energy* 22, 53-60 (1968).
32. M. V. Savin, Yu. A. Khokhlov, Yu. S. Zamyatnin, and I. N. Paramonova, "The Average Number of Prompt Neutrons in Fast-Neutron-Induced Fission of  $^{235}\text{U}$ ,  $^{239}\text{Pu}$ , and  $^{240}\text{Pu}$ ," Proc. 2nd Intern. Conf. Nuclear Data for Reactors, Helsinki, June 15-19, 1970 (IAEA, Vienna, 1970), 2, 157-165.
33. V. G. Nesterov, B. Nurpeissov, L. I. Prokhorova, G. N. Smirenkin, and Yu. M. Turchin, "Average Number of Prompt Neutrons in the Fission of Uranium-235 and Plutonium-239 by Neutrons," Proc. 2nd Intern. Conf. Nuclear Data for Reactors, Helsinki, June 15-19, 1970 (IAEA, Vienna, 1970), 2, 167-175.
34. G. C. Hanna, C. H. Westcott, H. D. Lemmel, B. R. Leonard, Jr., J. S. Story, and P. M. Attree, "Revision of Values for the 2200 m/s Neutron Constants for Four Fissile Nuclides," *At. Energy Rev.* 7, No. 4, 3-92 (1969).
35. G. R. Keepin, "Delayed Fission Data in Reactor Kinetics and Design," in Delayed Fission Neutrons (IAEA, Vienna, 1968), p. 3ff.
36. V. I. Shpakov, K. A. Petrzhalak, M. A. Bak, S. S. Kovalenko, and O. I. Kostochkin, "Delayed-Neutron Yields from the Fission of  $\text{Pu}^{239}$  and  $\text{Th}^{232}$  by 14.5 MeV Energy Neutrons," *Atomnaya Energiya* (Eng. Trans.) 11, 1190-1191 (1961); *Atomnaya Energiya* 11, 539-540 (1961).
37. A. E. Evans, M. M. Thorpe, and M. S. Krick, "Revised Delayed-Neutron Yield Data," *Nucl. Sci. Eng.* 50, 80-82 (1973). These data replace the values previously reported by M. S. Krick and A. E. Evans, "The Measurement of Total Delayed-Neutron Yields as a Function of the Energy of the Neutron Inducing Fission," *Nucl. Sci. Eng.* 47, 311-318 (1972).
38. C. F. Masters, M. M. Thorpe, and D. B. Smith, "The Measurement of Absolute Delayed-Neutron Yields from 3.1- and 14.9-MeV Fission," *Nucl. Sci. Eng.* 36, 202-208 (1969).
39. J. F. Conant and P. F. Palmedo, "Measurement of the Delayed-Neutron Fractions for Thermal Fission of Uranium-235, Plutonium-239, and Uranium-233," *Nucl. Sci. Eng.* 44, 173-179 (1971).
40. E. Barnard, A. T. G. Ferguson, W. R. McMurray, and I. J. Van Heerden, "Time-of-Flight Measurements of Neutron Spectra from the Fission of  $\text{U}^{235}$ ,  $\text{U}^{238}$ , and  $\text{Pu}^{239}$ ," *Nucl. Phys.* 71, 228-240 (1965).
41. L. M. Belov, M. V. Blinov, N. M. Kazarinov, A. S. Krivokhatetskii, and A. M. Protopopov, "Spectra of Fission Neutrons of  $\text{Cm}^{244}$ ,  $\text{Pu}^{242}$ , and  $\text{Pu}^{239}$ ," *Sov. J. Nucl. Phys.* 9, 421-423 (1969); *Yad. Fiz.* 9, 727-731 (1969).
42. Yu. S. Zamyatnin, I. N. Safina, E. K. Gutnikova, and N. I. Ivannova, "Spectra of Neutrons Produced by 14-MeV Neutrons in Fissile Materials," *Atomnaya Energiya* (Eng. Trans.) 4, 443-449 (1958); *Atomnaya Energiya* 4, 337-342 (1958).
43. H. Condé and G. During, "Fission Neutron Spectra: Part II, Fission Neutron Spectra of  $\text{U}^{235}$ ,  $\text{Pu}^{239}$ , and  $\text{Cf}^{252}$ ," *Arkiv Fysik* 29, 313-319 (1965).
44. G. N. Smirenkin, "Comparison of Effective Temperatures of Spectra of Neutrons Emitted in Fission of  $\text{U}^{235}$  and  $\text{Pu}^{239}$  by Fast and Thermal Neutrons," *JETP Lett.* 10, 1286-1287 (1960); *Zh. Eksp. Teor. Fiz.* 37, 1822-1824 (1959).
45. F. Bertrand and J. Voignier, "Inelastic Scattering of 14 MeV Neutrons by  $\text{Pu}^{239}$ ," Commissariat à l'Energie Atomique report CEA-R-3936 (1970).
46. A. B. Smith, "Note on the Prompt-Fission-Neutron Spectra of Uranium-235 and Plutonium-239," *Nucl. Sci. Eng.* 44, 439-442 (1971).
47. J. C. Hopkins and B. C. Diven, "Neutron Capture to Fission Ratios in  $\text{U}^{233}$ ,  $\text{U}^{235}$ ,  $\text{Pu}^{239}$ ," *Nucl. Sci. Eng.* 12, 169-177 (1962).
48. G. deSaussure, L. W. Weston, R. Gwin, R. W. Ingle, J. H. Todd, R. W. Hockenbury, R. R. Fullwood, and A. Lottin, "Measurement of the Neutron Capture and Fission Cross-Sections and of their Ratio Alpha for  $\text{U}^{233}$ ,  $\text{U}^{235}$ , and  $\text{Pu}^{239}$ ," Proc. Conf. Nuclear Data for Reactors, Paris, October 17-21, 1966 (IAEA, Vienna, 1967), 2, 233-249.
49. R. E. Hunter, J.-J. H. Berlijn, and C. C. Cremer, "Neutron Cross Sections for  $\text{Pu}^{239}$  and  $\text{Pu}^{240}$  in the Energy Range 1 keV to 14 MeV," Los Alamos Scientific Laboratory report LA-3528 (July 1968).
50. C. M. Lederer, J. M. Hollander, and I. Perlman, Table of Isotopes (2nd Ed.) (Wiley and Sons, New York, 1967).
51. V. N. Andreev, "Inelastic Scattering of Neutrons of the Fission Spectrum and Neutrons with an Energy of 0.9 MeV in  $\text{U}^{235}$  and  $\text{Pu}^{239}$ ," in Soviet Progress in Neutron Physics (Consultants Bureau, New York, 1963), p. 211-215.
52. L. A. Cranberg, "Neutron Scattering by  $\text{U}^{235}$ ,  $\text{Pu}^{239}$ , and  $\text{U}^{238}$ ," Los Alamos Scientific Laboratory report LA-2177 (January 1959).
53. J. L. Kammerdiener, "Neutron Spectra Emitted by  $\text{Pu}^{239}$ ,  $\text{U}^{238}$ ,  $\text{U}^{235}$ , Pb, Nb, Ni, Al, and C Irradiated by 14-MeV Neutrons," Lawrence Livermore Laboratory report UCRL-51232 (1972).
54. A. H. Wapstra and N. B. Gove, "The 1971 Atomic Mass Evaluation," *Nucl. Data Tables* 9, 265-468 (1971).

55. P. P. Whalen and D. R. Worlton, private communication (LASL Groups TD-3 and TD-4), 1972.
56. A. B. Smith, P. Lambropoulos, and J. F. Whalen, "Fast Neutron Total and Scattering Cross Sections of Plutonium-240," *Nucl. Sci. Eng.* 47, 19-28 (1972).
57. M. V. Savin, Yu. S. Zamyatnin, Yu. A. Khokhlov, and I. N. Paramonova, "Fission Cross-Section Ratios of  $^{235}\text{U}$ ,  $^{239}\text{Pu}$ ,  $^{240}\text{Pu}$  for Fast Neutrons," International Nuclear Data Committee report INDC(CCP)-8/U (1970).
58. P. Ruddick and P. H. White, "The Measurement of the Neutron Fission Cross Section of  $^{240}\text{Pu}$  in the Energy Range 60-500 keV," *J. Nucl. Energy* 18, 561-567 (1964).
59. V. G. Nesterov and G. N. Smirenkin, "0.04-4.0 MeV Neutron Fission Cross Section of  $^{240}\text{Pu}$ ," *Atomnaya Energiya* (Eng. Trans.) 9, 511-515 (1960); *Atomnaya Energiya* 9, 16-20 (1960); *J. Nucl. Energy* 16, 51-55 (1962).
60. W. B. Gilboy and G. Knoll, "The Fission Cross-Sections of Some Plutonium Isotopes in the Neutron Energy Range 5-150 keV," *Kernforschungszentrum* report KFK-450 (1966).
61. B. D. Kuzminov, "Average Number of Prompt Neutrons in  $^{240}\text{Pu}$  Fission by 3.6- and 15-MeV Neutrons," in *Soviet Progress in Neutron Physics* (Consultants Bureau, New York, 1961), pp. 181-182.
62. M. de Vroey, A. T. G. Ferguson, and N. Starfelt, "A Measurement of  $\bar{v}$  for Neutron-Induced Fission of  $^{240}\text{Pu}$ ," *J. Nucl. Energy* 20, 191-200 (1966).
63. J. Terrell, "Prompt Neutrons from Fission," Proc. Symp. Physics and Chemistry of Fission, Salzburg, March 22-26, 1965 (IAEA, Vienna, 1965), 2, 3-24.
64. T. A. Pitterle and M. Yamamoto, "Evaluated Neutron Cross Sections of Pu-240 for the ENDF/B File," Atomic Power Development Associates report APDA-218 (1968).
65. D. E. Kusner, S. Kellman, and R. A. Dannells, "ETOQ-1, a FORTRAN IV Program to Process Data from the ENDF/B File to the MUFT, GAM, and ANISN Formats," Westinghouse Electric Corporation report WCAP-3845-1 (1969).
66. T. J. Hiron and M. E. Battat, "Calculations of Fast Critical Assemblies Using LASL and ENDF/B Version II Data," *Trans. Am. Nucl. Soc.* 14, 348-349 (1971).
67. T. J. Hiron, "Calculations of ENDF/B Fast Reactor Benchmark Cases Using the LASL-TD Cross Section Library," *Trans. Am. Nucl. Soc.* 14, 813-814 (1971).
68. M. E. Battat and T. J. Hiron, "Calculations of Reflected Fast Critical Assemblies and Comparison with Experiment," *Trans. Am. Nucl. Soc.* 15, 458 (1972).
69. J.-J. H. Berlijn, R. E. Hunter, and C. C. Cremer, "Neutron Cross Sections for  $^{235}\text{U}$  and  $^{238}\text{U}$  in the Energy Range 1 keV to 14 MeV," Los Alamos Scientific Laboratory report LA-3527 (August 1968).
70. K. D. Lathrop, "DTF-IV, a FORTRAN-IV Program for Solving the Multigroup Transport Equation with Anisotropic Scattering," Los Alamos Scientific Laboratory report LA-3373 (November 1965).
71. L. B. Engle, G. E. Hansen, and H. C. Paxton, "Reactivity Contributions of Various Materials in Topsy, Godiva, and Jezebel," *Nucl. Sci. Eng.* 8, 543-569 (1960).
72. C. C. Cremer, R. E. Hunter, J.-J. H. Berlijn, and D. R. Worlton, "Comparison of Calculations with Integral Experiments for Plutonium and Uranium Critical Assemblies," Los Alamos Scientific Laboratory report LA-3529 (October 1969).
73. G. E. Hansen and H. C. Paxton, "Reevaluated Critical Specifications of Some Los Alamos Fast-Neutron Systems," Los Alamos Scientific Laboratory report LA-4208 (September 1969).
74. H. C. Paxton, "Los Alamos Critical-Mass Data," Los Alamos Scientific Laboratory report LAMS-3067 (May 1964).
75. W. G. Davey and A. L. Hess, "Additional Fast Reactor Benchmarks for Phase II Data Testing of ENDF/B," Argonne National Laboratory memo to CSEWG, Feb. 21, 1969.